

Portland State University

PDXScholar

Dissertations and Theses

Dissertations and Theses

1993

Mechanism of Calcium Release from Skeletal Muscle Sarcoplasmic Reticulum

Edmond Buck

Portland State University

Follow this and additional works at: https://pdxscholar.library.pdx.edu/open_access_etds

Let us know how access to this document benefits you.

Recommended Citation

Buck, Edmond, "Mechanism of Calcium Release from Skeletal Muscle Sarcoplasmic Reticulum" (1993). *Dissertations and Theses*. Paper 1307.

<https://doi.org/10.15760/etd.1306>

This Dissertation is brought to you for free and open access. It has been accepted for inclusion in Dissertations and Theses by an authorized administrator of PDXScholar. Please contact us if we can make this document more accessible: pdxscholar@pdx.edu.

MECHANISM OF CALCIUM RELEASE FROM SKELETAL
MUSCLE SARCOPLASMIC RETICULUM

by

EDMOND BUCK


A dissertation submitted in partial fulfillment of the
requirements for the degree of


DOCTOR OF PHILOSOPHY
IN
ENVIRONMENTAL SCIENCES AND RESOURCES:
PHYSICS

Portland State University
1993

TO THE OFFICE OF GRADUATE STUDIES:

The members of the committee approve the dissertation
of Edmond Buck presented May 5, 1993


Jonathan J. Abramson, Chair


Erik Bodegem


Pavel K. Smetek


Robert L. Millette


Gordon L. Kilgour


Gary R. Brodowicz

APPROVED:

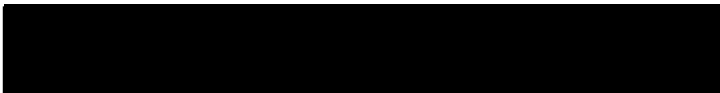

Robert O. Tinnin, Dean, College of Liberal Arts and Sciences

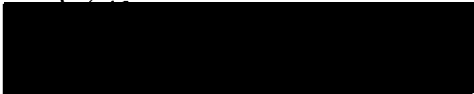

Roy W. Koch, Vice Provost for Graduate Studies

AN ABSTRACT OF THE DISSERTATION OF Edmond Buck for the
Doctor of Philosophy in Environmental Sciences and
Resources: Physics presented May 5, 1993.

Title: Mechanism of Calcium Release From Skeletal Muscle
Sarcoplasmic Reticulum.

APPROVED BY THE MEMBERS OF THE DISSERTATION COMMITTEE:

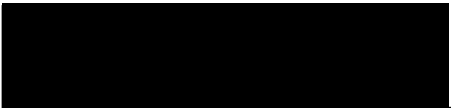

Jonathan J. Abramson, Chair


Erik Bodegom


Pavel K. Smejtek


Robert L. Millette


Gordon L. Kilgour


Gary R. Brodowicz

The sarcoplasmic reticulum (SR) is an intracellular membrane system dedicated to the active regulation of cytosolic calcium in muscle. The opening of Ca^{2+} channels in the SR results in a rapid increase in the myoplasmic Ca^{2+} concentration and the initiation of contraction. Closure of these channels allows the SR to re-accumulate the released Ca^{2+} which results in muscle relaxation. While it is known that a muscle fiber is stimulated to contract by the depolarization of the sarcolemma, it is not understood how this signal is communicated to the SR.

The focus of this dissertation is twofold. The first objective is to gain an understanding of the mechanism of Ca^{2+} release from the SR. To this end, three studies have been performed which indicate that Ca^{2+} release is mediated by an oxidation reaction. The second goal is to gain insight into the function of the Ca^{2+} release channel. This is addressed by a fourth study which characterizes the effect of the plant alkaloid, ryanodine, on channel operation.

The anthraquinones mitoxantrone, doxorubicin, daunorubicin, and rubidazone are shown to be potent stimulators of Ca^{2+} release from SR vesicles. Anthraquinone-induced Ca^{2+} release is shown to be via a specific interaction with the Ca^{2+} release system of the SR. In addition, a strong interaction between anthraquinone and caffeine binding sites on the Ca^{2+} release channel is observed when monitoring Ca^{2+} fluxes across the SR. It is

shown that Ca^{2+} release stimulated by anthraquinones is inhibited by preincubating the quinone with dithionite, a strong reducing agent. Spectrophotometric measurements show that the dithionite treated quinone is in a reduced state.

Previous work in this lab has shown that the photooxidizing xanthene dye rose bengal stimulates rapid Ca^{2+} release from skeletal muscle SR vesicles. In this thesis, it is shown that following fusion of vesicles to a bilayer lipid membrane (BLM), Ca^{2+} channel activity is stimulated by nanomolar concentrations of rose bengal in the presence of a broad-spectrum light source. This stimulation is shown to be independent of the Ca^{2+} concentration but is inhibited by μM ruthenium red. The photooxidation of rose bengal is shown to not affect either the K^+ or Cl^- channels which are present in the SR. Exposure of the Ca^{2+} release channel to 500 nM rose bengal in the presence of light is shown to reverse the modification to the channel induced by μM ryanodine. This apparent displacement of bound ryanodine by nanomolar concentrations of rose bengal is directly observed upon measurement of [^3H]ryanodine binding to TSR vesicles. Evidence is presented which suggests that Ca^{2+} release is mediated by singlet oxygen.

Micromolar concentrations of the porphyrin meso-Tetra(4-N-methylpyridyl)porphine tetraiodide ($\text{TMP}_{\text{Y}}\text{P}$) is shown to induce the rapid release of Ca^{2+} from skeletal muscle SR vesicles. Porphyrin-induced Ca^{2+} release is

stimulated by adenine nucleotides and $\mu\text{M Ca}^{2+}$, and is inhibited by mM Mg^{2+} and μM ruthenium red. High-affinity [^3H]ryanodine binding is also enhanced in the presence of the porphyrin. The presence of 1 mM Mg^{2+} in the assay medium sensitizes ryanodine binding to activation by Ca^{2+} . Porphyrin stimulated single channel activity is also sensitized to activation by Ca^{2+} in the presence of Mg^{2+} . Reduction of the porphyrin by dithionite, a strong reducing agent, prior to exposure to the Ca^{2+} release channel inhibited the ability of TMPyP to stimulate Ca^{2+} release.

These observations indicate that anthraquinones, rose bengal, and porphyrins induce a stimulation of the Ca^{2+} release protein from skeletal muscle SR by interacting with the ryanodine binding site. In addition, the mechanism of interaction for these compounds appears to be via an oxidation reaction.

Nanomolar to micromolar concentrations of ryanodine are shown to alter the gating kinetics of the Ca^{2+} release channel from skeletal muscle SR fused with bilayer lipid membranes. In the presence of asymmetric CsCl , 5 to 40 nM concentrations of ryanodine are shown to activate the channel by increasing the open probability (P_o) without changing the conductance. Statistical analysis of gating kinetics reveal that the open and closed dwell times exhibit bi-exponential distributions that are significantly modified by nM ryanodine. The altered channel gating kinetics seen

with low nM ryanodine is reversible and is shown to correlate with the binding kinetics of [^3H]ryanodine with its highest affinity site under identical ionic conditions. Ryanodine concentrations between 20 and 50 nM are observed to induce occasional 1/2 conductance fluctuations while ryanodine concentrations greater than 50 nM stabilize the channel into a 1/2 conductance state which is not reversible. These results are shown to correlate with [^3H]ryanodine binding to a second site having lower affinity than the first site. Ryanodine at concentrations greater than 70 μM are shown to produce a unidirectional transition from the 1/2 to a 1/4 conductance fluctuation, whereas ryanodine concentrations greater than 200 μM cause complete closure of the channel. The concentration of ryanodine required to stabilize either the 1/4 conductance transitions or channel closure do not directly correlate with the measured [^3H]ryanodine equilibrium binding constants. However, these results can be explained by considering the association kinetics of ryanodine concentrations greater than 200 nM in the presence of 500 mM CsCl.

These results indicate that ryanodine stabilizes four discrete states of the SR release channel and supports the existence of multiple interacting ryanodine binding sites on the channel protein.

ACKNOWLEDGEMENTS

Reflecting upon the last eleven years spent in pursuit of this degree, I realize that there have been far too many influential people in my life to include in a short acknowledgement. Nevertheless, I would like to thank each and every one who participated in my education. I would like to acknowledge and thank those who were my primary teachers; The Faculty and Staff of the Physics Department, past and present. I wish to thank Dr. Ray Sommerfeldt, Mrs. Dawn Dressler, and Dr. Arnold Pickar, each of whom recognized ability within me, even when I could not see it myself. I especially wish to acknowledge Dr. Pavel Smejtek, who has become a good friend and whose well timed comment initially motivated me to enter the Ph.D. program. The members of the Science Support Shop also deserve special mention. I especially wish to remember Garo Arakelian who helped me design my bilayer setup and eventually built it. I would also like to acknowledge the numerous people who have befriended and helped me over the years. To Maybell Trimm and all the other hard working Ladies of the Registrars Office, I thank you for remembering and taking care of me (all those boxes didn't go to waste). I also wish to thank Jerry and Marilyn Wilson for the opportunities they have provided. I wish for Brian Wilson tremendous success as a

clothier and grower of giant salt crystals. And finally, I wish to thank Dr. Ellen Magenis for providing me with a home and family when I needed it most. The rewards of a college education include the friendships which last a lifetime. To all those who made my college experience more than an eternity of study, I THANK YOU! I especially wish to remember Dr. Joe Walters, Dr. Hui Xiong, Dr. Eric Roth, and Dr. Jon Trimm, each of whom has shown me that there is indeed life after grad school. I would also like to acknowledge my good friends Jim Stapleton, Robin Dorociak, Susan Molitor, Margie Fyfield, and especially my brother Jeff. Time off would not be time off without you. To the members of the Biophysics group, I wish to say thanks for your support, camaraderie, and friendship over the years. I wish to thank Dr. Terry Favero, who showed me the meaning of the words productivity and chocoholic. To Keith Scott and Tony Zable, I wish you well. But the most important person I wish to acknowledge is my advisor, my mentor, and my friend, Jon Abramson, who has not only been instrumental in my development as a scientist, but whose integrity, honor, and high moral character will be a model for me for the rest of my life. Therefore, I dedicate this body of work to the only other person who understands all of it, Jon Abramson.

TABLE OF CONTENTS

	PAGE
ACKNOWLEDGEMENTS	iii
LIST OF TABLES	ix
LIST OF FIGURES	x
INTRODUCTION	1
Muscle and Contraction	1
Anatomy	
Contraction	
Sarcoplasmic Reticulum	9
Longitudinal SR	
Terminal SR	
Transverse Tubules and Triads	
Pharmacology of SR Ca ²⁺ Release	
Excitation-Contraction Coupling	15
Depolarization-induced Release	
Mechanical Coupling-induced Release	
Chemical Coupling-induced Release	
Ryanodine Receptor	23
Overview of the Dissertation	26
Oxidation-induced Ca ²⁺ Release	
Ryanodine Stabilized Conformational States	
of the SR Calcium Release Channel	
GENERAL METHODS	32
Introduction	32
Methods	32
Isolation of Sarcoplasmic Reticulum	

Ca ²⁺ Efflux Studies	
[³ H]Ryanodine Binding Studies	
Bilayer Lipid Membrane Studies	
MECHANISM OF ANTHRAQUINONE-INDUCED CALCIUM RELEASE FROM SKELETAL MUSCLE SARCOPLASMIC RETICULUM	44
Summary	44
Introduction	44
Methods and Materials	49
Preparation of SR Vesicles	
Ca ²⁺ Efflux Assays	
Skinned Fiber Assays	
[³ H]Ryanodine Binding Assays	
Materials	
Results	53
Anthraquinones Stimulate Ca ²⁺ Release from SR Vesicles	
Anthraquinones Induce Contractures in Skinned Muscle Fibers	
Anthraquinones Stimulate [³ H]Ryanodine Binding	
Effects of Caffeine	
Anthraquinones Interact with the Ca ²⁺ Release Channel via an Oxidation- Reduction Reaction	
Discussion	76
ROSE BENZAL ACTIVATES THE CALCIUM RELEASE CHANNEL FROM SKELETAL MUSCLE SARCOPLASMIC RETICULUM	82
Summary	82
Introduction	83
Methods and Materials	85
Preparation of SR Vesicles	
Bilayer Lipid Membrane Studies	
Measurement of Ca ²⁺ Efflux	
[³ H]Ryanodine Binding Dissociation Assay	
Materials	
Results	87
Rose Bengal Activates the Ca ²⁺ Release Channel from SR	

Stimulation of Ca^{2+} Release by Rose Bengal is Independent of Ca^{2+} concentration	
Activation of the Ca^{2+} Release Channel by Rose Bengal is Side Independent	
Rose Bengal Displaces Bound Ryanodine from its Receptor	
Rose Bengal Reverses the Effect of Micromolar Ryanodine on the Ca^{2+} Release Channel	
Discussion	99
PORPHYRIN-INDUCED CALCIUM RELEASE FROM SKELETAL MUSCLE SARCOPLASMIC RETICULUM	102
Summary	102
Introduction	103
Methods and Materials	104
Preparation of SR Vesicles	
Measurement of Ca^{2+} Efflux	
[^3H]Ryanodine Binding Assay	
Bilayer Lipid Membrane Studies	
Materials	
Results	107
Porphyrins Stimulate Ca^{2+} Release from SR Vesicles	
Porphyrins Stimulate [^3H]Ryanodine Binding	
Single Channel Measurements	
Effects of Reducing Agents	
Discussion	124
RYANODINE STABILIZES MULTIPLE CONFORMATIONAL STATES OF THE CALCIUM RELEASE CHANNEL FROM SARCOPLASMIC RETICULUM	127
Summary	127
Introduction	127
Methods and Materials	129
Preparation of SR Vesicles	
[^3H]Ryanodine Binding Assays	
Bilayer Lipid Membrane Studies	
Materials	
Results	132

[³ H]Ryanodine Receptor Binding in the Presence of CsCl Nanomolar Ryanodine and Single Channel Kinetics Ryanodine Stabilizes 1/2 Conductance States of the Ca ²⁺ Release Channel Ryanodine Stabilizes 1/4 Conductance States of the Ca ²⁺ Release Channel	
Discussion	148
CONCLUDING REMARKS	154
REFERENCES	161

LIST OF TABLES

TABLE		PAGE
I	Modulators of Ca^{2+} release from SR vesicles .	15
II	Mitoxantrone-induced Ca^{2+} release	59
III	Effect of doxorubicin on the affinity, cooperativity, and occupancy of [^3H]ryanodine binding sites	64
IV	Reversibility of doxorubicin-stimulated [^3H]ryanodine binding	66
V	Caffeine inhibition of doxorubicin-stimulated [^3H]ryanodine binding	68
VI	Kinetic analysis of doxorubicin-stimulated Ca^{2+} release	72
VII	TMPyP-induced Ca^{2+} release is irreversible .	124
VIII	Effect of 500 mM CsCl and temperature on binding constants of [^3H]ryanodine	136
IX	Association rate constants (k_{obs}) for [^3H]ryanodine binding in the presence of CsCl	138
X	Open probability, mean open time, and conductance of the Ca^{2+} release channel in the presence of 100 μM ryanodine ...	146

LIST OF FIGURES

FIGURE	PAGE
1. The internal membrane system of a skeletal muscle fiber	5
2. Electron micrograph showing striation pattern in skeletal muscle	6
3. Structure of quinones	46
4. Stepwise reduction of a simple quinone	47
5. Rate of Ca^{2+} release as a function of anthraquinone concentration	54
6. Inhibition of anthraquinone-induced Ca^{2+} release by Mg^{2+}	56
7. Rate of mitoxantrone-induced Ca^{2+} release as a function of free Ca^{2+} concentration ..	58
8. Phasic contractions of chemically skinned psoas muscle fibers triggered by mitoxantrone	61
9. Effect of doxorubicin on Ca^{2+} activation of [^3H]ryanodine binding in the presence of Mg^{2+} and Mg^{2+} -AMP-PCP	63
10. Daunorubicin-stimulated [^3H]ryanodine binding at 2 μM free Ca^{2+} and 1 mM free Mg^{2+} ...	65
11. Rate of daunorubicin-stimulated Ca^{2+} release as a function of caffeine concentration	69
12. Rate of Ca^{2+} release as a function of daunorubicin concentration in the absence and presence of caffeine	71
13. Rose bengal plus light activates the Ca^{2+} release channel	88

14.	The selectivity of the Ca^{2+} release channel is unaffected by rose bengal	89
15.	Activation of SR Ca^{2+} channels by rose bengal does not affect K^{+} channels	92
16.	Ca^{2+} dependence of rose bengal-induced Ca^{2+} release from skeletal muscle SR vesicles	94
17.	Activation of channel activity by rose bengal is side independent	95
18.	Displacement of [^3H]ryanodine from high- affinity receptor sites by rose bengal is light dependent	97
19.	Ryanodine modification of the Ca^{2+} release channel is reversed by rose bengal	98
20.	Rate of Ca^{2+} release as a function of TMP_YP concentration	108
21.	Rate of TMP_YP -induced Ca^{2+} release as a function of free Ca^{2+} concentration ...	109
22.	Rate of TMP_YP -induced Ca^{2+} release as a function of ATP concentration	111
23.	Rate of TMP_YP -induced Ca^{2+} release as a function of free Mg^{2+} concentration ...	112
24.	Ca^{2+} release induced by TMP_YP is inhibited by nanomolar concentration of ruthenium red	113
25.	Ca^{2+} dependence of TMP_YP stimulated high- affinity [^3H]ryanodine binding	115
26.	The effect of AMP-PCP and caffeine on TMP_YP stimulated ryanodine binding	116
27.	TMP_YP stimulates ryanodine binding by altering K_d and B_{max}	118
28.	Ca^{2+} release channels of SR are activated in the presence of TMP_YP	120
29.	Open probability of a single channel as a function of the Ca^{2+} concentration	121
30.	Selectivity of the Ca^{2+} release channel is decreased by 1 mM Mg^{2+}	122

31.	Equilibrium binding of 0.5-5050 nM [³ H]ryanodine in the presence of 500 mM CsCl and 100 μ M CaCl ₂	133
32.	Scatchard analysis of specific binding in the range 0.5-5050 nM ryanodine	134
33.	Biphasic association rate of [³ H]ryanodine binding in the presence of 500 mM CsCl	137
34.	Nanomolar concentrations of ryanodine increase channel open time	140
35.	Nanomolar concentrations of ryanodine increase channel open time in a reversible manner	141
36.	Ryanodine produces both occasional and persistent 1/2 conductance fluctuations with increasing concentration	143
37.	Addition of 100 μ M ryanodine causes SR channels to fluctuation in both 1/2 and 1/4 subconducting states	145
38.	Current-voltage plot of control and ryanodine modified Cs ⁺ conducting Ca ²⁺ channel ...	147

INTRODUCTION

Contraction and relaxation of muscle is the means by which animals locomote, manipulate their environment, and control visceral function. The contractile state of muscle is determined by the intracellular free Ca^{2+} concentration.

The sarcoplasmic reticulum (SR) is a highly specialized, internal membrane system which dynamically controls the Ca^{2+} concentration of muscle cells. When stimulated, Ca^{2+} channels in the SR open and Ca^{2+} is released into the cytosol. This results in the rapid increase in the myoplasmic Ca^{2+} concentration and the initiation of contraction. Closure of the Ca^{2+} release channels allows the Mg^{2+} - Ca^{2+} ATPase, through the hydrolysis of ATP into ADP and P_i , to actively sequester Ca^{2+} against a concentration gradient into the SR lumen, lowering the free Ca^{2+} concentration and producing relaxation.

The focus of this thesis is the study of the mechanism of Ca^{2+} release from skeletal muscle sarcoplasmic reticulum.

MUSCLE AND CONTRACTION

Vertebrate muscle can be divided into two broad categories based on morphology. Striated muscle displays a

distinct banding pattern (or cross-striations) when viewed under a light microscope, while smooth muscle lacks these striations.

Skeletal muscle comprises the largest group of muscles found in the body. These striated muscles are primarily involved in locomotion, maintenance of posture, and heat production. They also account for over a quarter of the body's mass and a major part of its energy expenditure (Keynes *et al.*, 1991). Skeletal muscle can be further characterized depending on its response to stimulation. Fast twitch skeletal muscle fibers respond to stimulation by a rapid twitch, while slow twitch muscle fibers contract more slowly and maintain the contraction for a longer period of time.

Cardiac muscle is the specialized tissue found in the walls of the heart. Like skeletal muscle, it also is striated. When viewed under a microscope, cardiac muscle tissue is seen to form a branching network of uninucleate cells which connect to each other at their ends. The juncture between cells is bounded by intercalated disks, which serve to provide an electrically conductive pathway between the cells, as well as to allow them to pull on one another. However, while most skeletal muscle is under voluntary control, cardiac muscle functions involuntarily. Despite these differences, the histology of the two tissues is remarkably similar.

Smooth muscle is fundamentally different from either skeletal or cardiac muscle. The fact that it is non-striated serves to illustrate this point. While smooth muscle contains the same contractile machinery as striated muscle, its orientation and regulation are under different control. Smooth muscle function is not considered in this thesis.

Anatomy

Skeletal muscle is composed of a large number of multinucleate cells, termed muscle fibers. Aligned longitudinally in the direction of contraction, fibers run the entire length of the muscle. Skeletal muscle fibers range from 10-100 μm in diameter and can be up to 30 cm long (Aidley, 1989). Enclosing the muscle fiber is the sarcolemma, or cell membrane, to which a thin layer of connective tissue called the endomysium is attached. The endomysia of individual fibers are continuous with a larger sheet of connective tissue, the perimysium, which serves to bind many fibers into bundles. These perimysia enclosed bundles are further grouped together by an outer sheet of connective tissue, the epimysium, which surrounds the entire muscle. The perimysium and epimysium of skeletal muscle are continuous with the insertions and tendons which attach these muscles to the skeleton.

The organization of a striated muscle fiber, as reviewed by Peachy (1965), is shown in Figure 1. Grouped around the periphery, but contained within the sarcoplasm of

a skeletal muscle fiber are the nuclei and mitochondria. The bulk of the fiber consists of the myofibrils.

Myofibrils represent the contractile apparatus of muscle fibers. Each fiber contains a large number of myofibrils which lie next to each other and run the length of the cell. Myofibrils, individually, are 1-2 μm in diameter and show a characteristic banding pattern when fixed, stained, and viewed under a microscope. Within the fiber, the banding pattern on one myofibril is in transverse register with the banding pattern of adjacent myofibrils and leads to the large scale striation pattern seen in both skeletal and cardiac muscle tissue. This pattern, as seen by low power electron microscopy, is shown in Figure 2. The two main bands seen in this figure are the dark A band and the lighter I band. The dark line in the center of the A band is termed the M line and the dark line in the center of the I band is termed the Z line (see also Figure 1).

The structural basis of the striation pattern was obscure until Huxley and Hanson (1954) determined that myofibrils were composed of two interdigitating sets of filaments. The appearance of striations follows from the fact that there are both thick and thin filaments, called myofilaments. Thick filaments, composed of myosin, make up the bulk of the A band. These filaments are approximately 16 nm in diameter, 1.6 μm long and attach at their centers along the dark M line. Thin filaments, which make up the

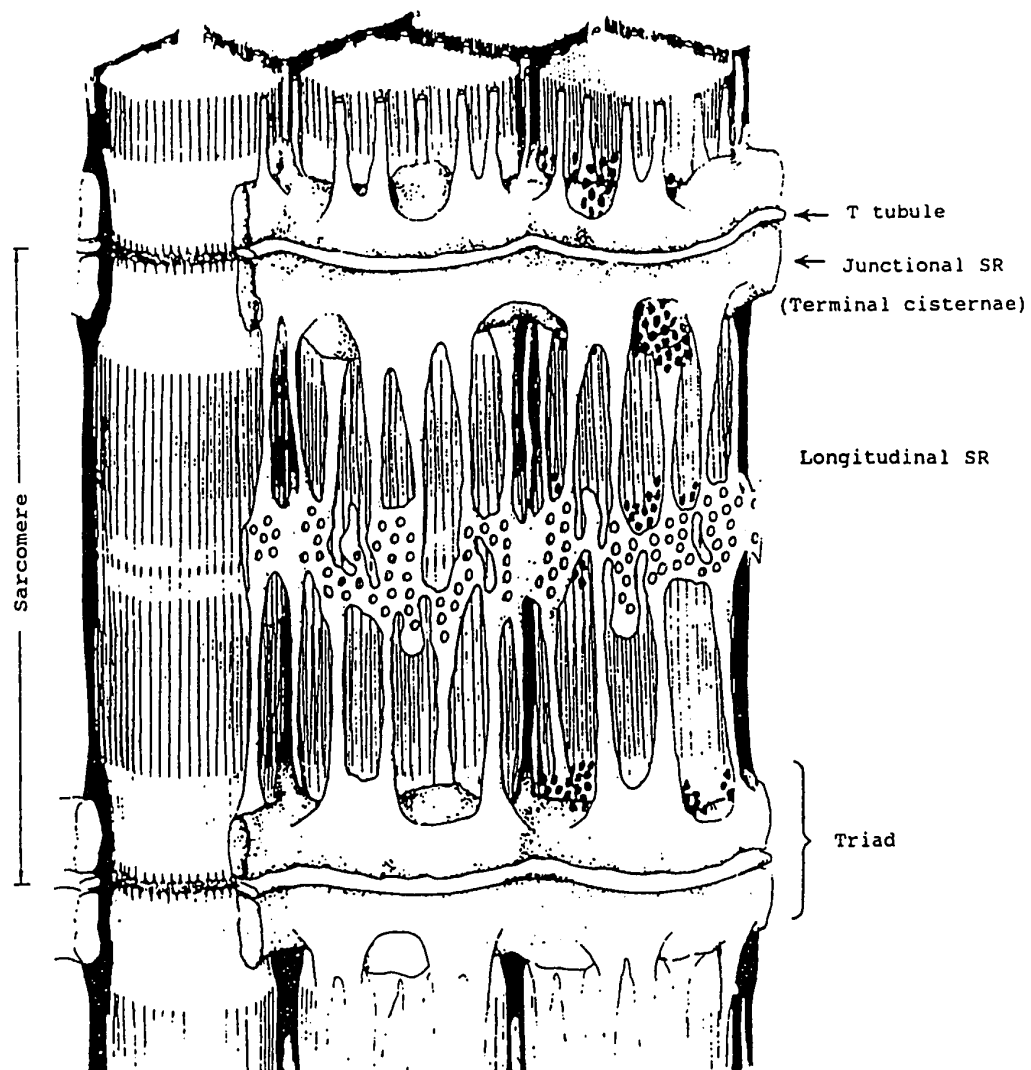


Figure 1. The internal membrane system of a skeletal muscle fiber. Reproduced from Peachy, 1965.

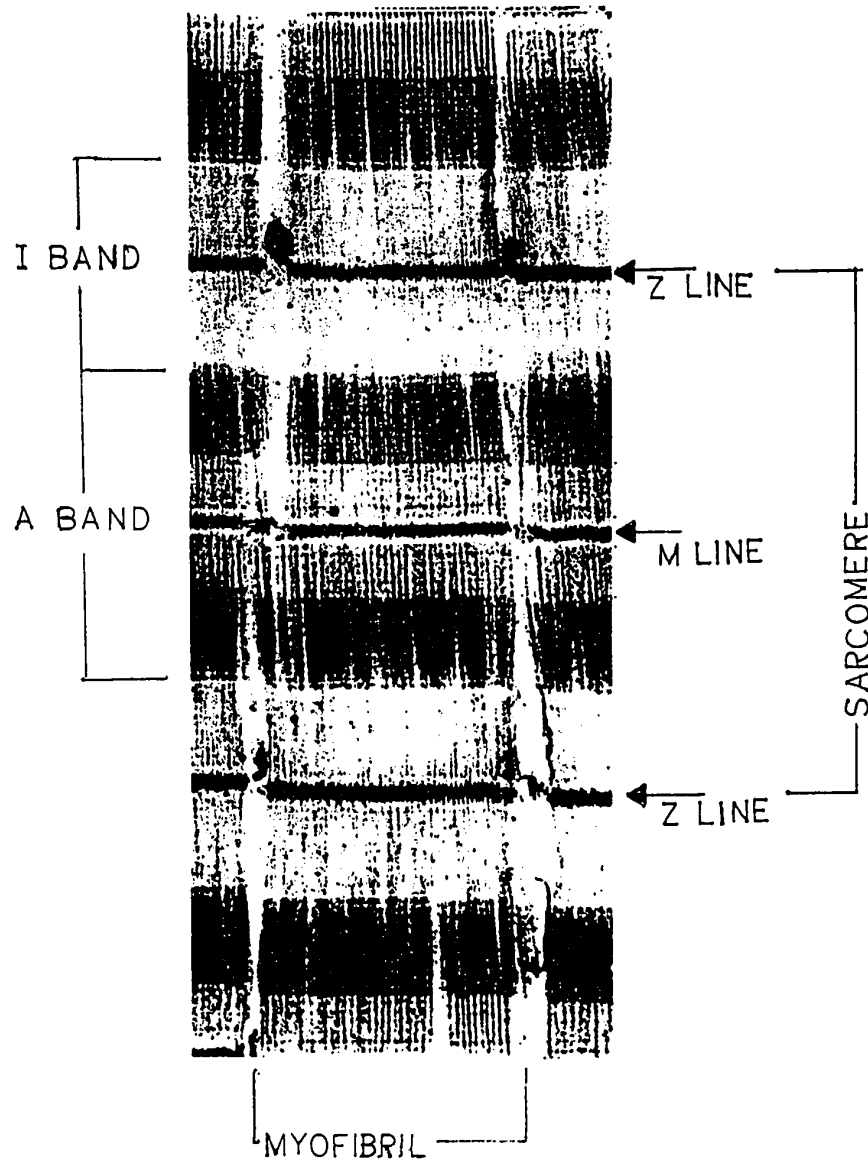


Figure 2. Electron micrograph showing striation pattern in skeletal muscle. Reproduced from Aidley, 1971.

bulk of the I band, are composed primarily of actin and are approximately 6 nm in diameter and 2.0 μm long. Actin filaments attach at their centers along the dark Z line. Since M lines and Z lines locate the centers of myosin and actin filaments, respectively, and since these lines alternate with each other along the length of the myofibril, then so do the regions where the two myofilaments interdigitate. The Z lines serve to define the boundary of a contractile unit which is repeated along the length of the myofibril. This repeating structure is called the sarcomere and represents the basic unit of contractile machinery in a muscle fiber.

Contraction

While it has long been known that depolarization of the sarcolemma stimulates a fiber to contract, the importance of Ca^{2+} in this process was only recently recognized. Niedergerke (1956) investigated the effect of Ca^{2+} on K^{+} induced contractions in heart muscle and found that contractures eventually failed in the absence of Ca^{2+} . Caldwell et al. (1963) developed a technique in which solutions were injected into muscle fibers. It was found that while injections of K^{+} , Na^{+} , Mg^{2+} , or ATP did not produce contraction, injections of small amounts of Ca^{2+} did. By injecting known quantities of Ca^{2+} and EGTA into skeletal muscle, Portzehl et al. (1964) determined that the threshold for contraction was 10^{-6} M. A further

demonstration of the involvement of Ca^{2+} in muscle contraction was performed by Ashley et al. (1970) in which aequorin, a bioluminescent protein which emits light in the presence of Ca^{2+} , was injected into muscle fibers. When the fibers were electrically depolarized, they produced a faint glow indicating the presence of Ca^{2+} .

The process by which Ca^{2+} interacts with the myofibrils to produce contraction has been worked out in great detail and is embodied in the sliding filament model of contraction. This model, proposed independently by H.E. Huxley and J. Hanson (1954) and A.F. Huxley and R. Niedergerke (1954), accounts for the observation that during contraction myofilaments are seen to move past each other with no change in filament length.

The biophysical basis of this model rests on the idea that filament motion is achieved through a cyclic, ratchet-like formation and breakage of cross bridges which extend from the myosin filaments to active sites on the actin filaments. In resting muscle (i.e. low Ca^{2+}), contraction is physically inhibited by tropomyosin, a component of the actin filaments. Tropomyosin's position shields actin's active site from the myosin heads of the cross bridges, sterically blocking the interaction of the two myofilaments. Bound to tropomyosin is troponin, a regulatory protein which binds Ca^{2+} in a concentration dependent manner. The formation of a Ca^{2+} -troponin complex induces tropomyosin to

shift its position, which exposes actin's active site. Thus, the inhibition of cross bridge formation is removed and contraction ensues.

SARCOPLASMIC RETICULUM

The sarcoplasmic reticulum (SR) was first identified in electron micrographs by Bennet *et al.* (1953) using chicken breast muscle. They showed that within the sarcoplasm and between the myofibrils, there is a reticular membrane system which is distributed in repeating units related to the sarcomeres of the myofibrils. This observation was repeated and amplified by other researchers and by the late 50's the major structures of the SR were described (for review, see Porter *et al.*, 1961). These structures include the longitudinal SR and terminal cisternae, which can be seen as a single membrane system spanning the length of a sarcomere, and a closely associated membrane system called the transverse tubules.

Longitudinal SR

Longitudinal SR (LSR) appears as a network of tubules which surround the body of the sarcomere (Franzini-Armstrong, 1970). LSR has been isolated and characterized (Meissner, 1975). It was found that LSR contains 90% of the total concentration of the Mg^{2+} Ca^{2+} ATPase found in the SR membrane. Based on density gradient sedimentation profiles, longitudinal SR is also frequently called light SR (LSR).

Terminal SR

In electron micrographs, the membrane system called the terminal cisternae (TSR) appears as large dilated sacs into which the LSR tubules connect. These sacs are formed at the ends of the LSR network, near the Z lines which mark the sarcomere boundary. While TSR was found to accumulate Ca^{2+} in a similar manner as LSR, it was also capable of releasing the stored Ca^{2+} when placed into a medium with a low Ca^{2+} concentration (Meissner, 1975). In addition, it was observed that TSR contained a large number of non-specific Ca^{2+} binding sites which LSR lacked. Based on density gradient sedimentation profiles, terminal SR is also frequently called heavy SR (HSR).

A number of electron microscopists have reported the presence of a delicate meshwork of granular particles seen to fill the TSR compartment (Revel, 1962; Peachey, 1965; Pellegrino et al., 1969; Franzini-Armstrong, 1970, 1987). This meshwork has also been seen in TSR vesicles (Meissner, 1975). Since SR accumulates large quantities of Ca^{2+} , it was proposed that there may be a protein component in the interior of the SR which would bind Ca^{2+} with low affinity (Weber, 1966). The discovery of a Ca^{2+} binding protein, called calsequestrin (MacLennan et al., 1971), in the SR lumen led to the conclusion that the meshwork seen by the electron microscopists was, in fact, calsequestrin. It thus appears that LSR is primarily involved with Ca^{2+}

accumulation, while TSR performs the function of Ca^{2+} storage and release.

Transverse Tubules and Triads

When viewed with the electron microscope there appears at the position of the Z lines in frog muscle, or at the boundary of the A-I band in other striated muscle, a structure in which a central element is situated in close apposition to the two terminal cisternae of the adjacent sarcomeres. In favorable micrographs, it can be seen that this central element is a portion of a tubule system which is continuous with the sarcolemma and extends across the entire fiber (Franzini-Armstrong et al., 1964). The orientation of these tubules is perpendicular to the axis of the muscle fiber, and so they have come to be known as transverse tubules, or t-tubules. This repeating structure of TSR/t-tubule/TSR, first identified by Porter et al. (1957), are termed triads. The function of the t-tubule was addressed by Huxley et al. (1955) where by locally depolarizing a myofibril at the location of a Z line, a contraction could be induced in the adjacent sarcomere without stimulating the whole fiber. This observation, coupled with the identification of the triads by Porter, lead researchers to the conclusion that the t-tubules serve to communicate the depolarization of the sarcolemma to the triads.

Franzini-Armstrong (1970) made a detailed study of triads from frog muscle. From electron micrographs it was determined that the TSR and t-tubule membranes are not in direct physical contact, but are separated by a distance of 120-140 Å. This separation is maintained by two parallel rows of evenly spaced projections of the SR, termed SR feet. Less dense projections associated with the t-tubule membrane were also observed. These projections appeared to be in contact with the feet structures. Since these projections provide the only physical connection between the t-tubule and TSR, many investigators believe they play a central role in the coupling of the two membranes. While this issue is approaching resolution, the complete function of SR feet has remained unresolved.

Pharmacology of SR Ca^{2+} Release

Many compounds have been found to modulate the flux of Ca^{2+} from SR vesicles. These modulators either inhibit or stimulate Ca^{2+} release. The most common of these compounds are listed in Table I.

Inhibitors of Ca^{2+} Release. Compounds which inhibit the release of Ca^{2+} from the SR can play an important diagnostic role in the study of the Ca^{2+} release system. For example, two inhibitors of Ca^{2+} release, ruthenium red and Mg^{2+} , are presumed to act directly on the release channel. Thus, any method of inducing Ca^{2+} release which is inhibited by these compounds is presumed to activate the Ca^{2+} release system.

Ruthenium red has been shown to inhibit Ca^{2+} uptake by mitochondria (Moore et al., 1977), to inhibit the Ca^{2+} release mechanism of isolated SR vesicles (Ohnishi, 1979; Meissner et al., 1986; Salama et al., 1984; Trimm et al., 1986), and to abolish the gating of single channels in the bilayer lipid membrane (BLM) (Smith et al., 1985). This powerful inhibitor of Ca^{2+} release is effective at concentrations of less than 5 μM .

Mg^{2+} has long been known to inhibit muscle fiber contraction (Ford et al., 1970; Endo, 1970). It has also been shown to inhibit Ca^{2+} release from isolated SR vesicles (Fairhurst et al., 1970; Ohnishi, 1979; Meissner et al., 1986) and to modulate the gating of single channels (Smith et al., 1986). Mg^{2+} inhibits Ca^{2+} release in SR vesicles at concentrations of less than 5 mM. It is a less effective inhibitor than ruthenium red, but is more physiologically relevant since it occurs naturally in the cell. The physiological Mg^{2+} concentration in muscle cells is generally accepted to be 0.6 to 1.0 mM.

Stimulators of Ca^{2+} Release. There are a large number of compounds which stimulate the release of Ca^{2+} from SR. These activators include caffeine, heavy metals, sulfhydryl oxidizing agents, adenine nucleotides, and Ca^{2+} .

Caffeine activates muscle fiber contraction (Howell, 1969; Endo, 1975) and stimulates Ca^{2+} release from SR vesicles (Fairhurst et al., 1970; Ohnishi, 1979). It is

often used for standardizing the results of muscle fiber studies because of its ability to directly induce Ca^{2+} release without affecting other components of the fibers (Howell, 1969; Endo, 1975).

Heavy metals, in particular Hg^{2+} and Ag^+ , stimulate rapid Ca^{2+} release from isolated SR vesicles (Abramson et al., 1983; Salama et al., 1984) and induce contractions in muscle fibers (Oba et al., 1984). The site of action of heavy metals appears to be a sulfhydryl group. Heavy metal-stimulated Ca^{2+} release is inhibited by all known inhibitors of Ca^{2+} release and hence appears to involve a direct interaction with the Ca^{2+} release system (Salama et al., 1984).

Compounds which contain adenine nucleotide, such as ATP, cAMP, and the non-hydrolyzable analogues of ATP, are known to stimulate Ca^{2+} -induced Ca^{2+} release (Meissner, 1986), heavy metal-induced Ca^{2+} release (Abramson et al., 1983; Salama et al., 1984), sulfhydryl oxidation-induced Ca^{2+} release (Trimm et al., 1986), and ryanodine-stimulated Ca^{2+} release (Pessah et al., 1987).

Ca^{2+} is unique among the activators in that it has a biphasic effect on the Ca^{2+} release system of skeletal muscle. Ca^{2+} induces a concentration dependent stimulation of Ca^{2+} release at free Ca^{2+} concentrations of less than 1 μM . Concentrations greater than 1 mM are inhibitory to the Ca^{2+} release system.

TABLE I
MODULATORS OF Ca^{2+} RELEASE FROM SR VESICLES

Stimulators	Effective Concentration	Inhibitors	Effective Concentration
Ca^{2+}	> 1 μM	Ca^{2+}	> 1 mM
Adenine		Mg^{2+}	> 2 mM
nucleotides	1-5 mM	Ruthenium	
Caffeine	> 0.5 mM	red	< 5 μM
Ag^+	15 μM	Procaine	10 μM
Cu^{2+} /cysteine	2-10 μM	Tetracaine	0.6 μM
Ryanodine	< 200 μM	Ryanodine	> 200 μM

EXCITATION-CONTRACTION COUPLING

The term excitation-contraction (EC) coupling was initially developed to describe the causal relationship between depolarization of the sarcolemma and the resulting fiber contraction. More recently, however, it has come to refer to the unknown connection between depolarization of a t-tubule membrane and the subsequent release of Ca^{2+} from the associated SR (Numa et al., 1990).

Since the t-tubule and SR membranes are maintained separate by the SR feet, several hypotheses have been developed to explain how depolarization of the t-tubule is communicated to the Ca^{2+} release channels of the SR. These include (1) an electrical coupling, (2) a mechanical coupling, (3) a chemical coupling, or (4) some combination of the above. A number of theories are discussed below.

Depolarization-induced Release

The notion that depolarization of the SR is a first step in the release of Ca^{2+} is an attractive hypothesis. Since depolarization of the t-tubule leads to Ca^{2+} release and since the t-tubule is in close apposition to the SR, it is possible that the SR is also depolarized. Franzini-Armstrong (1971) addressed the question of depolarization-induced release in studies of the triad and concluded that the separation between the two membrane systems is too large to provide an efficient capacitive coupling between them. Additionally, several investigators have attempted to directly depolarize SR vesicles by rapidly altering their ionic conditions. Meissner (1976) and Ikemoto et al. (1984) performed depolarization experiments in which the ionic conditions were changed while minimizing any effects due to osmotic shock. No Ca^{2+} release was observed. In a different approach, Fabiato (1985b) used a variety of electrical techniques to stimulate the SR of skinned fibers while measuring potential changes in the interior of these fibers. Chemical stimulation of SR Ca^{2+} release yielded no changes in potential, nor did direct electrical stimulation of the SR activate Ca^{2+} release. Finally, Meissner (1976) determined that the permeability of the SR membrane to K^+ and Cl^- was too large to allow any transport system to develop a significant membrane potential. It would seem, then, that the coupling between the SR and t-tubule is not electrical and this hypothesis has fallen into disfavor.

Mechanical Coupling-induced Release

The model of mechanical coupling between the t-tubule and SR membranes was originally proposed by Schneider and Chandler (1973). This hypothesis is attractive because the membranes are physically connected via the SR feet.

Schneider and Chandler (1973) observed a voltage-dependent intramembrane charge movement located within the t-tubule membrane. Based on the magnitude of the current produced by the motion of these charges, Schneider and Chandler (1973) calculated the density of charged groups to be roughly equal to the density of SR feet proteins as described by Franzini-Armstrong (1970). Since Ca^{2+} release from the SR is preceded by depolarization of the t-tubule, they proposed that the charged groups may be mechanically linked, via the feet, to the activation mechanisms of the Ca^{2+} channels of the SR.

While the Schneider-Chandler model has never been directly tested, recent work has lent support to the hypothesis that a direct mechanical connection between the two membranes may be important in signalling Ca^{2+} release. For example, there has been some evidence for the presence of voltage gated channels in the SR (Hals et al., 1989). In addition, a protein called triadin has recently been isolated and characterized which appears to bind to both the SR foot protein and the t-tubule voltage sensor (Caswell et al., 1991).

Chemical Coupling-induced Release

An alternative interpretation of the Schneider and Chandler (1973) data is that the voltage-dependent charge movement is coupled to the release of a chemical transmitter which diffuses across the gap between the two membranes, binds to activating sites on the SR, and stimulates Ca^{2+} release. This hypothesis, which can be called the chemical-transmitter model, is supported by the fact that a large number of ligands affect the opening and closing of Ca^{2+} release channels. Since the gap between the two membranes is on the order of 140 Å, the diffusion of a small molecule or ion from one side to the other would take only a few tens of microseconds (Franzini-Armstrong, 1971). This is a small fraction of the total time involved in EC coupling. Possible mechanisms of chemical-transmitter induced release include Ca^{2+} -induced Ca^{2+} release, IP_3 -induced Ca^{2+} release, and sulfhydryl oxidation-induced Ca^{2+} release.

Ca^{2+} -induced Ca^{2+} Release. The process termed Ca^{2+} -induced Ca^{2+} release was initially observed in skinned muscle fibers (Ford et al., 1970; Endo et al., 1970). Using fibers preloaded with 10^{-6} M Ca^{2+} , the addition of 10^{-4} M Ca^{2+} induced a rapid, transient contraction which was larger in magnitude than could be explained by the added Ca^{2+} alone. Subsequent work confirmed that the additional Ca^{2+} was released from internal stores during the contraction process (Ford et al., 1972).

Briefly, the proposed mechanism of Ca^{2+} -induced Ca^{2+} release is as follows: The concentration of free Ca^{2+} within the lumen of the t-tubules is greater than 10^{-6} M, while the cytoplasmic Ca^{2+} concentration in resting muscle is maintained below 10^{-7} M. T-tubule depolarization triggers the opening of the Ca^{2+} selective channels of the t-tubule, allowing Ca^{2+} to enter the gap between the two membranes. This Ca^{2+} then diffuses to the TSR membrane, where it binds to Ca^{2+} receptors and stimulates the subsequent rapid release of Ca^{2+} from the SR.

In support of the Ca^{2+} -induced Ca^{2+} release hypothesis is the discovery of voltage-dependent dihydropyridine-sensitive (DHPR) Ca^{2+} channels in the t-tubule membrane (for review see Bean et al., 1989). These DHPR channels have been shown to also be the source of the charge movement identified by Schneider and Chandler (1973). Therefore, there is a t-tubule membrane bound protein which acts both as a voltage sensor and a source of cytoplasmic Ca^{2+} . This, coupled with the observation that the permeability of SR vesicles (Meissner et al., 1986) and the gating activity of single Ca^{2+} release channels (Smith et al., 1985) are strongly Ca^{2+} dependent lends support for the existence of a Ca^{2+} -induced Ca^{2+} release mechanism.

The mechanism of Ca^{2+} -induced Ca^{2+} release has been well-documented in cardiac muscle and is believed to be the method by which contraction is induced in this muscle (for

review, see Fabiato, 1983). The role of Ca^{2+} -induced Ca^{2+} release as the physiological Ca^{2+} release mechanism of skeletal muscle has remained controversial (Martinosi, 1984; Costantin, 1975).

IP_3 -induced Ca^{2+} Release. Inositol 1,4,5-trisphosphate (IP_3) is an intracellular second messenger which has been shown to trigger Ca^{2+} release from the endoplasmic reticulum of several tissues (Berridge et al., 1984). Since the SR membrane is derived from the endoplasmic reticulum (MacLennan, 1986), researchers have investigated the Ca^{2+} releasing properties of IP_3 on SR. There have been several reports which claim that IP_3 induces Ca^{2+} release in smooth muscle, cardiac muscle, and skeletal muscle (Suematsu, 1984; Watras, 1987, 1989; Hirata et al., 1984; Volpe et al., 1985; Vergara et al., 1985; Hasegawa et al., 1989).

The proposed mechanism of IP_3 -induced Ca^{2+} release is similar to that of Ca^{2+} -induced Ca^{2+} release in that depolarization of the t-tubule triggers the production of IP_3 which diffuses to the SR, binds to a receptor, and stimulates Ca^{2+} release from the SR. This hypothesis is supported by the observation that an enzyme responsible for the breakdown of IP_3 , IP_3 -5 phosphatase, has been found in the SR (Vergara et al., 1985).

While it is generally accepted that IP_3 is the signal which leads to Ca^{2+} release in smooth muscle (for review, see Garcia et al., 1990), IP_3 has remained controversial as

the mechanism of Ca^{2+} release in either cardiac or skeletal muscle. Specifically, the results obtained with skeletal muscle have been disputed. Several investigators have published reports which claim that IP_3 does not induce Ca^{2+} release from either SR vesicles, or from skeletal muscle Ca^{2+} release channels expressed from cDNA (Scherer *et al.*, 1985; Mikos *et al.*, 1987; Pessah *et al.*, 1987; Penner *et al.*, 1989). In addition, many researchers argue that the conditions which favor IP_3 -induced Ca^{2+} release in skeletal muscle are not physiological. Chu *et al.*, (1991) and Suares-Isla *et al.*, (1991) recently published reports using isolated SR Ca^{2+} channels in a bilayer lipid membrane (BLM) in which they were only able to achieve IP_3 -induced Ca^{2+} release at Ca^{2+} concentrations of less than 10^{-7} M. When the Ca^{2+} concentration was increased, IP_3 -induced Ca^{2+} release was inhibited.

Sulfhydryl Oxidation-induced Ca^{2+} Release. Much of the work performed in the Abramson laboratory over the last ten years has focused on a mechanism of Ca^{2+} release which involves the oxidation of critical sulfhydryls on the SR.

Interest in sulfhydryl oxidation-induced Ca^{2+} release initially stemmed from the observation that micromolar concentrations of heavy metals (Hg^{2+} , Cu^{2+} , Ag^+ and Cd^{2+}) stimulated rapid Ca^{2+} release from SR vesicles (Abramson *et al.*, 1983). It was found that the Ca^{2+} releasing potency of these metals paralleled their binding affinity to sulfhydryl

(SH) groups. Activation of the Ca^{2+} release system by heavy metals was verified by testing the effect of known modulators of Ca^{2+} release on heavy metal-induced release. Abramson et al. (1983) showed that Ag^{+} -induced Ca^{2+} release was modulated by inhibitors and activators of Ca^{2+} release in a manner which paralleled modulation of other methods of Ca^{2+} release with the single exception that Ag^{+} -induced Ca^{2+} release occurred at physiological Mg^{2+} concentrations (Salama et al., 1984).

Recognizing that Ca^{2+} release induced by heavy metals probably has no physiological basis, the authors suggested that the effect of heavy metals was to implicate a role for sulfhydryl oxidation in the Ca^{2+} release process. Further demonstration of the involvement of sulfhydryls in Ca^{2+} release came from a study by Trimm et al. (1986), in which it was shown that the Cu^{2+} catalyzed oxidation of mercaptans induced a dramatic increase in the Ca^{2+} permeability of SR vesicles. It was found that the rate of Ca^{2+} release paralleled the rate of oxidation of the mercaptans and that the effect could be reversed by the addition of dithiothreitol (DTT), a reducing agent. As in the case of heavy metal-induced release, Cu^{2+} /mercaptan-induced release was also modulated by known inhibitors and activators of Ca^{2+} release.

Many other compounds known to participate in oxidation-reduction reactions have been shown to induce release of

Ca^{2+} from the SR. These include phthalocyanine dyes (Abramson et al., 1988), anthraquinones (Chapter III), rose bengal (Stuart et al., 1992; Chapter IV), and porphyrins (Chapter V). These results strongly suggest that the oxidation of critical sulfhydryls on the SR is involved in the regulation of Ca^{2+} release.

The sulfhydryl reactivity of the Ca^{2+} release channel has provided investigators with a means to isolate and purify a unique protein from SR membranes (Zaidi et al., 1989). By using biotin-avidin chromatography, a 106 kDa protein was isolated and characterized. When incorporated into a BLM this isolated protein was found to be inhibited by ruthenium red and Mg^{2+} and to have a similar Ca^{2+} conductance (107 pS) and selectivity ($P_{\text{Ca}^{2+}}/P_{\text{Tris}} = 7.4$) to the native channel (Xiong, 1990).

RYANODINE RECEPTOR

Ryanodine is a neutral alkaloid isolated from the stems of the plant *Ryania speciosa* Vahl. Initially used as an insecticide, it was shown to have profound effects on muscle from both vertebrates and invertebrates. In vertebrates, these effects include irreversible contracture in skeletal muscle and a negative inotropic effect on cardiac muscle.

Fairhurst and Jenden (1966) showed that high concentrations of ryanodine stimulated the uptake of Ca^{2+} into SR of skeletal muscle. Sutko et al. (1985) proposed

that this stimulation was due to an increased efficiency of the pump due to a decrease in the Ca^{2+} permeability of the SR. Using radiolabeled ryanodine, Pessah et al. (1985) demonstrated that under appropriate conditions ryanodine remained tightly bound, with nanomolar affinity, to a single class of receptor sites on the SR. The observation that high-affinity ryanodine binding occurred only in the TSR (Pessah et al., 1986; Campbell et al., 1987), and that this binding had all the ligand binding pharmacology of the Ca^{2+} release channel (Pessah et al., 1985, 1986), strongly indicated that ryanodine was acting on the Ca^{2+} release site.

The ability to radiolabel the ryanodine receptor allowed for the identification and isolation of a membrane bound protein from muscle homogenates by a number of investigators (Imagawa et al., 1987; Lai et al., 1988a,b; Smith et al., 1988; Rardon et al., 1989). When this purified 450 kDa protein was inserted into a BLM and monitored, it demonstrated Ca^{2+} selective channels with similar conductance as native Ca^{2+} release channels (Smith et al., 1988). In addition, these channels were inhibited by micromolar concentrations of ruthenium red and millimolar concentrations of Mg^{2+} . The large molecular weight of this protein and its apparent localization to TSR lead investigators to compare the morphological characteristics of the purified protein with that of the feet structures as

identified by Franzini-Armstrong (1971). Electron micrographs showed that the isolated protein appeared as tetrameric structures which were similar in appearance to the SR feet (Inui et al., 1987a,b).

SR vesicles incorporated into a BLM exhibit a rapidly fluctuating, full conductance Ca^{2+} channel in the presence of μM Ca^{2+} . When this channel behavior is monitored in the presence of ryanodine, it is observed that low micromolar concentrations of ryanodine induce the Ca^{2+} channel to undergo slow transitions of 1/2 the normal channel conductance. In contrast, millimolar concentrations of ryanodine close the channel entirely.

The pharmacology of the ryanodine receptor suggests that the alkaloid interacts directly with the Ca^{2+} release channels. Ryanodine binding is stimulated in the presence of adenine nucleotides, caffeine, Ca^{2+} , and all other known activators of Ca^{2+} channel activity. Ryanodine binding is also inhibited by Mg^{2+} and ruthenium red, both inhibitors of channel activity. Investigators have come to believe that the effect of channel activators and inhibitors on ryanodine binding reflects the fact that ryanodine binds only when the channel is in an open configuration.

Based on the above observations, many researchers have concluded that the feet structures, the ryanodine receptor, and the Ca^{2+} release channel are synonymous. However, this conclusion remains controversial. Procedures designed to

purify the 450 kDa protein appear to copurify a 106 kDa protein (Abramson, unpublished observation). In addition, the 106 kDa protein has been shown to have many of the characteristics of the Ca^{2+} release channel when isolated and inserted into a BLM (Xiong, 1990). It is unresolved if some of the effects credited to the 450 kDa protein are, instead, artifacts introduced by a contaminating presence of the 106 kDa protein. Alternatively, both proteins may be associated in a required functional complex in order to reconstitute the Ca^{2+} release channel.

OVERVIEW OF THE DISSERTATION

The focus of this dissertation is twofold. The first objective is to gain an understanding of the mechanism of Ca^{2+} release from the SR. To this end, three separate studies have been performed which indicate that Ca^{2+} release is mediated by an oxidation reaction. The second goal is to gain insight into the function of the Ca^{2+} release channel. This is addressed by a fourth study which characterizes the effect of the plant alkaloid, ryanodine, on channel operation.

Oxidation-induced Ca^{2+} Release

Three studies examining oxidation-induced Ca^{2+} release were performed with three classes of compounds known to participate in oxidation-reduction reactions. These studies were motivated from, and are extensions of, work performed

by our group which indicates that oxidation of a critical sulfhydryl is involved in SR Ca^{2+} release. The compounds studied here include anthraquinones (Chapter III), rose bengal (Chapter IV), and porphyrins (Chapter V).

Anthraquinone-induced Ca^{2+} Release. The anthraquinones doxorubicin, mitoxantrone, daunorubicin and rubidazole are shown to be potent stimulators of Ca^{2+} release from skeletal muscle SR vesicles.

The effect of anthraquinones is shown to be specific for the Ca^{2+} release system of the SR. Ca^{2+} release by anthraquinones is inhibited by mM Mg^{2+} and μM ruthenium red, and enhanced by adenine nucleotides. This study also shows that channel activation by doxorubicin and daunorubicin exhibits a sharp dependence on the Ca^{2+} concentration in the presence of adenine nucleotides and at physiological Mg^{2+} concentrations.

A strong interaction between the anthraquinone and caffeine binding sites on the Ca^{2+} release channel is observed when monitoring Ca^{2+} fluxes across the SR. Millimolar caffeine both inhibits anthraquinone-stimulated Ca^{2+} release and reduces anthraquinone-stimulated [^3H]ryanodine binding without altering the affinity of anthraquinone for its binding site.

Quinones, which occur frequently in biological systems, are known to play a role in oxidation-reduction reactions. Results presented here show that Ca^{2+} release stimulated by

anthraquinones is inhibited by preincubating the quinone with dithionite, a strong reducing agent. Spectrophotometric measurements show that the dithionite treated quinone is in a reduced state.

Rose Bengal-induced Ca^{2+} Release. Previous work in this lab has shown that the photooxidizing xanthene dye rose bengal stimulates rapid Ca^{2+} release from skeletal muscle SR vesicles. This thesis shows that following fusion of vesicles to a BLM, Ca^{2+} channel activity is stimulated by nanomolar concentrations of rose bengal in the presence of a broad-spectrum light source.

Interestingly, this stimulation is found to be independent of the Ca^{2+} concentration but is inhibited by μM ruthenium red. Also, photooxidation of rose bengal is shown to not affect either the K^+ or Cl^- channels which are present in the SR.

Ryanodine at a concentration of $10 \mu\text{M}$ is known to alter the gating characteristics of the Ca^{2+} release channel (Smith et. al., 1988). The addition of 500 nM rose bengal in the presence of light is shown to reverse the effect induced by μM ryanodine. This apparent displacement of bound ryanodine by nanomolar concentrations of rose bengal is directly observed upon measurement of [^3H]ryanodine binding to TSR vesicles.

These observations indicate that photooxidation of rose bengal causes a stimulation of the Ca^{2+} release protein from

skeletal muscle SR by interacting with the ryanodine binding site.

Porphyrim-induced Ca^{2+} Release. Micromolar concentrations of the porphyrin meso-Tetra(4-N-methylpyridyl)porphine tetraiodide (TMPyP) is shown to induce the rapid release of Ca^{2+} from skeletal muscle SR vesicles. This porphyrin-induced Ca^{2+} release is stimulated by adenine nucleotides and μM Ca^{2+} , and is inhibited by mM Mg^{2+} and μM ruthenium red. High-affinity [^3H]ryanodine binding is also enhanced in the presence of the porphyrin. The presence of 1 mM Mg^{2+} in the assay medium sensitizes ryanodine binding to activation by Ca^{2+} . Porphyrin stimulated single channel activity is also sensitized to activation by Ca^{2+} in the presence of Mg^{2+} .

These observations show that porphyrin induces Ca^{2+} release via a direct interaction with the Ca^{2+} release protein from SR.

Ryanodine Stabilized Conformational States of the SR Calcium Release Channel

Nanomolar to micromolar concentrations of ryanodine are shown to alter the gating kinetics of the Ca^{2+} release channel from skeletal muscle SR fused with bilayer lipid membranes.

In the presence of asymmetric CsCl , 5 to 40 nM concentrations of ryanodine are shown to activate the channel by increasing the open probability (P_o) without

changing the conductance. Statistical analysis of gating kinetics reveal that the open and closed dwell times exhibit bi-exponential distributions that are significantly modified by nM ryanodine. The altered channel gating kinetics seen with low nM ryanodine is reversible and is shown to correlate with the binding kinetics of [^3H]ryanodine with its highest affinity site under identical ionic conditions.

Ryanodine concentrations between 20 and 50 nM are observed to induce occasional 1/2 conductance fluctuations while ryanodine concentrations greater than 50 nM stabilize the channel into a 1/2 conductance state which is not reversible. These results are shown to correlate with [^3H]ryanodine binding to a second site having lower affinity than the first site.

Ryanodine at concentrations greater than 70 μM are shown to produce a unidirectional transition from the 1/2 to a 1/4 conductance fluctuation, whereas ryanodine concentrations greater than 200 μM cause complete closure of the channel. The concentration of ryanodine required to stabilize either the 1/4 conductance transitions or channel closure do not directly correlate with the measured [^3H]ryanodine equilibrium binding constants. However, these results can be explained by considering the association kinetics of ryanodine concentrations greater than 200 nM in the presence of 500 mM CsCl.

These results indicate that ryanodine stabilizes four discrete states of the SR release channel and supports the existence of multiple interacting ryanodine binding sites on the channel protein.

GENERAL METHODS

INTRODUCTION

A number of biophysical and biochemical techniques have been used to accumulate the data presented in Chapters III through VI. While much of the methodology is common to all chapters, there are also techniques which are specific to the goals of the associated study. This chapter reviews only those techniques which are common to all studies. Specific techniques will be reviewed in an appropriate methods section within each chapter.

METHODS

Isolation of Sarcoplasmic Reticulum

Preparation of SR Vesicles. For all studies, rabbit skeletal muscle sarcoplasmic reticulum vesicles were prepared according to the method of MacLennan et al. (1970). A 2 to 3 kg New Zealand White rabbit was anesthetized with 3 ml pentobarbitol, injected interthoracically. The animal was then bled by cutting the jugular vein. The back and hind leg muscles were quickly removed and put on ice. The muscles were then trimmed of connective tissue and fat, diced, and placed into 1500 ml of ice-cold buffer A (120 mM NaCl, 10 mM imidazole, 100 μ M dithiothreitol, pH 7.4). The muscle tissue

was homogenized with an Omnimixer (Omni Int., Waterbury CT) until the homogenate had an even, smooth consistency and connective tissue was no longer trapped by the blades. The resulting suspension was centrifuged for 10 minutes at 1,600 x g (3,100 rpm in the large Sorval GSA rotor) to sediment the connective tissue and muscle debris. The supernatant liquid was separated, strained through four layers of cheesecloth, and the pH adjusted to 7.4 with dry imidazole. The supernatant liquid was then centrifuged for 15 minutes at 10,000 x g (8000 rpm in the large Sorval GSA rotor). The resulting supernatant liquid was again strained through four layers of cheesecloth and the brown mitochondrial pellet discarded. The fluid collected was then centrifuged for 70 minutes at 44,000 x g (19,000 rpm in the Ti19 rotor). The clear supernatant liquid was carefully pipetted off and discarded. The portion of the pellet above the brown mitochondrial ring was carefully removed and re-suspended in buffer A to a final concentration of approximately 10 mg/ml with a Wheaton tissue homogenizer. The pH was again adjusted to 7.4 with dry imidazole and the suspension was centrifuged for 10 minutes at 7,500 x g (11,000 rpm in the Ti60 rotor). The supernatant liquid was carefully pipetted off and kept. Care was taken to not disturb the remaining large flocculent myosin pellet (which is discarded). The supernatant liquid was centrifuged for 70 minutes at 78,000 x g (35,000 rpm in the Ti60 rotor). The resulting pellet contains SR. The

supernatant liquid was discarded and the pellet re-suspended at approximately 25 mg/ml (approximately 15 ml final volume) in 100 mM KCl, 20 mM Hepes-Tris, pH 7.0. The SR was stored frozen at -70°C until needed.

Preparation of Light and Heavy SR Vesicles. SR vesicles prepared by the method of MacLennan, as described above, were further fractionated into light and heavy SR components on a 29-45% (w/w) discontinuous sucrose gradient. This protocol consists of 1) preparation of a 45% (w/w) stock sucrose solution, 2) removal of any trace metals in this stock solution, and finally 3) formation of the gradient and fractionation of the SR. These procedures are described below.

700 ml of a 45% (w/w) sucrose stock solution was prepared by dissolving 378.9 g ultrapure sucrose into 650 ml of a 10 mM Hepes-Tris, pH 7.0 solution and then adjusting the final volume to 700 ml.

Prior to use, the sucrose solution to be used in the gradient was subjected to an ion-exchange protocol in order to remove any trace metal contamination. A coarse grade (50-100 mesh) Chelex-100 ion-exchange column was prepared in the following manner: Chelex-100 (Bio-Rad) ion-exchange beads were suspended in approximately 500 ml of a 10 mM Hepes-Tris, pH 7.0 solution. The mixture was stirred and the beads were allowed to settle. The excess Hepes solution was poured off and fresh solution was added. The above procedure was

repeated until the Chelex suspension stabilized at pH 7.0. A 2.5 x 75 cm glass chromatography column (Bio-Rad), which had been rinsed several times with dilute HCl and distilled water, was supported upright with a stand and partially filled with the Hepes solution. The Chelex/Hepes suspension was then slowly poured into the column and the beads allowed to settle until a bed of approximately 3-4 cm in thickness formed on the bottom. Excess solution was allowed to run through the column until the beads were covered by only a few millimeters of solution. Care was taken to keep the beads wet at all times. The sucrose solution was gently poured into the ion-exchange column and the beads allowed to settle. The column was opened and sucrose was allowed to slowly run through. The first 25 to 50 ml of solution removed from the column was discarded and the remaining trace metal free sucrose solution was collected in a beaker which had also been acid washed and rinsed thoroughly with 1 mM ethylene glycol bis(β -aminoethyl ether)*N,N'*-tetraacetic acid (EGTA). The flow rate of sucrose through the column was approximately 10 ml per minute.

The sucrose gradient was formed in the following manner. Using the density of sucrose solutions (CRC Handbook of Chemistry and Physics) as a guide, the stock solution was diluted with 10 mM Hepes-Tris buffer, pH 7.0 to the following percentages and volumes:

29%	(50 ml)	=	30.5 ml	45% sucrose	+	19.5 ml	buffer
30%	(90 ml)	=	57.0 ml	45% sucrose	+	33.0 ml	buffer
35%	(150 ml)	=	113.3 ml	45% sucrose	+	36.7 ml	buffer
38.5%	(90 ml)	=	75.6 ml	45% sucrose	+	14.4 ml	buffer
41%	(90 ml)	=	81.2 ml	45% sucrose	+	8.8 ml	buffer
45%	(130 ml)	=	130 ml	45% sucrose	+	0 ml	buffer

The density of each dilution was verified with an Abbe refractometer (Bausch & Lomb, Rochester NY). The volumes reported above are sufficient for two gradients.

Six sucrose gradient tubes (Beckman SW28 swinging-bucket rotor), using disposable polyallomer inserts, were allowed to chill in the cold room. The gradient was formed in each tube by carefully adding the following volumes of each solution in the order specified and in such a manner as to minimize the mixing between layers:

4 ml	of	45% sucrose
7 ml	of	41% sucrose
7 ml	of	38.5% sucrose
12 ml	of	35% sucrose
7 ml	of	30% sucrose
4 ml	of	29% sucrose

Finally, 2 ml of SR vesicles prepared as described in "Preparation of SR Vesicles" were placed on the top of each gradient. The tubes were placed into the buckets of a Beckman SW28 swinging-bucket rotor, balanced, and placed on the rotor head. The SR/sucrose gradient was then centrifuged for 12 h at 22,000 rpm (Beckman Analytical Centrifuge L-2B) at 4°C. The centrifuge was allowed to stop without braking to avoid mixing. Fractions from the 38.5-41% sucrose step contained the SR component identified as 'heavy' SR (TSR),

while fractions from the 29-30% interface contain 'light' SR (LSR). These two protein bands were carefully withdrawn using a 10 ml syringe fitted with an 18-gauge needle. The protein was diluted 2-3x with a solution consisting of 100 mM KCl, 20 mM Hepes-Tris, pH 7.0 and centrifuged for 90 minutes at 41,000 x g (18,500 rpm in the SS-34 Sorvall rotor). The pellet was then re-suspended at a protein concentration of approximately 10 mg/ml in the KCl/Hepes buffer described above and stored at -70°C until needed.

Protein Concentration Determination. Protein concentrations were determined by absorption spectroscopy. 10 μ l of an SR suspension with an unknown protein concentration was diluted 1:100 in a 1% sodium dodecyl sulfate (SDS) solution and the absorbance measured at 230, 260 and 280 nm. The protein concentration was determined from the following formula, generated from Kalckar (1947) and Thorley-Lawson et. al. (1977):

$$\begin{aligned}\text{Protein (mg/ml)} &= 100 (1.45 \text{ Abs}_{280} - 0.74 \text{ Abs}_{260}) \\ \text{Protein (mg/ml)} &= 100 (0.183 \text{ Abs}_{230} - 0.075 \text{ Abs}_{260})\end{aligned}$$

A second 10 μ l addition of SR was added, the absorbance remeasured, and the protein concentrations recalculated. The results of this second calculation were divided by 2 to obtain the correct result since the above equations are normalized to a 100 fold dilution of the SR from baseline and two additions of SR result in only a 50 fold dilution. The above procedure is repeated for a third 10 μ l SR

addition and the results of from all calculations are averaged together and expressed as mean \pm SD.

Ca²⁺ Efflux Studies

Active Ca²⁺ Efflux. Ca²⁺ release rates from actively loaded SR vesicles were assayed using a calcium selective electrode (WPI, Cal-1) which was interfaced through an analog-to-digital converter (Scientific Solutions, TM-40) with an IBM-XT computer. This system was calibrated by adding at least four aliquots of 10 μ M Ca²⁺ to a buffer of 100 mM KCl, 1 mM MgCl₂, 20 mM Hepes-Tris, pH 7.0. Millivolt readings from the calcium selective electrode, referenced to an Ag/AgCl electrode (WPI, Mere-1), were read into the computer after each addition of Ca²⁺. An in-house program internally generates a plot of the potential difference vs. the logarithm (base 10) of the Ca²⁺ concentrations. This procedure corrects for Ca²⁺ present in the buffer (usually 2-3 μ M) before the addition of Ca²⁺ and displays the slope of the plot (29 ± 1 mV per decade of Ca²⁺ concentration). The linearity of response of the Ca²⁺ electrode was verified in the range of Ca²⁺ concentration from 0.2-20 μ M with Ca²⁺/EGTA buffered solutions using the stability constants $k_1 = 10.716$, $k_2 = 5.33$ as published by Fabiato and Fabiato (1979). The response time of the Ca²⁺ electrode was typically 0.2-0.3 s.

In a typical experiment, SR vesicles were suspended at 0.2 mg/ml in 100 mM KCl, 1 mM MgCl₂, 20-30 μ M CaCl₂, 20 mM

Hepes-Tris, pH 7.0. The uptake of Ca^{2+} was initiated by the addition of either Mg^{2+} -ATP (0.5 mM) or acetyl phosphate (AcPO_4) (1 mM). Upon completion of uptake and leveling off of the signal, the external Ca^{2+} concentration was adjusted to the desired level by additions of 1-2 μM Ca^{2+} from a 100x stock. Ca^{2+} release was initiated by the addition of an effluxing agent.

Data are digitized at a frequency of 10 Hz and stored in the computer. An analysis program converts millivolt readings to free Ca^{2+} concentrations, displays the data as a function of time, and calculates the maximal Ca^{2+} efflux rate ((nmol/mg)/sec) or fits the data to an exponential and calculates the first order rate constant, $k(\text{sec}^{-1})$.

Passive Ca^{2+} Efflux. Passive Ca^{2+} efflux was measured using a time-sharing dual-wavelength spectrophotometer (custom manufactured by the University of Pennsylvania machine shop). Prior to efflux measurements, SR vesicles were loaded with Ca^{2+} by equilibration at a protein concentration of 10 mg/ml in a buffer containing 100 mM KCl, 1 mM CaCl_2 , 1 mM MgCl_2 , 20 mM Hepes-Tris, pH 7.0, at room temperature for at least two hours.

Efflux measurements were made by diluting the sample 50-fold into a buffer containing 100 mM KCl, 1 mM MgCl_2 , 20 mM Hepes-Tris, 100 μM arsenazo III, pH 7.0. (Arsenazo III, a polycationic indicator dye, responds to the presence of Ca^{2+} by increasing its absorbance at 675 nm in a Ca^{2+}

concentration dependent manner.) The extravesicular Ca^{2+} concentration was monitored by measuring the differential absorption changes at 675-685 nm. The maximal slope of the time-dependent absorbance change is related to the maximum Ca^{2+} efflux rate expressed in (nmol/mg)/sec. The loading capacity of the vesicles was determined by adding 0.4 $\mu\text{g/ml}$ of the Ca^{2+} ionophore A23187 at the completion of each experiment. An aliquot of Ca^{2+} was added at the end of each run to calibrate the absorption changes of the Ca^{2+} indicator dye.

[^3H]Ryanodine Binding Studies

Preparation of SR for [^3H]ryanodine Binding Studies.

For all [^3H]ryanodine binding studies, rabbit skeletal muscle sarcoplasmic reticulum vesicles were prepared according to the method of Inui et al. (1978). SR vesicles were prepared as described under "Preparation of SR Vesicles" except that female New Zealand White rabbits were used. This was followed by isolation of the heavy SR component as described under "Preparation of Light and Heavy SR Vesicles" with the following modifications: 1) The SR fraction used in these studies was collected from the 38/45% interface on a 15-45% (w/w) sucrose gradient which had been prepared as described. 2) The sucrose steps used in this gradient were 15, 27, 32, 34, 38, and 45% sucrose. 3) The SR fraction isolated was diluted, pelleted, and re-suspended as described, at a protein concentration of 4-6 mg/ml, in a

solution consisting of 250 mM KCl, 15 mM NaCl, 20 mM Hepes-Tris, pH 7.1.

[³H]Ryanodine Binding Assay. Terminal SR membranes (30 mg/ml), prepared as described in the previous section, were incubated at 37°C for 3 h in a medium containing 250 mM KCl, 15 mM NaCl, 50 μ M CaCl₂, 1.0 nM [³H]ryanodine, 20 mM Hepes-Tris, pH 7.1. Depending on the conditions of the assay, various concentrations of Ca²⁺ channel activators or inhibitors were included in the incubation.

Assays were terminated by addition of 5 ml of ice-cold wash medium (consisting of 250 mM KCl, 15 mM NaCl, 20 mM Hepes-Tris, pH 7.1), followed by rapid filtration through GF/B glass fiber filters in a cell harvester (Brandel, Gaithersburg, MD). One additional 5 ml wash was used to rinse the filters.

Radioactivity was measured by scintillation counting with an efficiency of approximately 43%. In all cases, non-specific [³H]ryanodine binding was defined by the addition of a 100-fold excess of non-labeled ryanodine. Filter binding of [³H]ryanodine in the absence of vesicles was negligible.

Bilayer Lipid Membrane Studies

SR Vesicle Preparation. SR vesicles were prepared for reconstitution with the bilayer lipid membrane in the following manner. SR vesicles initially prepared as described in "Preparation of SR Vesicles" were suspended at

a protein concentration of 1.5 mg/ml in a solution consisting of 0.3 M sucrose, 100 mM CsCl, 20 mM Hepes-Tris, pH 7.0, to a final volume of 1 ml. This suspension was placed on ice and stored in the refrigerator overnight. The following day, the equilibrated SR was portioned into 50 μ l aliquots and stored at -70°C until needed.

Reconstitution of SR vesicles. Reconstitution experiments were carried out by the fusion of a single SR vesicle to a planar bilayer lipid membrane (BLM). Bilayers, made from a 5:3 mixture of phosphatidylethanolamine (PE) and phosphatidylserine (PS) suspended at 50 mg/ml in decane, were formed across a 150 micron hole drilled into the side of a polystyrene cup which separates two chambers of 0.7 ml each.

The *cis* chamber (defined as the side to which the SR vesicles are added) contained 500 mM CsCl, 350 μ M CaCl₂, 5 mM Hepes-Tris, pH 7.0, while the *trans* chamber contained 100 mM CsCl, 5 mM Hepes-Tris, pH 7.0. The fusion process was initiated by adding 5 μ l SR (10 μ g protein) to the *cis* chamber. Following fusion of a single vesicle, 0.7 mM EGTA, pH 7.0 was quickly added to the *cis* chamber to stop further fusions. The chamber was then quickly perfused with an identical buffer which contained no added Ca²⁺ or EGTA.

Data Acquisition. Current through the open channel was recorded as a function of voltage, and channel activity was measured at various holding potentials with respect to the

trans (ground) side. A bilayer clamp amplifier (Warner Instruments, model BC-525A) was used to amplify picoampere currents. The data were processed unfiltered with an Instratech Digital Data Recorder (model VR-10), stored on VCR tape, and subsequently analyzed for channel activity.

In a typical experiment, 100-300 μM Ca^{2+} was added to the *cis* chamber to achieve a channel which gates with the desired activity. This control channel activity was recorded for at least 1 minute. Various concentrations of Ca^{2+} channel activators or inhibitors were then added and the change in channel activity was again recorded for at least 1 minute.

For analysis, data were passed through a Krohn-Hite low pass filter (model 3202) at 1.5 kHz, digitized with a Scientific Solutions analog to digital converter (Labmaster DMA) and subsequently analyzed for channel activity using the pCLAMP program (version 5.5, Axon Instruments, Burlingame, CA).

MECHANISM OF ANTHRAQUINONE-INDUCED CALCIUM RELEASE FROM SKELETAL MUSCLE SARCOPLASMIC RETICULUM

SUMMARY

This chapter shows that micromolar concentrations of the anthraquinones doxorubicin, mitoxantrone, daunorubicin, and rubidizone trigger a large and rapid Ca^{2+} release from skeletal muscle sarcoplasmic reticulum (SR) vesicles and induce phasic contractions in skinned psoas muscle fibers. These effects of quinones are shown to be modulated by known modifiers of the Ca^{2+} release system in SR. [^3H]Ryanodine binding studies show that doxorubicin alters the Ca^{2+} sensitivity of ryanodine binding and that millimolar concentrations of caffeine inhibit doxorubicin-stimulated ryanodine binding. These results indicate that anthraquinones induce release via a direct stimulation of the SR Ca^{2+} release channel. Evidence is presented which suggests that anthraquinone-stimulated Ca^{2+} release is via an oxidation reaction.

INTRODUCTION

Quinones are aromatic dioxo compounds derived from benzene or multiple-ring hydrocarbons. They are characterized by the presence of two carbonyl groups,

generally para, attached to the center ring. The number of rings which make up the backbone of this molecule determines its classification. Benzoquinones have one ring, naphthoquinones have two rings, and three rings define an anthraquinone. Figure 3 shows some examples of quinones, including those used in this study.

Quinones are widely distributed in nature and are found in higher plants, fungi, and throughout the animal kingdom. They are mostly involved in electron transport systems such as cellular respiration and photosynthesis, but are also prevalent as environmental pollutants. For example, quinones have been found in atmospheric particulate matter (Fox et al., 1979), cigarette smoke (Pryor et al., 1982) and diesel exhaust (Scheutzle, 1983).

One of the major biological functions of quinones is to participate in oxidation-reduction reactions. Figure 4 shows the stepwise reduction of the simplest quinone (1,4-benzoquinone) to its semiquinone and hydroquinone states. While in a reduced state, quinones are capable of auto-oxidizing to their next higher oxidation state (i.e. hydroquinone to semiquinone, or semiquinone to quinone) through the loss of an electron. In this figure, the auto-oxidation of the reduced species is shown with O_2 as the oxidizing agent (electron acceptor). During this process, the O_2 is itself reduced to the superoxide anion radical

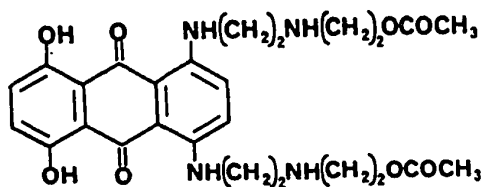
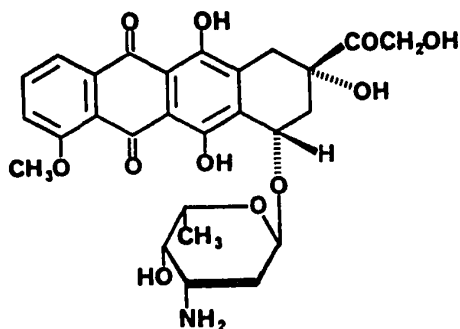
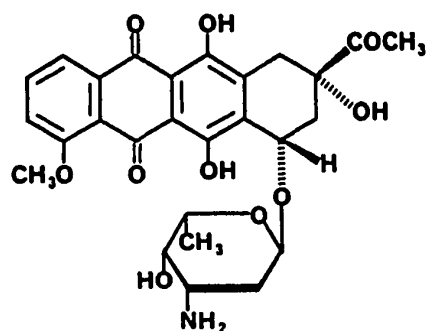
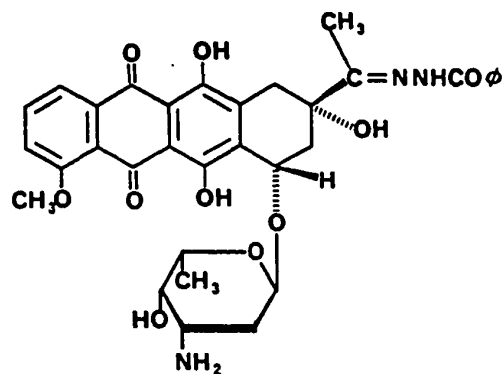
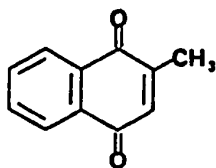
**Mitoxantrone diacetate****Doxorubicin****Daunorubicin****Rubidazone****Menadione**

Figure 3. Structure of quinones. Representative structures of the anthraquinones (mitoxantrone, doxorubicin, daunorubicin, and rubidazone), and naphthoquinones (menadione) used in this study.

(O_2^-), which is a potentially toxic species. In general, semiquinones are easily oxidized, while hydroquinones tend to be more stable in aqueous environments. Since most semiquinone radicals rapidly react with O_2 to form superoxide, the one electron reduction of quinones to the semiquinone state and the subsequent auto-oxidation of the semiquinone back to the quinone state results in the production of large quantities of superoxide. This oxidation-reduction process is known as redox cycling and the resulting formation of superoxide is held responsible for much of the oxidative injury to biological systems caused by quinones.

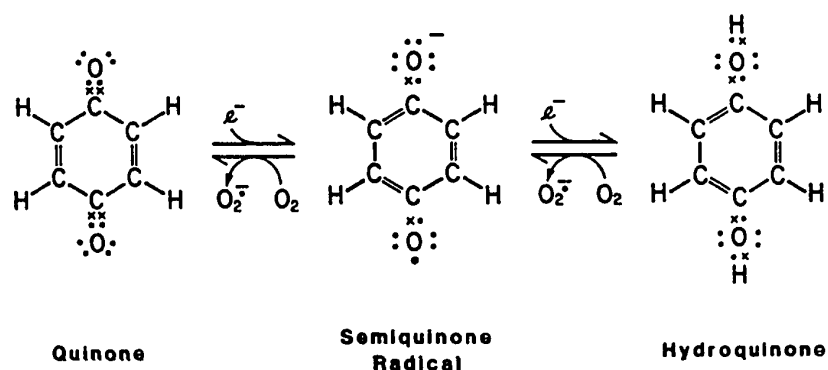


Figure 4. Stepwise reduction of a simple quinone. The reduction of the quinone 1,4-benzoquinone to its semiquinone and hydroquinone states is shown.

The anthraquinones doxorubicin and daunorubicin are of interest clinically because they are widely used in the treatment of cancers. They show a broad range of antitumor

activity with doxorubicin being the most widely used anticancer drug in the world (Weiss et al., 1984). Unfortunately, the use of these drugs is limited by several side effects, the most serious of which is chronic cardiotoxicity. This toxicity is morphologically characterized by myofibrillar loss, vacuolization of the SR, and swelling of the mitochondria (Ferrans, 1978). The leading hypothesis for the mechanism of toxicity involves quinone induced free radical damage and non-specific oxidation of cardiac membranes (Doroshov et al., 1983).

Initial interest in the interaction between quinones and the Ca^{2+} release system stems from a report that doxorubicin induces rapid Ca^{2+} release from SR vesicles and contractions in skinned muscle fibers (Zorzato et al., 1985). This, along with the observation that the naphthoquinone plumbagin also causes Ca^{2+} release from SR vesicles (Trimm et al., 1986), lead us to inquire whether other quinones were capable of interacting with the Ca^{2+} release system from SR.

In this chapter all figures were generated by E. Buck, with the following exceptions: Figure 8 was generated by Salama et al. at the University of Pennsylvania. Figures 9 and 10 were generated by Pessah et al. at the University of California, Davis. Both Salama and Pessah were collaborators on the associated publication and these figures were

included here for completeness. This work was published in the Journal of Biological Chemistry (Abramson et al., 1988).

METHODS AND MATERIALS

Preparation of SR Vesicles

For all Ca^{2+} efflux assays, rabbit skeletal muscle sarcoplasmic reticulum vesicles were prepared according to the method of MacLennan et al., as described in detail under "Preparation of SR Vesicles" in Chapter II. For efflux assays using LSR or TSR, light and heavy SR vesicles were prepared as described in detail under "Preparation of Light and Heavy SR Vesicles" in Chapter II.

Protein concentrations were determined as described in Chapter II.

Ca^{2+} Efflux Assays

Ca^{2+} efflux measurements were performed either actively or passively, depending on the conditions of the assay.

Active Ca^{2+} Efflux. Ca^{2+} release rates from actively loaded SR vesicles were measured using a calcium selective electrode as described in detail under "Active Ca^{2+} Efflux" in Chapter II, with the following modifications: For experiments designed to measure the rate of Ca^{2+} release as a function of either the quinone concentration or the caffeine concentration, the free Ca^{2+} concentration was adjusted to 1.5 μM prior to the addition of the effluxing agent.

For experiments designed to measure the Ca^{2+} or Mg^{2+} dependence of mitoxantrone or doxorubicin-induced release, the Ca^{2+} or Mg^{2+} concentration was adjusted to the value shown on the abscissa prior to stimulation of release.

In all other respects the experiments were performed as described.

Passive Ca^{2+} Efflux. Passive Ca^{2+} efflux was measured using a time-sharing dual-wavelength spectrophotometer as described in detail under "Passive Ca^{2+} Efflux" in Chapter II.

Skinned Fiber Assays

Fiber Preparation. Chemically skinned fibers are prepared from psoas muscles of New Zealand White rabbits according to the method of Wood et al. (1975). Small bundles of several hundred fibers were removed from the muscle, tied to Teflon sticks at 110-120% of rest length, and 'skinned' in a solution containing 170 mM K^{+} -gluconate, 2.5 mM Mg^{2+} -gluconate, 2.5 mM Na^{+} -ATP, 5 mM EGTA, 5 mM imidazole, pH 6.75. After 24 h at 0°C, the bundles were transferred to a solution of the same ionic composition, with 50% glycerol, and stored at -20°C for up to six weeks.

Fiber Method. Following skinning, bundles of 2-4 fibers were mounted between stainless steel rods and held in place with either an acetone based glue or a pair of microclamps. One of the rods or clamps remained fixed while the other was attached to the headstage of a force transducer system

(Cambridge 400A) for the measurement of isometric force. Fibers were stretched to 120% of resting length and suspended in a Chelexed relaxing solution containing 2.5 mM Na₂-ATP, 1 mM MgSO₄, 10 mM MOPS, pH 6.75. The solution was maintained at 23°C and was magnetically stirred. Under these conditions, the free Ca²⁺ and Mg²⁺ concentrations are 150 nM and 100 μM, respectively. The calculated free Ca²⁺ concentration was the same as measured using a Ca²⁺ selective electrode (WPI, Cal-1). At the start of each experiment, the SR is loaded by successive additions of Ca²⁺-gluconate. The loading procedure allowed the SR to accumulate sufficient Ca²⁺ to produce large phasic contractions in response to a Ca²⁺ channel activator.

[³H]Ryanodine Binding Assays

Preparation of SR Vesicles. For all [³H]ryanodine binding studies, rabbit skeletal muscle SR vesicles were prepared according to the method of Inui et al., as described in detail under "Preparation of SR for [³H]Ryanodine Binding Studies" in Chapter II, with the following modification: Following isolation of the heavy SR fraction, the vesicles were suspended in 115 mM KCl, 15 mM NaCl, 40 mM Tris, pH 7.1. In all other respects the SR was prepared as described.

Equilibrium Binding Assay. Equilibrium [³H]ryanodine binding was performed as described in detail under "[³H]Ryanodine Binding Assay" in Chapter II, with the

following modification: The incubation medium consisted of 115 mM KCl, 15 mM NaCl, 1 mM MgCl₂, 2.5 nM [³H]ryanodine, 40 mM Tris, pH 7.1. Free Ca²⁺ concentrations below 80 μM were adjusted with EGTA based on stability constants for the Ca²⁺-EGTA complex derived from Sillen and Martell (1964).

For experiments designed to measure the influence of doxorubicin or daunorubicin on Ca²⁺ activation of [³H]ryanodine binding, the assay was performed under competitive conditions such that SR was added as a final step (to initiate the binding reaction). In all cases, the samples were equilibrated for 180 minutes at 37°C before the reaction was quenched.

In all other respects these assays were the same as described in Chapter II.

Materials

All reagents were analytical grade. [³H]Ryanodine was synthesized as described by Pessah et al. (1985). Hepes was obtained from Research Organics (Cincinnati, OH). MgCl₂ and CaCl₂ were purchased from J.T. Baker Chemical Co.. ATP and A23187 are from Calbiochem. Menadione and plumbagin were purchased from Aldrich Chemical Co.. Doxorubicin, daunorubicin, and all other chemicals were obtained from Sigma Chemical Co. (St. Louis, MO). Some of the doxorubicin (Adriamycin) used in this study was provided by Adria Laboratories (Dublin, OH). Mitoxantrone diacetate and rubidazone were gifts from the Drug Synthesis and Chemistry

Branch, Division of Cancer Treatment, National Cancer Institute.

RESULTS

Anthraquinones Stimulate Ca^{2+} Release from SR Vesicles

Since it had been shown that doxorubicin, an anthraquinone, and plumbagin, a naphthoquinone, were capable of stimulating Ca^{2+} release from SR vesicles, we investigated if other quinones were also capable of inducing Ca^{2+} release. We report here that (1) all of the benzoquinones tested were totally ineffective in stimulating efflux, (2) only a few naphthoquinones, most notably menadione (2-methyl-1,4 naphthoquinone) and plumbagin (5-hydroxy-2-methyl-1,4 naphthoquinone), were capable of inducing Ca^{2+} release, and (3) the most effective stimulators of Ca^{2+} release were the anthraquinones.

The most potent anthraquinone tested was mitoxantrone, followed by doxorubicin, daunorubicin, and rubidazone (Figure 5). Since many compounds stimulate Ca^{2+} release from the SR in a Ca^{2+} dependent manner, the Ca^{2+} concentration in the assay medium was carefully adjusted to $1.5 \mu\text{M}$ prior to addition of the anthracycline. The Ca^{2+} efflux rates observed at low mitoxantrone or doxorubicin concentrations ($<10 \mu\text{M}$) are relatively large, despite the facts that 1 mM Mg^{2+} was present in the assay medium and the Ca^{2+} concentration was low.

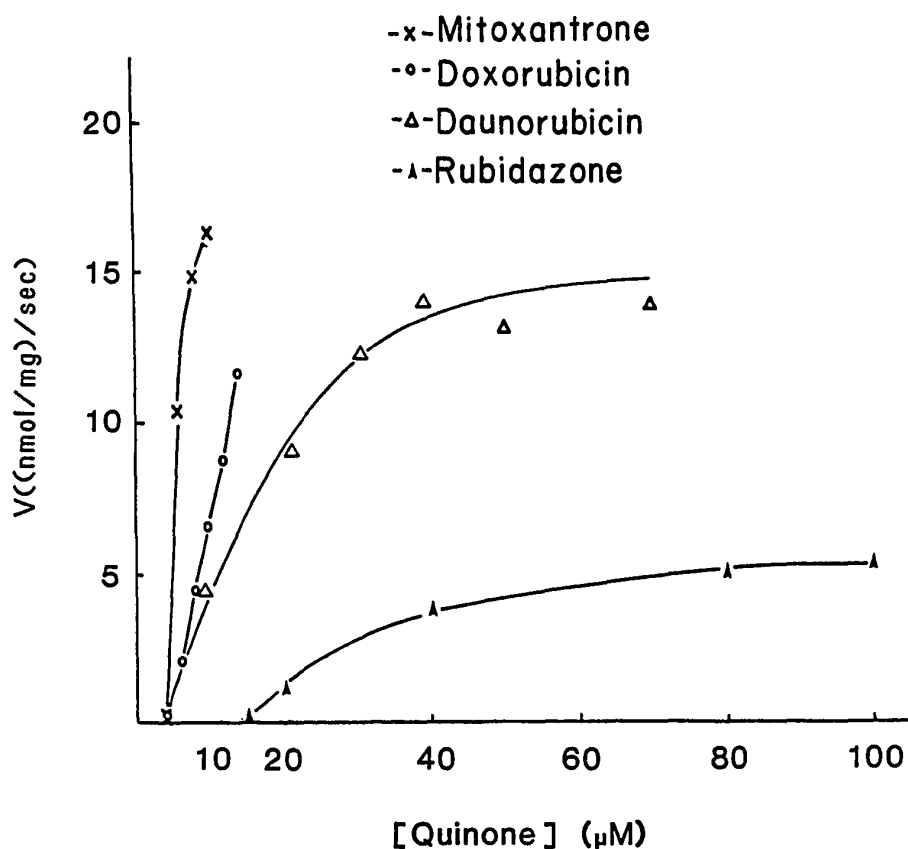


Figure 5. Rate of Ca^{2+} release as a function of anthraquinone concentration. SR vesicles are suspended in 100 mM KCl, 1 mM MgCl_2 , 20 μM CaCl_2 , 20 mM HEPES-Tris, pH 7.0, at a protein concentration of 0.2 mg/ml. Ca^{2+} uptake is initiated by the addition of 0.5 mM Mg^{2+} -ATP. The free Ca^{2+} concentration is adjusted to 1.5 μM prior to the addition of the quinone. Data shown is (x) mitoxantrone, (o) doxorubicin, (Δ) daunorubicin, and (▲) rubidazone.

Since a quinone activated, non-specific pathway could be mediating the observed efflux of Ca^{2+} from the SR, the influence of several known modulators of SR Ca^{2+} release were investigated. These include inhibition by Mg^{2+} and ruthenium red, stimulation by Ca^{2+} and adenine nucleotides, and localization of release to the terminal cisternae region of the SR.

Inhibition of Ca^{2+} Release from SR Vesicles. Millimolar concentrations of Mg^{2+} and micromolar concentrations of ruthenium red have been shown to inhibit Ca^{2+} release from SR vesicles and to inhibit contractions in skinned muscle fibers (Endo, 1977). Figure 6 shows Ca^{2+} release induced by either 10 μM mitoxantrone or 10 μM doxorubicin is strongly inhibited by low concentrations of Mg^{2+} . Over this range of Mg^{2+} concentrations, and at the anthracycline concentration used, neither the amount of Ca^{2+} loading nor the response time of the Ca^{2+} selective electrode was affected. Inhibition of anthraquinone-induced Ca^{2+} release by ruthenium red was also observed to be very effective, with half-inhibition occurring at a ruthenium red concentration of 100 nM (data not shown).

Stimulation of Ca^{2+} Release from SR Vesicles. One of the primary mechanisms proposed for triggering Ca^{2+} release from the SR involves the binding of Ca^{2+} to a site on the Ca^{2+} release protein. The observed rate of Ca^{2+} efflux is

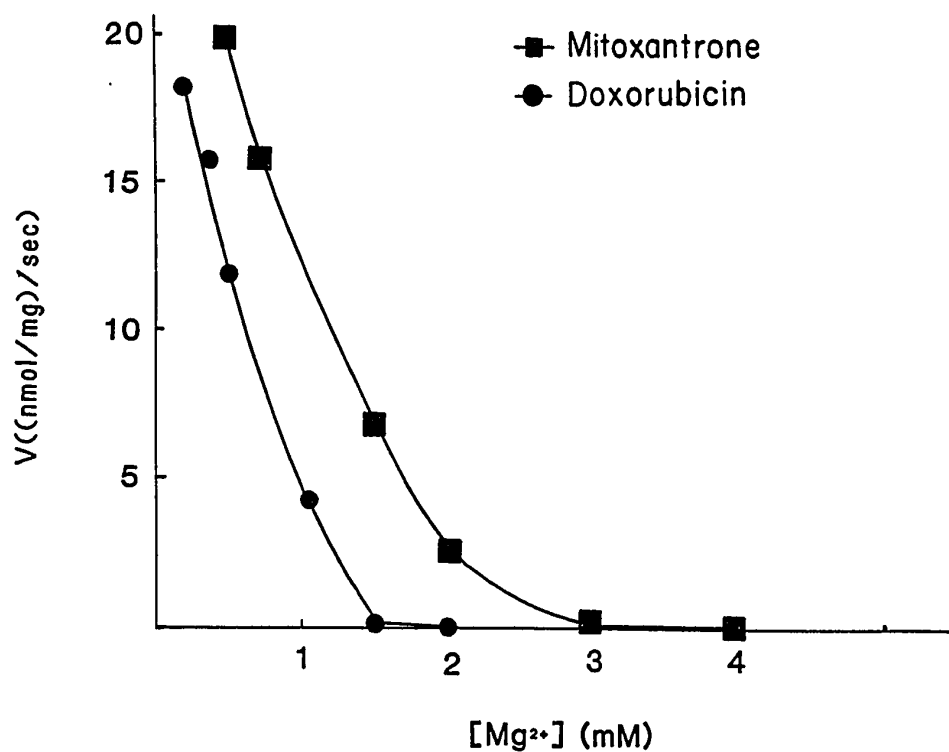


Figure 6. Inhibition of anthraquinone-induced Ca^{2+} release by Mg^{2+} . SR vesicles are actively loaded with Ca^{2+} as described in Figure 5 in buffers containing various free Mg^{2+} concentrations. Ca^{2+} release is initiated by the addition of $10\ \mu\text{M}$ mitoxantrone (■) or $10\ \mu\text{M}$ doxorubicin (●).

decreased significantly at Ca^{2+} concentrations less than 10 μM and at Ca^{2+} concentrations greater than 1 mM (Meissner, 1984).

In Figure 7, shows that activation of Ca^{2+} release triggered by mitoxantrone is strongly dependent on the free Ca^{2+} concentration. The concentrations shown on the abscissa are the free Ca^{2+} concentration when the anthraquinone is added, as determined by the Ca^{2+} electrode. A similar sharp Ca^{2+} dependence is also observed when Ca^{2+} release is triggered by the addition of doxorubicin.

Ca^{2+} release from SR vesicles is known to be stimulated by the presence of adenine nucleotides (Meissner, 1986). In Table II, the rates of Ca^{2+} release triggered by 10 μM mitoxantrone in the presence of either ATP, beta gamma-methylenadenosine 5'-triphosphate (AMP-PCP), or the non-adenine containing substrate, acetyl phosphate (AcPO_4), are compared. The amount of Ca^{2+} loading by the SR was unaffected by the choice of substrate, nevertheless, mitoxantrone-induced Ca^{2+} release was stimulated 4-7 fold in the presence of adenine nucleotide containing substrates. As observed with other modes of triggering Ca^{2+} release from SR vesicles, ATP is a more effective stimulator than AMP-PCP (Meissner et al., 1986).

Physiologically, Ca^{2+} release is believed to occur through the terminal cisternae region of the SR. As shown in Table II, Ca^{2+} release induced by 10 μM mitoxantrone is also

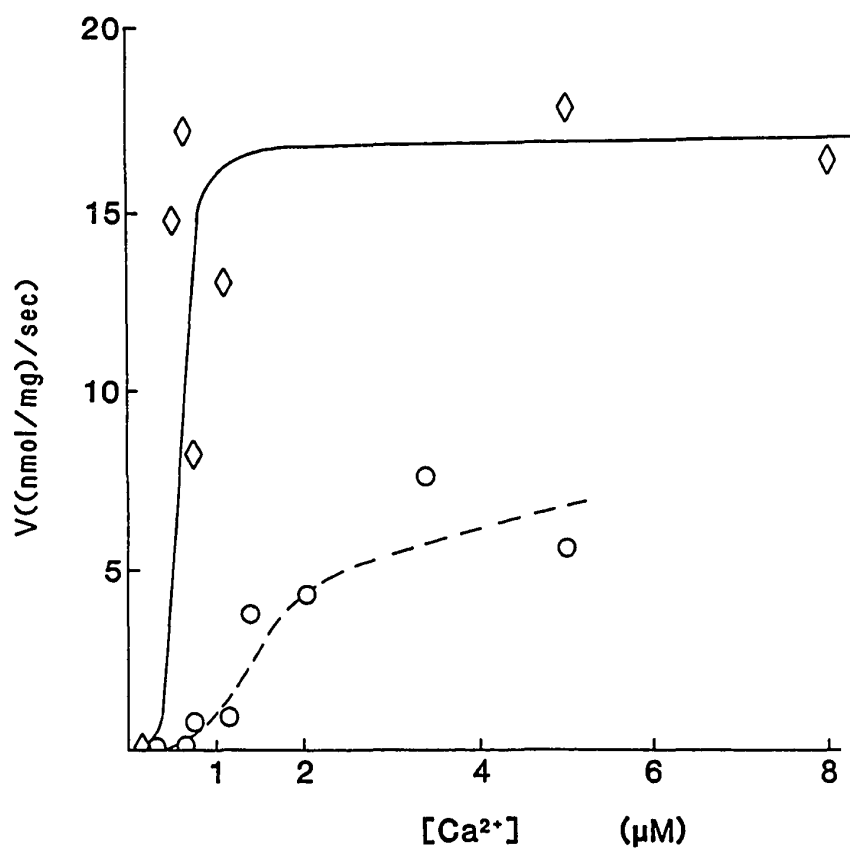


Figure 7. Rate of mitoxantrone-induced Ca^{2+} release as a function of free Ca^{2+} concentration. SR vesicles were actively loaded as described in Methods. The free Ca^{2+} concentration was adjusted to the level shown on the abscissa prior to release. Ca^{2+} release was initiated by the addition of 5 μM (○) or 10 μM (◇) mitoxantrone.

specific for SR derived from the terminal cisternae region (TSR). Both the Ca^{2+} release rate and the amount of Ca^{2+} released is four to five times larger with TSR vesicles than with vesicles derived from the longitudinal region of the SR (LSR).

TABLE II
MITOXANTRONE-INDUCED Ca^{2+} RELEASE

SR	Pump substrate	Ca^{2+} released (%)	Efflux Rate (nmol/mg)/s	Pretreatment
SR	ATP	53	19.0	Na ₂ S ₂ O ₄ Na ₂ S ₂ O ₄ + O ₂
SR	AcPO ₄	46	2.8	
SR	AcPO ₄ +AMP-PCP	48	10.6	
LSR	ATP	10	3.9	
TSR	ATP	40	18.3	
SR	ATP	26	2.8	
SR	ATP	35	18.3	

Ca^{2+} release rates and percent Ca^{2+} released are affected by adenine nucleotides, dithionite reduction, and regional specificity. Ca^{2+} uptake is initiated by either 0.5 mM Mg^{2+} -ATP (ATP), 0.5 mM AcPO₄, or 0.5 mM AcPO₄ plus 0.5 mM Mg^{2+} -AMP-PCP (AcPO₄ + AMP-PCP), in a buffer containing 100 mM KCl, 1 mM MgCl_2 , 20 μM CaCl_2 , 20 mM Hepes-Tris, pH 7.0. Ca^{2+} release is initiated by the addition 10 μM mitoxantrone. Pretreatment with a 5 fold molar excess of dithionite (Na₂S₂O₄) over mitoxantrone is carried out in a de-aired environment generated by extensive bubbling of all solutions with argon gas. In control experiments, dithionite is oxidized by bubbling in O₂ before preincubation with mitoxantrone (Na₂S₂O₄ + O₂). The standard deviation of each efflux rate is approximately 10%.

Anthraquinones Induce Contractures in Skinned Muscle Fibers

Ca^{2+} release triggered by mitoxantrone is also observed in skinned psoas muscle fibers. These fibers are chemically skinned and prepared as described in Methods. As shown in

Figure 8, Ca^{2+} loaded fibers respond to the addition of 25 μM mitoxantrone with a transient contraction (trace A). Subsequent additions of mitoxantrone repeatedly stimulate transient contractions. Mitoxantrone at lower concentrations was also able to induce twitches, but only after a time delay. The addition of a saturating Ca^{2+} concentration at the end of each experiment reveals that Ca^{2+} released by mitoxantrone generates 85 to 95% ($n=5$) of the maximum force generated by the fiber.

Caffeine induces contractions in skinned muscle fibers (Endo, 1975). As shown in Figure 8, skinned fibers were still capable of responding to 2 mM caffeine after stimulation by 25 μM mitoxantrone. A comparison of contractions induced by caffeine before and after exposure to mitoxantrone shows that the anthracycline does not interact directly with the contractile apparatus of the cell. The maximum contracture possible is not affected by mitoxantrone and is equivalent to a transient contraction generated by 2 mM caffeine. As in vesicle experiments, 10 μM ruthenium red completely blocks contractions caused by both mitoxantrone and caffeine (trace B).

Anthraquinones Stimulate [^3H]Ryanodine Binding

[^3H]Ryanodine binds in a Ca^{2+} dependent manner with high specificity and nanomolar affinity to the Ca^{2+} release channel of the SR. The characteristics of [^3H]ryanodine

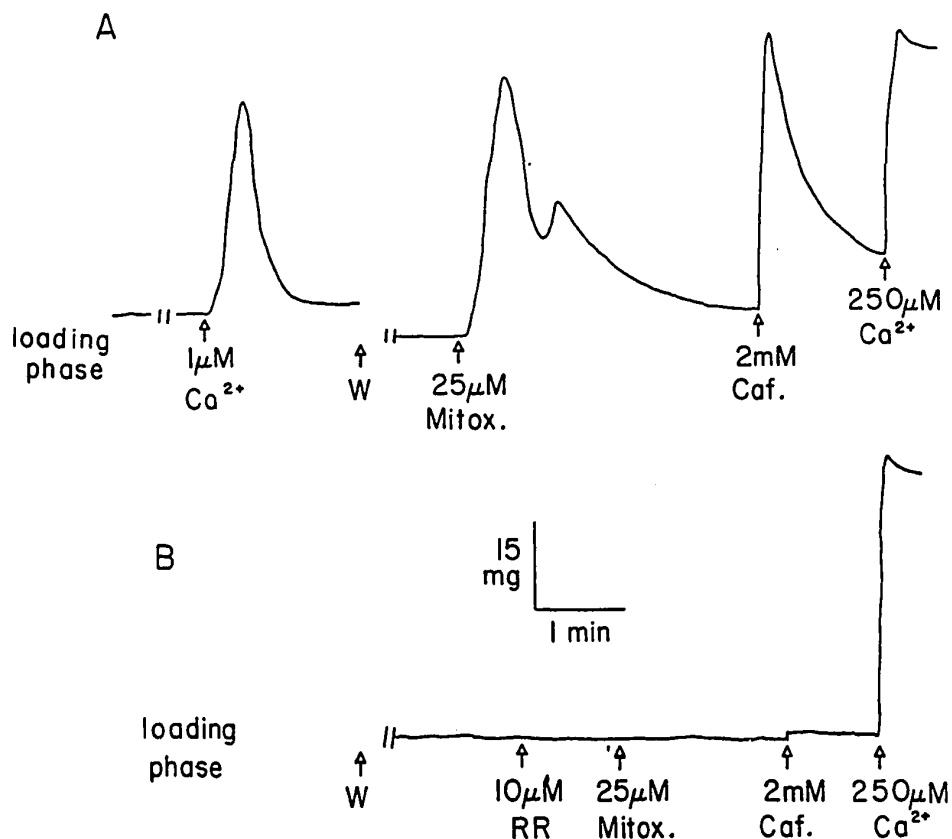


Figure 8. Phasic contractions of chemically skinned psoas muscle fibers triggered by mitoxantrone. Fibers are skinned and suspended in a solution containing 170 mM K^+ -gluconate, 2.5 mM $\text{Na}_2\text{-ATP}$, 1 mM MgSO_4 , 10 mM MOPS, pH 6.75. (A) The SR of the fibers is loaded with Ca^{2+} during the 'loading phase'. Further addition of Ca^{2+} leads to a Ca^{2+} induced contraction. The fiber is returned to the initial buffer (W) and exposed to $25\mu\text{M}$ mitoxantrone (Mitox.), 2 mM caffeine (Caf.), and finally, a saturating level of Ca^{2+} . (B) In a parallel experiment, addition of $10\mu\text{M}$ ruthenium red (RR) blocks both mitoxantrone and caffeine induced contractions.

binding suggest that the alkaloid recognizes only the open state of the channel and can serve as a functional probe (Pessah et al., 1987). To determine the mechanism by which anthraquinones influence Ca^{2+} release, the direct effects of doxorubicin and daunorubicin on [^3H]ryanodine binding to TSR vesicles were examined.

Doxorubicin. As is shown in Figure 9, in the presence of 1 mM Mg^{2+} -AMP-PCP and 1 mM free Mg^{2+} , doxorubicin induces a concentration dependent decrease in the Ca^{2+} sensitivity of [^3H]ryanodine binding without increasing the maximum level of binding. Table III is a quantification of the data in Figure 9. It can be seen that the normalized binding constant (K_d/Ca^{2+}) decreases from a control value of 15.4 μM to 0.6 μM in the presence of 60 μM doxorubicin. Over this range of doxorubicin concentrations the cooperativity (h) and occupancy of binding sites (B_{max}) remain unchanged.

In general, we have observed that doxorubicin elicits little or no influence on ryanodine binding unless the assay medium contains either a physiologically relevant Mg^{2+} concentration (approximately 1 mM), a Ca^{2+} concentration suboptimal for activation of the Ca^{2+} release channel, or both. This evidence suggests doxorubicin does not induce additional ryanodine binding over that achieved by optimal binding conditions.

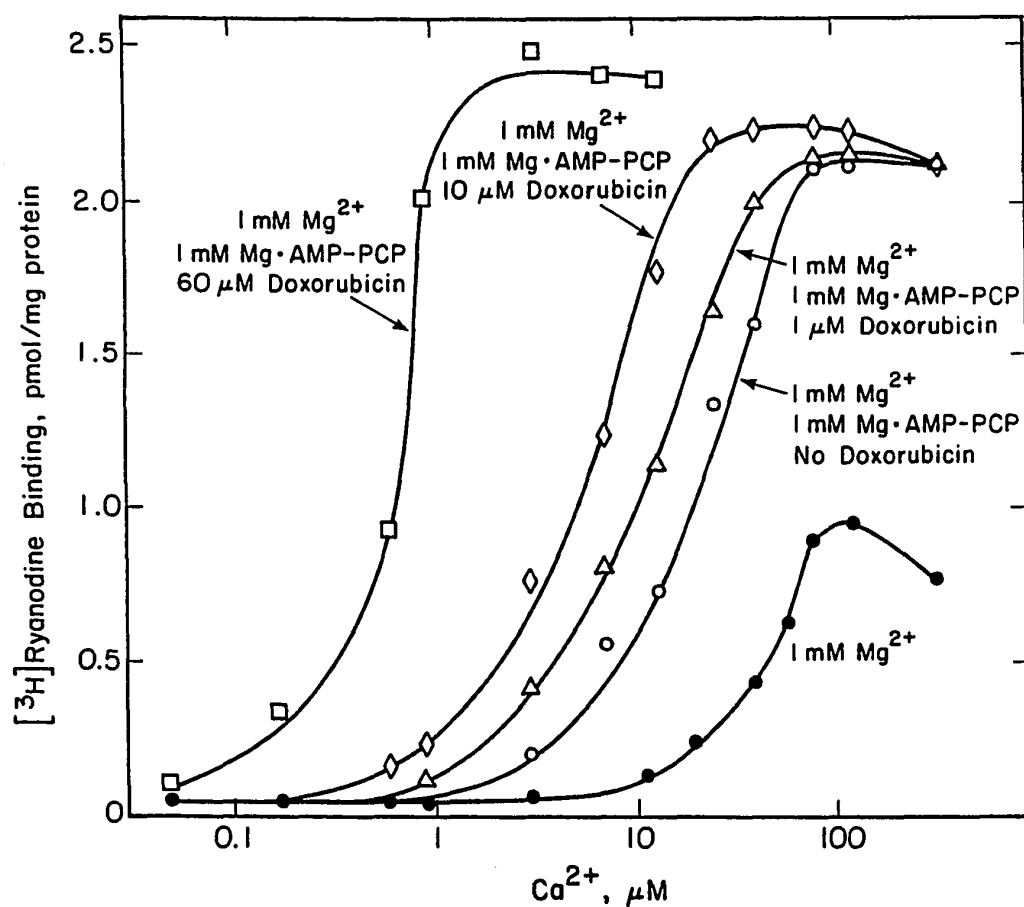


Figure 9. Effect of doxorubicin on Ca^{2+} activation of $[^3\text{H}]$ ryanodine binding in the presence of Mg^{2+} and Mg^{2+} -AMP-PCP.

Daunorubicin. Like doxorubicin, the anthraquinone daunorubicin also sensitizes Ca^{2+} activation of $[^3\text{H}]$ ryanodine binding in a concentration dependent manner. In Figure 10, $[^3\text{H}]$ ryanodine binding is measured as a function of the daunorubicin concentration. These

TABLE III

EFFECT OF DOXORUBICIN ON THE AFFINITY, COOPERATIVITY, AND OCCUPANCY OF $[^3\text{H}]$ RYANODINE BINDING SITES.

Additions	Affinity (K_d/Ca^{2+}) (μM)	Cooperativity (h)	Occupancy (B_{max}) (pmol/mg)
1 mM Mg^{2+}	24.7 ± 2.5	1.5 ± 0.2	0.5-0.9
1 mM Mg^{2+} plus Mg^{2+} -AMP-PCP	15.4 ± 1.1	1.3 ± 0.1	1.7-2.1
+ 1 μM doxo	9.7 ± 1.1	1.6 ± 0.2	1.7-2.1
+ 10 μM doxo	5.3 ± 0.4	1.3 ± 0.1	2.2-2.3
+ 60 μM doxo	0.6 ± 0.2	1.7 ± 0.3	2.4-2.7

Junctional SR membranes (50 $\mu\text{g}/\text{ml}$) were incubated in an assay buffer containing 2.5 nM $[^3\text{H}]$ ryanodine and 0.05-320 μM free Ca^{2+} . Each Ca^{2+} titration contained the indicated concentration of Mg^{2+} , Mg^{2+} -AMP-PCP, and doxorubicin (doxo). K_d/Ca^{2+} , h, and their standard errors were obtained directly from linear regression of Hill plots, while B_{max} is given as a range of three experiments.

experiments are performed in the absence and presence of 0.5 mM Mg^{2+} -AMP-PCP and 1 mM caffeine. As can be seen from this figure, a daunorubicin concentration of 55 μM half-maximally stimulates $[^3\text{H}]$ ryanodine binding in the presence of 2 μM Ca^{2+} and 1 mM Mg^{2+} (upper trace). Doxorubicin, which exhibits a half-activation constant of 20 μM , is nearly threefold more potent than daunorubicin (not shown).

Reversibility of Doxorubicin-Stimulated [^3H]Ryanodine Binding

High-affinity [^3H]ryanodine binding to TSR vesicles was measured in the presence of $1\ \mu\text{M}\ \text{Ca}^{2+}$, $1\ \text{mM}\ \text{Mg}^{2+}$, and $1\ \text{mM}\ \text{cAMP}$. Addition of $30\ \mu\text{M}$ doxorubicin increased ryanodine

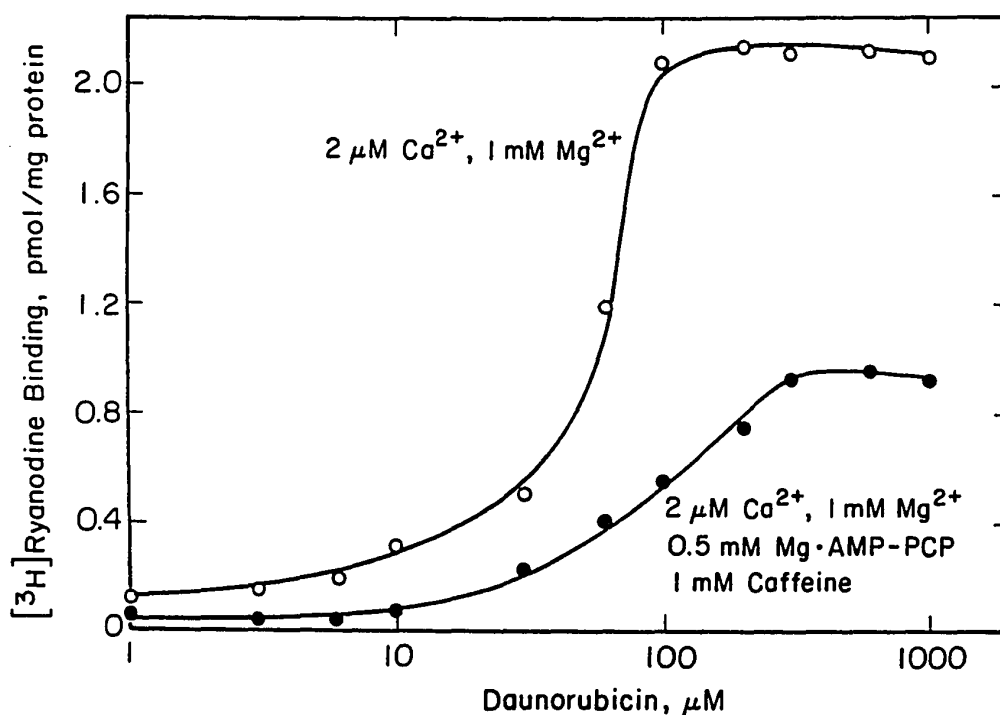


Figure 10. Daunorubicin-stimulated [^3H]ryanodine binding at $2\ \mu\text{M}$ free Ca^{2+} and $1\ \text{mM}$ free Mg^{2+} . Data was acquired in the absence (○) or presence (●) of Mg^{2+} -AMP-PCP and caffeine. Concentrations of daunorubicin required for half-maximal activation are $55\ \mu\text{M}$ and $72\ \mu\text{M}$, respectively.

binding approximately 250% (Table IV). The vesicles were then pelleted, rinsed, resuspended in a standard buffer, and [^3H]ryanodine binding remeasured. The wash procedure

decreased high-affinity binding to levels similar to those prior to the addition of doxorubicin, however, binding was

TABLE IV
REVERSIBILITY OF DOXORUBICIN-STIMULATED
[³H]RYANODINE BINDING

Additions	[³ H]ryanodine bound (%)
1 mM Mg ²⁺ , 1 mM cAMP	100
+ 50 μ M Ca ²⁺	0.7 \pm 0.1
+ 1 μ M Ca ²⁺	248 \pm 34
+ 1 μ M Ca ²⁺ + 30 μ M doxorubicin	
+ wash	4.0 \pm 5.6
+ wash + 30 μ M doxorubicin	254

One millimolar aliquots of TSR membranes (2-3 mg/ml), some pretreated with 30 μ M doxorubicin for 10-15 minutes at room temperature, were pelleted (15,000 x g for 15 minutes at 4°C) and the supernatant siphoned with a Pasteur pipette. The tubes containing the SR pellets were gently rinsed and resuspended in an assay buffer at their original concentration. Aliquots (15-20 μ l) were added to the assay medium containing the indicated additions and 2.5 nM [³H]ryanodine. The specific binding was determined as described under Methods. Values shown are mean \pm SD (n=3).

still capable of being reactivated by the addition of 30 μ M doxorubicin. It would thus appear, at least on the short time scale of these experiments, that the interaction of doxorubicin with the Ca²⁺ release channel is completely reversible.

Effects of Caffeine

The effect of caffeine on [³H]ryanodine binding has been shown to be via an interaction with a site distinct from the adenine nucleotide binding site (Pessah et al.,

1987). The sensitizing effect of doxorubicin on Ca^{2+} activation of [^3H]ryanodine binding is observed to be similar to that observed with caffeine. Since caffeine and doxorubicin appear to behave similarly, we investigated their possible interaction.

Although both doxorubicin and caffeine increase the Ca^{2+} sensitivity of [^3H]ryanodine binding, doxorubicin is much more effective than caffeine. Analysis of Table III shows that 60 μM doxorubicin reduces K_d/Ca^{2+} twenty-seven fold, while 20 mM caffeine is required to obtain an effect of equal magnitude (Pessah et al., 1987).

Caffeine Reduces Anthraquinone-Stimulated [^3H]Ryanodine Binding. To ascertain whether doxorubicin and caffeine interact at the same site on the Ca^{2+} release protein, varying concentrations of caffeine were titrated in the presence of 60 μM doxorubicin. Table V shows that an increase in the caffeine concentration reduces doxorubicin-stimulated [^3H]ryanodine binding. While approximately 4 mM caffeine is sufficient to achieve half inhibition, a caffeine concentration as high as 60 mM does not completely inhibit doxorubicin-stimulated ryanodine binding.

Daunorubicin-stimulated ryanodine binding is also observed to be inhibited by caffeine. Figure 10 shows that in the presence of 1 mM caffeine, [^3H]ryanodine binding is reduced at all daunorubicin concentrations.

TABLE V
CAFFEINE INHIBITION OF DOXORUBICIN-STIMULATED
[³H]RYANODINE BINDING

Additions	Specific binding (pmol/mg)	Percent inhibition (%)
2 μ M Ca ²⁺ , 1 mM Mg ²⁺ + 60 mM caffeine	0.03 \pm 0.01 1.38 \pm 0.07	0.0
2 μ M Ca ²⁺ , 1 mM Mg ²⁺ + 60 μ M doxorubicin	2.29 \pm 0.05	
+ 0.1 mM caffeine	2.16 \pm 0.06	14.3
+ 1.0 mM caffeine	2.01 \pm 0.10	30.8
+ 10 mM caffeine	1.72 \pm 0.07	62.7
+ 60 mM caffeine	1.59 \pm 0.02	76.9

The incubation buffer contains 1 mM Mg²⁺ and 2 μ M free Ca²⁺, adjusted with 80 μ M CaCl₂ and 85 mM EGTA, as described in Methods. 50 μ g/ml TSR membrane is added last to initiate the binding reaction which is equilibrated for 180 minutes. Reactions are quenched as described in Methods. Standard deviations of triplicate samples are shown.

Caffeine Inhibits Anthraquinone-Stimulated Ca²⁺ Release from SR Vesicles. Not only does caffeine decrease doxorubicin-stimulated ryanodine binding (Table V) and sensitize Ca²⁺ activation of ryanodine binding (Pessah et al., 1987), but it also inhibits daunorubicin-stimulated Ca²⁺ release from SR vesicles, as is shown in Figure 11. Under the conditions of this experiment, addition of caffeine after completion of Ca²⁺ uptake causes a small increase in the Ca²⁺ permeability of the SR, which is negligible compared to the release rates measured in the

absence of caffeine. Nevertheless, the primary action of millimolar caffeine is to inhibit the Ca^{2+} release activity of daunorubicin. A caffeine concentration of 0.7 mM was sufficient to cause a 50% reduction in the Ca^{2+} release rate

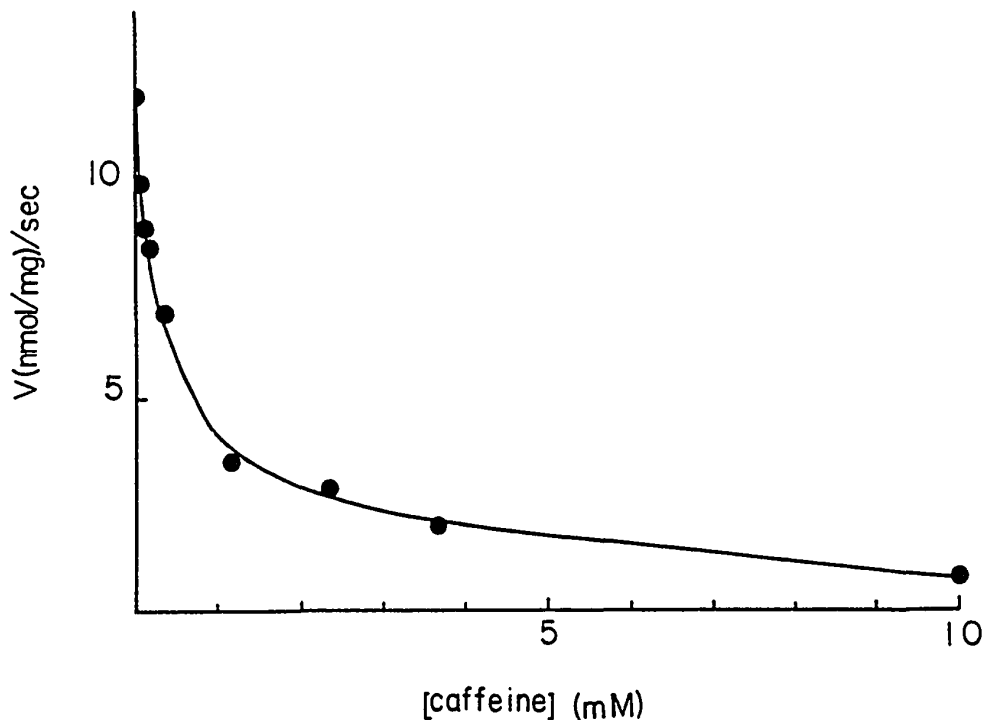


Figure 11. Rate of daunorubicin-stimulated Ca^{2+} release as a function of caffeine concentration. SR vesicles were actively loaded with $30 \mu\text{M}$ Ca^{2+} in the presence of various caffeine concentrations. Ca^{2+} release was initiated by the addition of $30 \mu\text{M}$ daunorubicin.

stimulated by $30 \mu\text{M}$ daunorubicin. At 2 mM caffeine the efflux rate is further reduced to approximately 20% of the zero caffeine control.

The inhibitory effect of caffeine is further demonstrated in Figure 12, in which the rate of Ca^{2+} release is measured as a function of the daunorubicin concentration, both in the absence and presence of 2 mM caffeine. Clearly, caffeine reduces daunorubicin-stimulated Ca^{2+} release at all daunorubicin concentrations. A similar inhibition by caffeine is also observed when examining the interaction between doxorubicin and caffeine.

Kinetic Analysis of Daunorubicin-Stimulated Ca^{2+} Release. The effect of caffeine on daunorubicin activation of Ca^{2+} release is analyzed in the absence and presence of adenine nucleotides, as summarized in Table VI. These results were calculated according to the method of Hill (1910), using a computer program developed by Trimm et al. (1986). For passively loaded SR vesicles, Ca^{2+} release was measured spectrophotometrically, while Ca^{2+} release was measured with the calcium selective electrode from SR vesicles which were actively loaded with either AcPO_4 or ATP as substrate for the pump.

Regardless of the loading method, the presence of caffeine decreased the maximal Ca^{2+} efflux rate (V_{max}) by approximately 50%. Caffeine also increased the degree of cooperativity (h), while not changing the effective dissociation constant ($(K_d)^{1/h}$) of daunorubicin's interaction with the Ca^{2+} release site. $(K_d)^{1/h}$ is the daunorubicin concentration at which the Ca^{2+} efflux rate is

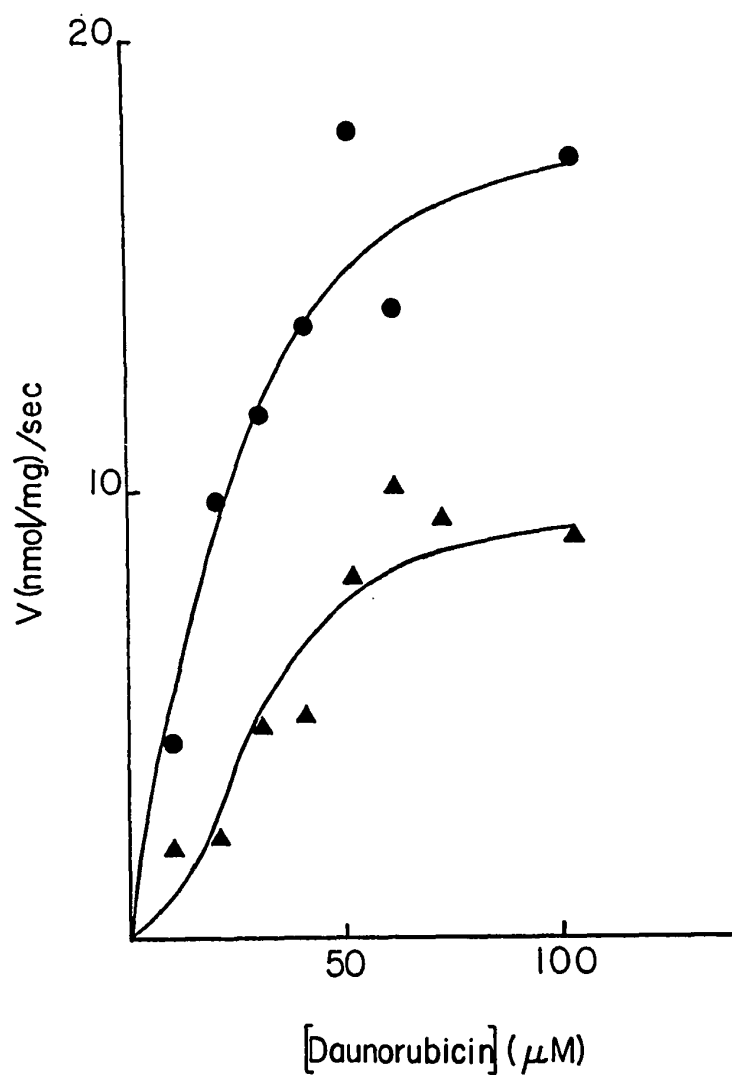


Figure 12. Rate of Ca^{2+} release as a function of daunorubicin concentration in the absence and presence of caffeine. SR vesicles were actively loaded with $30 \mu\text{M}$ Ca^{2+} in the absence (●) or presence (▲) of 2 mM caffeine. Ca^{2+} release is initiated by the addition of the indication concentration of daunorubicin.

half maximal, as derived by the Hill formalism. Comparison of Ca^{2+} release rates acquired in the absence of caffeine reveals that maximal Ca^{2+} release occurs in the presence of ATP and is from 10-40 fold faster than in the absence of

TABLE VI
KINETIC ANALYSIS OF DAUNORUBICIN-STIMULATED Ca^{2+} RELEASE

Loading method	Caffeine conc. (mM)	V_{\max} (nmol/mg) /s	h	$(K_d)^{1/h}$ (μM)
Passive	0	0.9 ± 0.2	1.5 ± 0.3	46 ± 36
	1	0.55 ± 0.02	2.8 ± 0.3	40 ± 16
1 mM AcPO_4	0	3.8 ± 0.1	1.67 ± 0.09	40 ± 8
	1	2.13 ± 0.01	2.20 ± 0.01	46 ± 1
0.5 mM ATP	0	37.0 ± 3.0	1.1 ± 0.1	23 ± 17
	0.7	23.0 ± 5.0	2.5 ± 0.1	23 ± 3

SR vesicles were loaded either passively or actively with 0.5 mM Mg^{2+} -ATP or 1.0 mM AcPO_4 as described in Methods in assay buffer containing the indicated caffeine concentrations. Ca^{2+} release is initiated by the addition of various concentrations of daunorubicin, and the data are analyzed according to the method of Hill. The derived values for the maximal efflux rate (V_{\max}), the Hill coefficient (h), and the concentration of daunorubicin at which the efflux rate is half-maximal (K_d)^{1/h} are determined by the iterative fitting method described by Trimm et al. (1986). Values given are mean \pm SD.

adenine nucleotides (AcPO_4 and passive). ATP also appears to sensitize the Ca^{2+} release mechanism to daunorubicin, since the effective dissociation constant for daunorubicin is decreased by a factor of two in the presence of ATP.

Caffeine Inhibition of Anthraquinone-induced Ca^{2+}

Release is Reversible. The reversibility of caffeine block

on anthraquinone-stimulated Ca^{2+} release was assayed. In the presence of 2 mM caffeine the rate of anthraquinone-induced Ca^{2+} release was reduced. The SR was then pelleted and washed to remove both anthraquinone and caffeine. The pellet/wash process resulted in a completely viable preparation such that the SR still actively accumulated Ca^{2+} . Addition of anthraquinone to this preparation resulted in the rapid release of Ca^{2+} which was inhibitable by the subsequent addition of caffeine.

Anthraquinones Interact with the Ca^{2+} Release Channel via an Oxidation-Reduction Reaction

To determine if anthraquinones stimulate Ca^{2+} release via an oxidation reaction, the effect of reducing agents on the ability of mitoxantrone to stimulate Ca^{2+} release from SR vesicles were measured.

Reduction by Dithionite Inhibits Mitoxantrone-stimulated Ca^{2+} Release. We have shown (Figure 5) that mitoxantrone is the most potent stimulator of Ca^{2+} release from the SR. Pretreatment of mitoxantrone with a fivefold excess of the reducing agent dithionite is sufficient to reduce the quinone, as determined spectrophotometrically. As seen in Table II, when this reduced mitoxantrone is added to the SR, Ca^{2+} release by the anthracycline is inhibited. Oxidation of the dithionite prior to adding it to the mitoxantrone abolishes its ability to reduce mitoxantrone. When a fivefold excess of previously oxidized dithionite is

added to mitoxantrone and this mixture added to actively loaded SR vesicles, the Ca^{2+} release rate is unaffected by the presence of the dithionite.

In a related experiment, if instead of pretreating the mitoxantrone with reduced dithionite, the dithionite is added directly to the buffer in which the SR has actively accumulated Ca^{2+} , the initial Ca^{2+} release caused by the addition of mitoxantrone is unaffected by the presence of the dithionite. However, on a time scale of approximately 10 seconds, the released Ca^{2+} is reaccumulated by the SR vesicles. Spectrophotometric measurements of the reduction of mitoxantrone by dithionite show that the time required for dithionite to completely reduce the quinone is also on the order of 10 seconds. It appears that chemical reduction of mitoxantrone inhibits mitoxantrone-stimulated Ca^{2+} release from SR vesicles.

Attempts to inhibit quinone-stimulated Ca^{2+} release by pre-treatment with other reducing agents such as dithiothreitol, cysteine, or ascorbate were unsuccessful. When measured spectrophotometrically, there was no change in the absorption spectrum or other evidence of reduction of mitoxantrone caused by these reducing agents. It appears that they were ineffective inhibitors of Ca^{2+} release because they were unable to reduce the quinone. A stronger reducing agent such as dithionite is needed to reduce

mitoxantrone and thus to inhibit Ca^{2+} release caused by this anthraquinone.

Ca^{2+} Release is not Stimulated by Superoxide. While extended use of anthracycline antibiotics, such as doxorubicin, is known to cause extensive damage to cardiac tissue, the primary site of this damage is not known. It has been proposed that non-specific oxidation caused by free radicals are responsible for anthraquinone cardiotoxicity (Doroshov et al., 1983). Since doxorubicin, mitoxantrone, and daunorubicin are quinones, they produce superoxide (O_2^-) by the mechanism of redox cycling. It is feasible that anthraquinones might stimulate Ca^{2+} release via a non-specific interaction with superoxide.

To determine if anthraquinone-stimulated Ca^{2+} release was caused by superoxide generated during the redox cycling of mitoxantrone or doxorubicin, 0.2 mg/ml superoxide dismutase was added to the SR prior to the addition of the anthraquinone. Superoxide dismutase catalyzes the aqueous disproportionation of superoxide to H_2O_2 and molecular oxygen, thus removing superoxide from possible interaction with the Ca^{2+} release system. The presence of superoxide dismutase had no effect on the Ca^{2+} release rate triggered by either mitoxantrone or doxorubicin. Thus, neither superoxide nor superoxide dismutase interact with the Ca^{2+} release system. It appears that anthraquinones induce Ca^{2+}

release by directly oxidizing some component of the Ca^{2+} release mechanism of the SR membrane.

DISCUSSION

In this chapter we have examined the interaction between quinones, caffeine, and the Ca^{2+} release mechanism of skeletal muscle SR.

Anthraquinones are shown to be extremely potent stimulators of Ca^{2+} release from SR vesicles. Naphthoquinones, such as menadione and plumbagin, at approximately 50 μM stimulate Ca^{2+} release from SR vesicles, but they are much less effective than the anthraquinones. Benzoquinones are totally ineffective in stimulating Ca^{2+} release from SR vesicles, as were most of the naphthoquinones tested. The ability of anthraquinones to stimulate Ca^{2+} release from SR vesicles is shown to depend on the anthraquinone concentration and to depend on the free Ca^{2+} concentration. Anthraquinone-stimulated Ca^{2+} release is also inhibited by millimolar Mg^{2+} and submicromolar ruthenium red, and is stimulated by adenine nucleotides. The Ca^{2+} release activity is specific for SR derived from the terminal cisternae region (TSR). These results demonstrate that anthraquinones interact with the Ca^{2+} release mechanism of SR vesicles.

Since mitoxantrone induces Ca^{2+} release via the Ca^{2+} release mechanism, we would expect that in a more intact

system such as a chemically skinned psoas muscle fiber, anthraquinones would also induce contractions. As shown in Figure 8, micromolar concentrations of mitoxantrone induce transient contractions that are completely inhibited by ruthenium red. Mitoxantrone appears to trigger contraction by releasing the same Ca^{2+} stores as that mobilized by caffeine (i.e. Ca^{2+} accumulated by the SR). This observation is similar to that reported by Zorzato et al. (1985) using doxorubicin as the Ca^{2+} releasing agent.

The binding of [^3H]ryanodine serves as a structural and functional probe for the Ca^{2+} release channel. [^3H]Ryanodine binding has been shown to be modified by Ca^{2+} , Mg^{2+} , adenine nucleotides, caffeine, and ruthenium red (Pessah et al., 1986, 1987; Lai et al. 1987, 1988; Campbell et al., 1987; Inui et al., 1987). Modulation of Ca^{2+} release by these compounds results in modification of a ryanodine binding site which is accessible to ryanodine only when the channel is in the open state.

Caffeine is known to decrease the threshold for Ca^{2+} activation of [^3H]ryanodine binding to TSR membranes. In the presence of 1 mM Mg^{2+} , 20 mM caffeine has been shown to increase the Ca^{2+} binding affinity associated with the [^3H]ryanodine receptor by about twenty fold (Pessah et al., 1987). This study shows that doxorubicin induces a similar concentration dependent increase in Ca^{2+} dependent [^3H]ryanodine binding, as derived from Figure 9 and Table

III. Not only does doxorubicin increase the Ca^{2+} sensitivity of [^3H]ryanodine binding, similar to that of caffeine, but it is considerably more potent. Activation of [^3H]ryanodine binding to TSR membranes by 60 μM doxorubicin is found to be 1.65 times greater than that of 60 mM caffeine. Finally, we have observed that an increase in the concentration of caffeine results in a decrease in the level of doxorubicin-stimulated [^3H]ryanodine binding (Table V). These results indicate that the mechanism by which anthraquinones stimulate Ca^{2+} release from the SR involves a direct interaction with the [^3H]ryanodine receptor complex.

Caffeine not only reduces the level of anthraquinone-stimulated [^3H]ryanodine binding, but it also reduces the rate of Ca^{2+} efflux from SR vesicles (Figure 11). The interaction between caffeine and anthraquinone binding sites is examined by measuring the rate of Ca^{2+} release from SR vesicles as a function of daunorubicin concentration, both in the absence and presence of caffeine (Table VI, Figure 12). Table VI shows that the degree of cooperativity between daunorubicin binding sites is enhanced by the presence of caffeine (h increases). Despite this increase in cooperativity, the effective dissociation constant (i.e., the concentration of daunorubicin at which the Ca^{2+} efflux rate is half maximal, K_d/Ca^{2+}) is not changed by caffeine. The increase in daunorubicin cooperativity induced by caffeine is similar to the finding that caffeine increases

the cooperativity of Ca^{2+} activation of ryanodine binding (Pessah *et al.*, 1987).

In addition to causing an increased interaction between daunorubicin binding sites, caffeine is also seen to decrease the maximal Ca^{2+} release rate. Using three different protocols, we observe that 1 mM caffeine causes an approximate 50% decrease in the maximal Ca^{2+} release rate induced by daunorubicin (Table VI). A decrease in the Ca^{2+} release rate without affecting the effective binding constant is characteristic of a non-competitive interaction between the anthraquinone and caffeine. This suggests that caffeine acts to increase the interaction between the anthraquinone and Ca^{2+} binding sites.

Although both the caffeine and anthraquinone binding sites interact strongly with each other, kinetic analysis suggests that these two sites are distinct. Binding of ligand to either binding site results in an enhancement of the Ca^{2+} sensitivity of [^3H]ryanodine binding. However, anthracyclines dramatically stimulate maximal [^3H]ryanodine binding, while caffeine does not. In addition, the binding of caffeine to its site results in an increase in the degree of cooperativity of daunorubicin-induced Ca^{2+} release (Table VI), while the binding of anthraquinone to its site does not result in a similar increase in the cooperativity of Ca^{2+} activation of ryanodine binding (Table III). These results suggest that millimolar concentrations of caffeine act to

non-competitively reduce the level of anthraquinone-stimulated [^3H]ryanodine binding.

Quinones, which readily participate in oxidation-reduction reactions, play a central role in many biological electron transport systems. Given the previous observation that Ca^{2+} release can be triggered by the oxidation of sulfhydryls (Trimm *et al.*, 1986; Abramson *et al.*, 1988), we were interested if anthraquinones also trigger Ca^{2+} release via an oxidation reaction. Chemical reduction of the anthraquinone with dithionite inhibited its Ca^{2+} release activity. Control experiments with oxidized dithionite indicate that side or end products of dithionite oxidation are not responsible for this inhibition. Also, reduced oxygen species generated during quinone redox cycling are not responsible for triggering Ca^{2+} release from SR vesicles. Addition of superoxide dismutase does not at all alter the Ca^{2+} release rates triggered by anthraquinones. Thus, superoxide produced during redox cycling does not induce Ca^{2+} release. It appears as if there is a direct oxidative coupling between the quinones and the Ca^{2+} release mechanism of the SR.

The anthraquinones doxorubicin and daunorubicin are commonly used anticancer agents. Unfortunately, these compounds induce a chronic cardiotoxicity which is progressive, and often fatal. One of the leading hypotheses for the molecular mechanism of this cardiotoxicity involves

anthraquinone generated free radical damage and non-specific oxidation of cardiac membranes (Doroshov et al., 1983).

There are a number of morphological and biochemical changes which point to an interaction of anthracyclines with the SR membrane. Most notable are extensive vacuolization of the SR in both cardiac and skeletal muscles (Ferrans, 1978; Doroshov et al., 1985), increased Ca^{2+} permeability in skeletal muscle SR (Zorzato et al., 1985), and decreased ability of cardiac SR to actively accumulate Ca^{2+} (Boucek et al., 1987). However, this study reports that anthraquinones directly interact with the Ca^{2+} release channel of skeletal muscle SR. Other investigators have verified that anthraquinones also directly interact with the Ca^{2+} release channel from cardiac muscle SR (Kim et al., 1989; Pessah et al., 1990). Therefore, it is possible that the cardiotoxic effects of anthraquinones are, instead, due to their interaction with an anthraquinone binding site on the Ca^{2+} release channel.

ROSE BENGAL ACTIVATES THE CALCIUM RELEASE CHANNEL
FROM SKELETAL MUSCLE SARCOPLASMIC RETICULUM

SUMMARY

Nanomolar concentrations of rose bengal have been shown to stimulate the rapid release of Ca^{2+} from skeletal muscle sarcoplasmic reticulum (SR) vesicles and to inhibit the binding of ryanodine to its site (Stuart, 1992). This chapter shows that following fusion of SR vesicles to a bilayer lipid membrane (BLM), nanomolar concentrations of rose bengal activate single channel activity in the presence of a broad spectrum light source. This effect of rose bengal is shown to be independent of the Ca^{2+} concentration. It is also shown that rose bengal does not activate the K^{+} channels present in the SR. In addition, the ryanodine induced modification of the Ca^{2+} release channel is shown to be reversed by the addition of rose bengal. This effect is correlated with the observation that rose bengal displaces bound [^3H]ryanodine from SR vesicles. These observations indicate that photooxidation of rose bengal stimulates Ca^{2+} release by directly interacting with the [^3H]ryanodine binding complex.

INTRODUCTION

Rose bengal is a photooxidizing dye of the xanthene family. Originally synthesized by Gnehm (1885) as a coloring for fabric, its name is related to the red spot worn by Bengali women to symbolize marriage (Neckers, 1988). Photoactivation of rose bengal in the presence of oxygen leads to the rapid generation of reactive oxygen intermediates such as superoxide (O_2^-), hydroxyl (OH^\cdot), and singlet oxygen (1O_2). These intermediates have been implicated in a variety of aspects of cellular injury.

The effect of abnormal quantities of reactive oxygen species on living tissue falls under the general heading of oxidative stress. Since several biological processes result in the production of free radicals, the body has developed enzymatic defense mechanisms (e.g., catalase, superoxide dismutase, glutathione peroxidase) and nonenzymatic antioxidants (e.g., vitamin E, ascorbate, vitamin A, and glutathione) (Cadenas, 1985). The physiological system becomes stressed when pathologic processes either inhibit these free radical scavenging systems or overwhelm them.

While much work surrounding the study of free radicals has focused on ischemia in the heart, lipid peroxidation, redox cycling, and enzymatic reduction (for review, see Sies, 1985), we have examined the effects of reactive oxygen species on skeletal muscle SR. The SR and the sarcolemma

appear to be especially sensitive to reactive oxygen species (Manning et al., 1984; Hess et al., 1984; Kim et al., 1987; Kukreja et al., 1988).

In a previous paper rose bengal was shown to stimulate the rapid release of Ca^{2+} from SR vesicles (Stuart et al., 1992). This effect of rose bengal was found to be independent of the Mg^{2+} concentration and required the presence of light. It was found that stimulation of rose bengal-induced release could be inhibited by removal of oxygen from the system. Additionally, the presence of histidine, an active scavenger for $^1\text{O}_2$, inhibited rose bengal-induced release, while superoxide dismutase had no effect. Even though photoactivation of rose bengal yields other reactive oxygen species, Stuart concluded that $^1\text{O}_2$ was most likely responsible for Ca^{2+} release.

This study was undertaken to extend the above described results to a single channel incorporated in the BLM and to further determine the nature of the interaction between rose bengal and the Ca^{2+} release system of SR.

In this chapter all figures were generated by E. Buck, with the following exceptions: Figure 16 was generated by J. Stuart at Portland State University, Figure 17 was generated by H. Xiong at Portland State University, and Figure 18 was generated by Pessah et al. at University of California, Davis. Stuart, Xiong, and Pessah were collaborators on the associated publication and the figures were included here

for completeness. This work was published in the Archives of Biochemistry and Biophysics (Xiong et al., 1992).

METHODS AND MATERIALS

Preparation of SR Vesicles

For all Ca^{2+} flux studies, and for single channel measurements, rabbit skeletal muscle sarcoplasmic reticulum vesicles were prepared according to the method of MacLennan et al., as described under "Preparation of SR Vesicles" in Chapter II.

Protein concentrations were determined as described in Chapter II.

Bilayer Lipid Membrane Studies

Reconstitution experiments were carried out by fusion of SR vesicles to a planar bilayer lipid membrane (BLM) as described in detail under "Bilayer Lipid Membrane Studies" in Chapter II, with the following modification: For those experiments in which rose bengal treated protein was exposed to light, the bilayer was illuminated with a halogen incandescent lamp of approximately 8000 lux, measured at the sample.

Measurement of Ca^{2+} Efflux

SR vesicles were passively loaded by incubation overnight at 0°C in a medium containing 100 mM KCl, 5 mM MgCl_2 , 1 mM $^{45}\text{CaCl}_2$, 50 mM HEPES, pH 7.0, at a protein

concentration of 10 mg/ml. The vesicles were then diluted 50-fold into a buffer containing 100 mM KCl, 5 mM MgCl₂, 50 mM Hepes, pH 7.0, with various additions of Ca²⁺ and EGTA. The final free Ca²⁺ concentration was calculated using stability constants reported by Fabiato and Fabiato (1979).

As a function of time, the amount of ⁴⁵Ca²⁺ remaining in the vesicles was measured by filtering aliquots of SR through a 0.45 μ m millipore filter. The samples were washed with 1 ml of an identical buffer containing 5 mM CaCl₂ and 5 mM MgCl₂. The amount of ⁴⁵Ca²⁺ remaining on the filter was measured by scintillation counting. The Ca²⁺ efflux rate was determined from the slope of the ⁴⁵Ca²⁺ remaining in the vesicles as a function of time.

In experiments designed to measure the effect of light on rose bengal-induced release, the samples were irradiated with a 360 Watt broad spectrum light source (intensity of approximately 10,000 lux, measured at the sample). A beaker of water was placed between the light source and the sample to screen out the effects of infrared light. Several experiments were also carried out in semidark conditions to minimize the effects of ambient lighting.

[³H]Ryanodine Binding Dissociation Assay

For all [³H]ryanodine binding studies, rabbit skeletal muscle sarcoplasmic reticulum vesicles were prepared according to the method of Inui et al., as described in

detail under "Preparation of SR for [^3H]Ryanodine Binding Studies" in Chapter II.

Junctional SR membranes were assayed for [^3H]ryanodine binding as described in detail under "[^3H]Ryanodine Binding Assay" in Chapter II, with the following exception: During the incubation procedure the samples were exposed to either 50 or 500 nM rose bengal either in the presence of white light (6500 lux) or in near darkness for various amounts of time. In all other respects the procedures were the same and the assays were quenched as described.

Materials

All reagents were analytical grade. Dithiothreitol and Hepes were obtained from Research Organics (Cincinnati, OH). Imidazole was purchased from Aldrich Chemical Co. [^3H]Ryanodine was purchased from New England Nuclear (Wilmington, DE) and ryanodine-dehydroryanodine was purchased from Agrisystems Int. (Wind Gap, PA). $^{45}\text{Ca}^{2+}$ was purchased from ICN (Irvine, CA). All other chemicals were obtained from Sigma Chemical Co. (St. Louis, MO).

RESULTS

Rose Bengal Activates the Ca^{2+} Release Channel from SR

The effect of rose bengal on SR vesicles fused to the BLM was examined. Figure 13, trace A shows a single Ca^{2+} channel gating in the presence of an asymmetric 5:1 CsCl gradient with 5 μM CaCl_2 on the *cis* side of the BLM. The

addition of 500 nM rose bengal, in the presence of light, increased channel open probability (P_o) from a control value of 0.28 to 0.88 (trace B). At these submicromolar concentrations of rose bengal, exposure to a broad spectrum

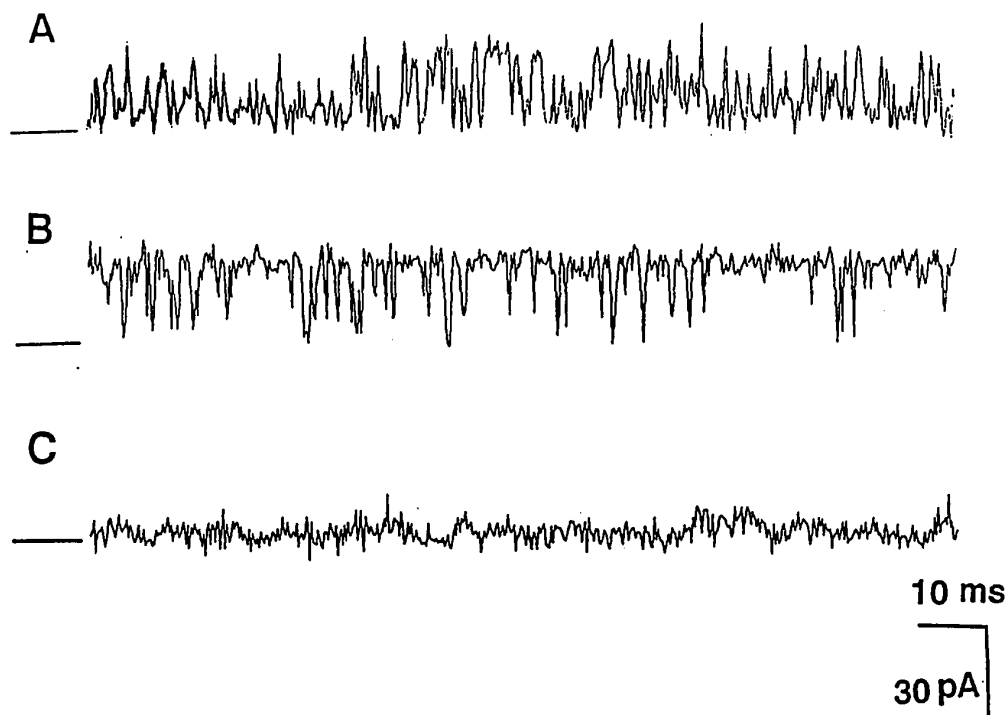


Figure 13. Rose bengal plus light activates the Ca^{2+} release channel. Single channel current fluctuations in a 5:1 CsCl gradient after fusion of SR vesicles to a BLM. (A) In the presence of 5 μM Ca^{2+} *cis*, the open probability (P_o) was 0.29. (B) Addition of rose bengal in the presence of a 8000 lux light source activated the channel ($P_o=0.88$). (C) Addition of 10 μM ruthenium red.

light source is necessary to activate the channel. In trace C, addition of 10 μM ruthenium red completely blocks the rose bengal activated channel. Figure 14 shows that although channel gating activity is stimulated, the conductance and

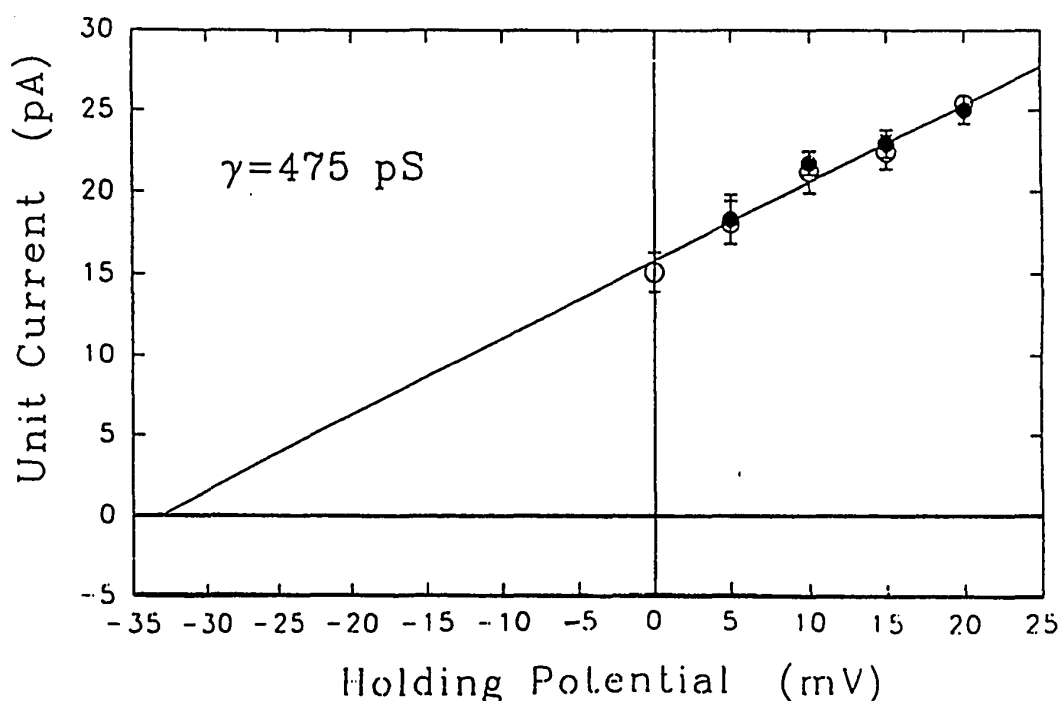


Figure 14. The selectivity of the Ca^{2+} release channel is unaffected by rose bengal. The data in Figure 13 was collected at different holding potentials in the absence (●) and presence (○) of rose bengal and light. The single channel conductance was calculated to be 475 pS ($n=5$).

selectivity of the channel remains unaffected by photooxidation of rose bengal. A calculation of the slope

from this plot yields a conductance of 475 pS. Both data sets (with and without rose bengal) have the same slope or conductance. The voltage intercept at zero current is related to the cation vs. anion permeability (the selectivity) of the membrane. It is seen that in the presence of rose bengal the channel remained highly cation selective ($P_{Cs+}/P_{Cl-} = 13$).

Rose Bengal does not Activate SR Cl^- Channels. Cl^- channels are present in relative abundance in the SR membrane. In BLM experiments, these channels are not regulatable and present themselves as a non-specific background current. The magnitude of the current due to these channels is seen to vary from one SR preparation to the next. Nevertheless, rose bengal activation of the Ca^{2+} channel resulted in no modification of either the background current level or the voltage intercept at zero current. Therefore, the Cl^- channels were unaffected by rose bengal.

Rose Bengal does not Activate SR K^+ Channels. Experiments were undertaken to determine if rose bengal is capable of activating K^+ channels which are also present in the SR. Vesicles were fused to the BLM in the presence of a 5:1 KCl gradient. A low Ca^{2+} concentration of 6 nM was maintained by the addition of EGTA. Under these conditions (i.e. a large KCl gradient and a low Ca^{2+} concentration), a K^+ channel was observed (Figure 15, trace A). Addition of 500 nM rose bengal, in the absence of light, had no effect

on these relatively slow fluctuations (trace B). However, upon addition of light, a high conductance, rapidly fluctuating channel was observed (trace C). The measured conductance of this channel (1000 pS) is similar to that reported by Smith et al. (1985) for the conductance of K^+ through the Ca^{2+} release channel. That rose bengal had activated the Ca^{2+} release channel was confirmed by the addition of 5 μM ruthenium red, which completely inhibited the large, rapid fluctuations without abolishing the slow, lower conductance K^+ channel gateings (trace D). Therefore, no stimulation of K^+ channels was observed by the photooxidation of rose bengal.

In addition, Coronado et al. (1979) has reported that Cs^+ inhibits the SR K^+ channel in a concentration dependent manner. The 170 pS K^+ channel observed in this study was inhibited 75% by the addition of 50 mM CsCl (data not shown). These results further indicate that rose bengal acts to preferentially activate the SR Ca^{2+} release channel.

Stimulation of Ca^{2+} Release by Rose Bengal is Independent of Ca^{2+} Concentration

A unique observation is that rose bengal, in the presence of light, activates the Ca^{2+} release channel despite a very low free Ca^{2+} concentration (Figure 15). Similarly, it is shown here that rose bengal-stimulated Ca^{2+}

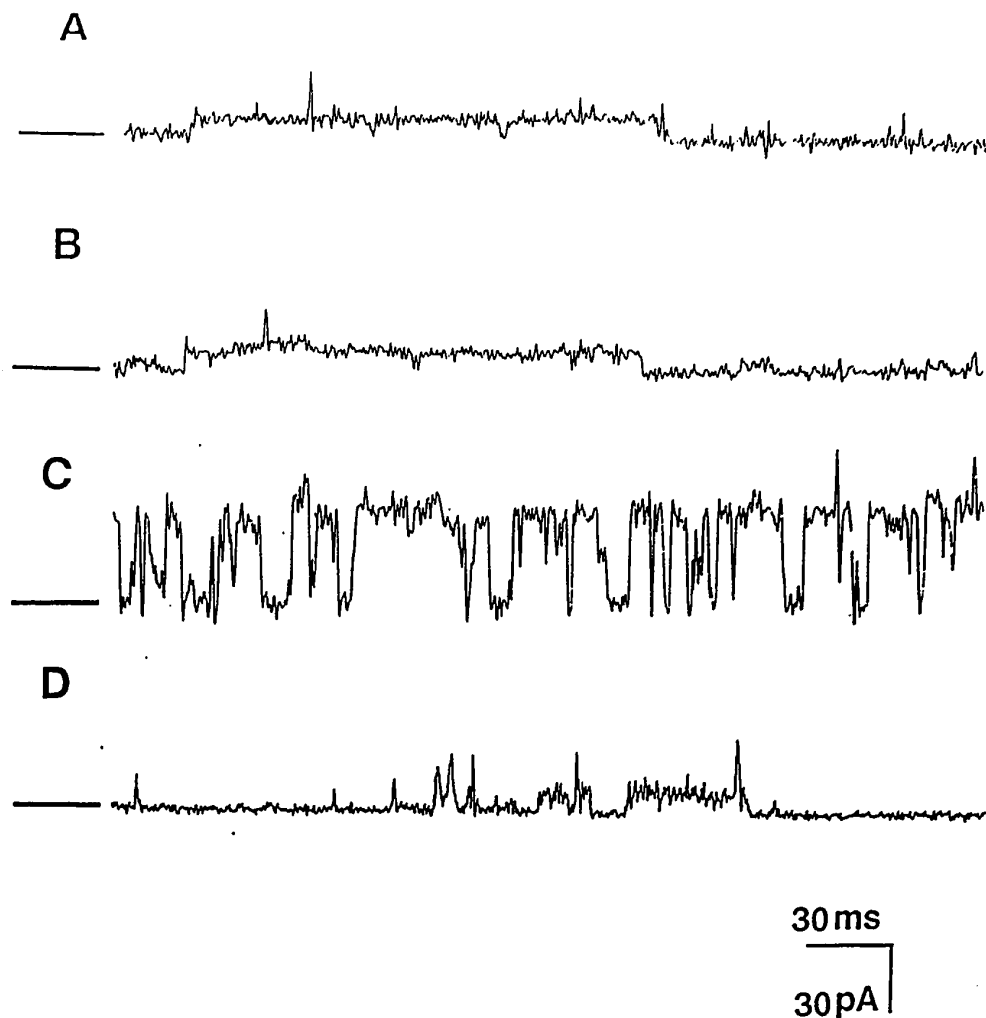


Figure 15. Activation of SR Ca^{2+} channels does not affect K^{+} channels. Fusion of SR vesicles to the BLM was carried out in the presence of a five fold KCl gradient (500 mM KCl, 5 mM Hepes, pH 7.2, *cis*; 100 mM KCl, 5 mM Hepes, pH 7.2, *trans*) as described in Methods. The free Ca^{2+} concentration was 6 nM. (A) Control K^{+} channels. (B) Addition of 500 nM rose bengal in the absence of light. (C) Following exposure to light (8000 lux for 15 s). (D) Addition of 5 μM ruthenium red to the *cis* chamber. The holding potential was +25 mV with respect to ground (*trans* side) for all traces ($n=3$).

release from passively loaded SR vesicles is insensitive to the free Ca^{2+} concentration.

Passive efflux experiments were performed, with and without light, in the presence of rose bengal and 5 mM Mg^{2+} . Figure 16 shows that following activation of Ca^{2+} release by rose bengal and light, no Ca^{2+} dependence of the release rates was observed. This result is in contrast with most other methods of stimulating Ca^{2+} release, which show a marked activation by micromolar Ca^{2+} . In the absence of light, no activation of channel activity was observed and the low release rates and absence of a measurable Ca^{2+} dependence in the control data were due to the high Mg^{2+} concentration used in these experiments.

Comparing the results of experiments performed with SR vesicles with those performed with a single channel in the BLM, it is clear that rose bengal stimulation of the Ca^{2+} release channel is independent of the Ca^{2+} concentration.

Activation of the Ca^{2+} Release Channel by Rose Bengal is Side Independent

Activation of the Ca^{2+} release protein by photooxidation of rose bengal is also independent of the side of the BLM to which the dye is added. In Figure 17, 1 μM rose bengal added to the *cis* side of the bilayer in the presence of light results in the activation of channel activity (trace B). Trace D shows the results of an

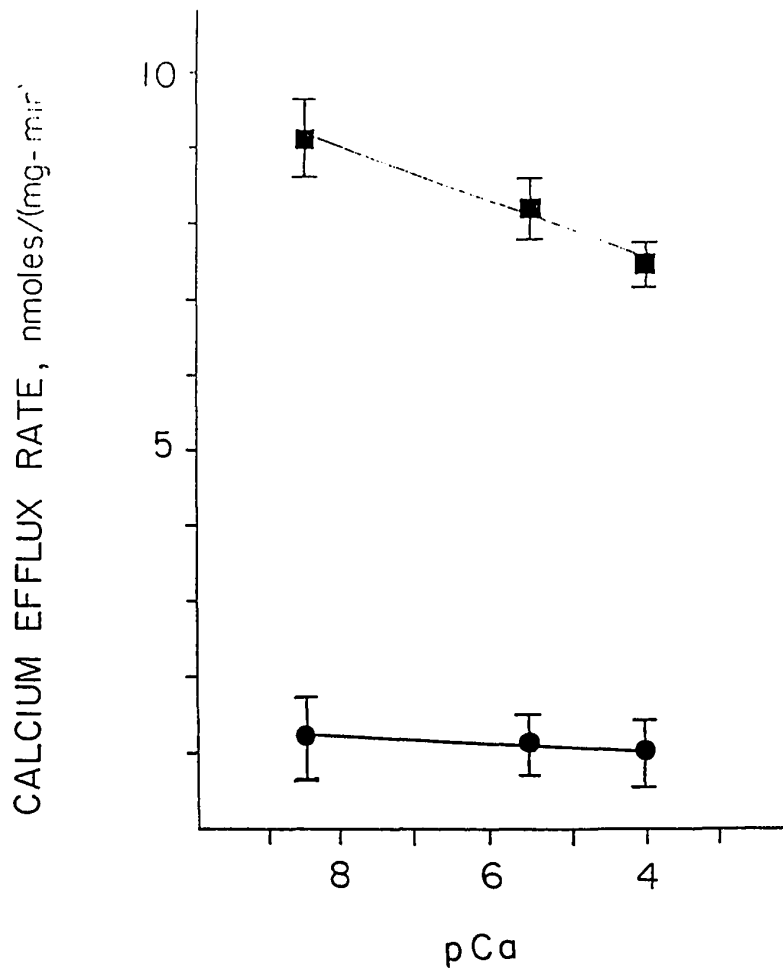


Figure 16. Ca^{2+} dependence of rose bengal-induced Ca^{2+} release from skeletal muscle SR vesicles. SR vesicles were passively loaded with $^{45}\text{CaCl}_2$ as described in Methods at a high Mg^{2+} concentration (5 mM). The vesicles were then diluted into solutions buffered with EGTA- Ca^{2+} which yield the pCa shown on the abscissa. The samples were then irradiated with a 360 Watt light source in the absence (●) or presence (■) of 200 nM rose bengal.

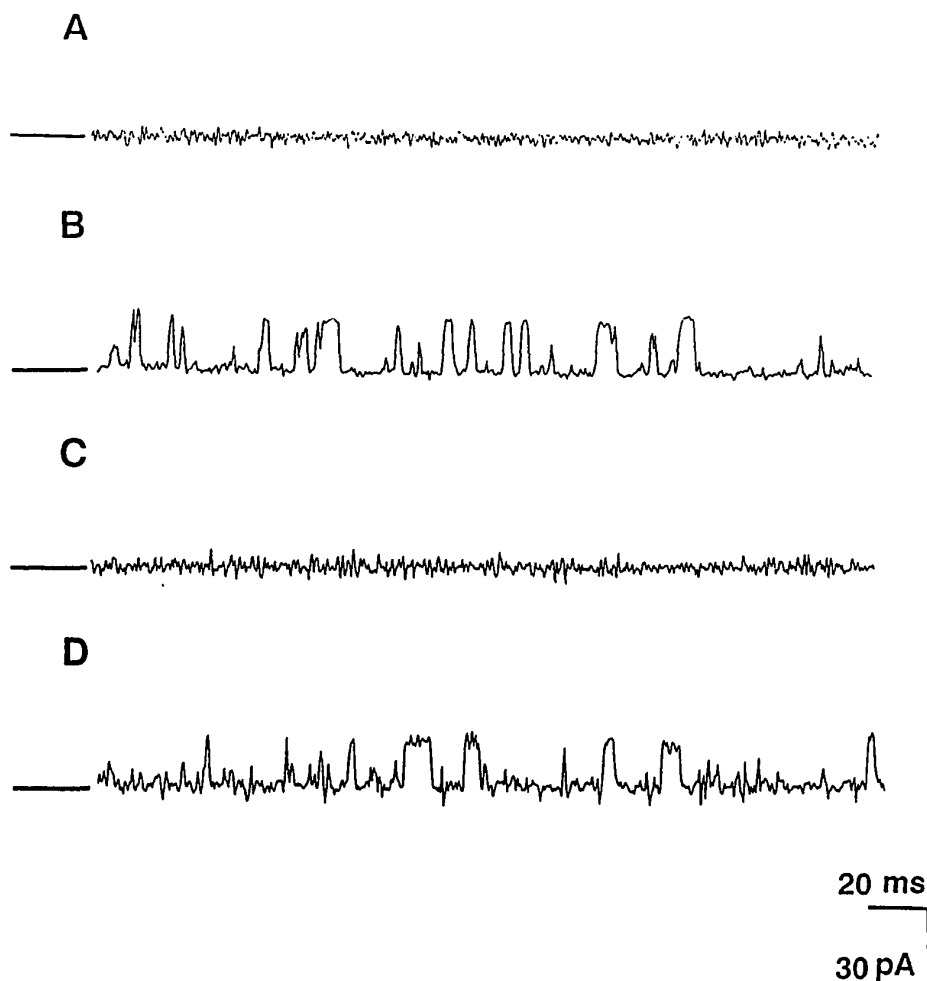


Figure 17. Activation of channel activity by rose bengal is side independent. Following fusion of SR vesicles to the BLM, Ca^{2+} -EGTA was buffered in the *cis* chamber to yield a free Ca^{2+} concentration of 160 nM. (A) Control trace with a 5:1 CsCl gradient as described in Figure 13. (B) Activation of the channel following addition of 1 μM rose bengal to the *trans* chamber in the presence of light. (C) Repeat of trace A (new bilayer). (D) Activation of the channel following addition of 1 μM rose bengal to the *cis* chamber in the presence of light. Holding potential is +20 mV ($n=6$).

identical experiment with the exception that the rose bengal was added to the *trans* side of the bilayer. The channel was again activated. Traces A and C are controls for the *cis* and *trans* sides, respectively.

Rose Bengal Displaces Bound Ryanodine from its Receptor

It has been shown by Stuart et al. (1992) that nanomolar concentrations of rose bengal inhibit highaffinity [^3H]ryanodine binding to its receptor in a light dependent manner. This result was extended by observing that nanomolar concentrations of rose bengal can rapidly displace [^3H]ryanodine from its receptor site. Figure 18 shows that the displacement of bound [^3H]ryanodine by either 50 or 500 nM rose bengal requires the presence of light. In addition, it is observed that the rate of displacement of bound [^3H]ryanodine is dependent on the rose bengal concentration, with higher concentrations of rose bengal displacing [^3H]ryanodine more rapidly.

Rose Bengal Reverses the Effect of Micromolar Ryanodine on the Ca^{2+} Release Channel

It has been well established that micromolar concentrations of ryanodine locks the Ca^{2+} release channel into a slowly fluctuating, half conductance state. The rapid displacement of bound ryanodine seen with the addition of rose bengal and light suggests that rose bengal may also be able to reverse the channel modifying effect of ryanodine.

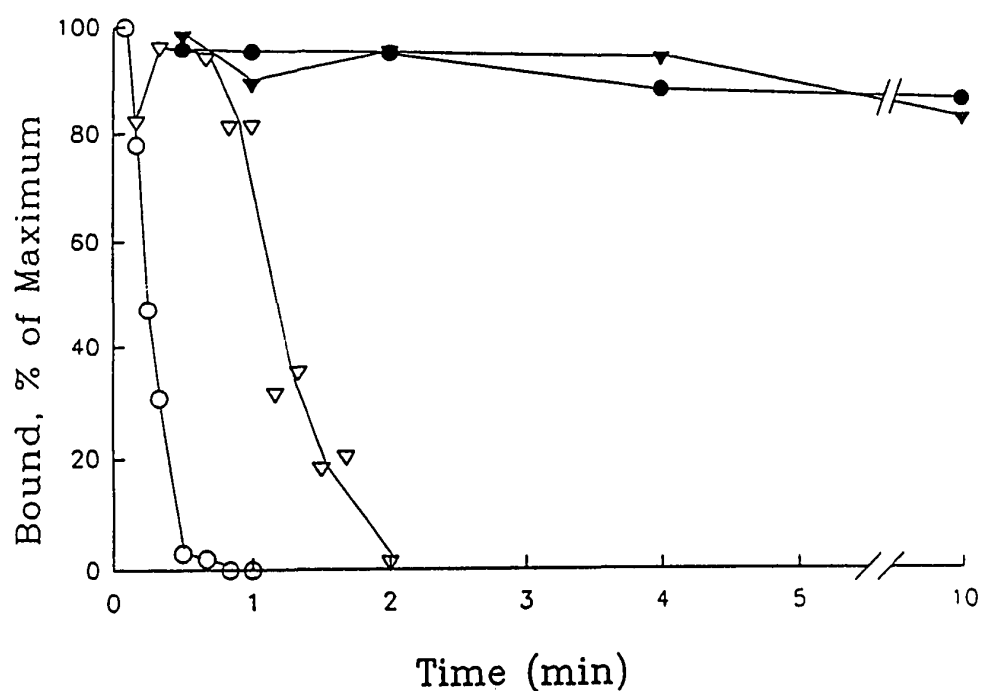


Figure 18. Displacement of [^3H]ryanodine from high-affinity receptor sites by rose bengal is light dependent. Light dependent dissociation of the [^3H]ryanodine receptor equilibrium complex by 50 nM (∇) and 500 nM (\circ) rose bengal. TSR membranes (30 μg) were equilibrated with 1 nM [^3H]ryanodine for 3 h. Rose bengal was added at indicated times in near complete darkness (\bullet , \blacktriangledown), or in the presence of white light (\circ , \triangledown).

Figure 19 shows, as expected, that the addition of 700 nM ryanodine to the *cis* chamber results in a slowly fluctuating channel of approximately 60% full conductance (trace A). The subsequent addition of 600 nM rose bengal to the *cis* chamber, followed by exposure to light, reverses the effect of ryanodine (trace B). The channel is seen to return

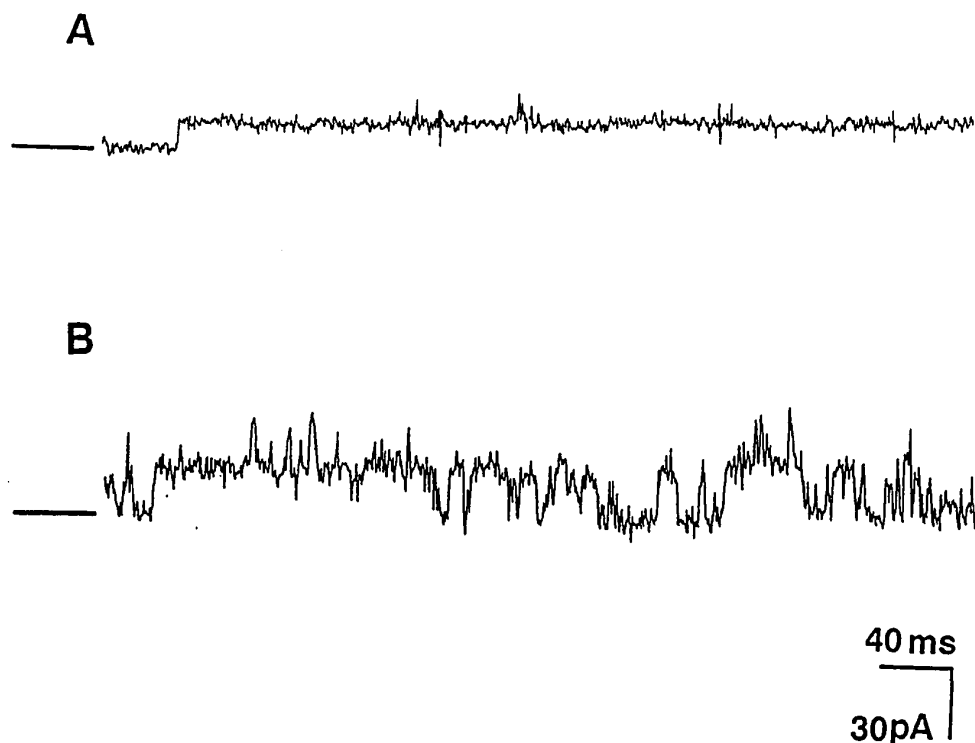


Figure 19. Ryanodine modification of the Ca^{2+} release channel is reversed by rose bengal. Following the protocol described in Figure 17, with the free Ca^{2+} concentration buffered at 100 μM , (A) 0.7 μM ryanodine was added to the *cis* chamber. (B) Following addition of 600 nM rose bengal and activation of light. The holding potential was maintained at +20 mV ($n=3$).

to a rapidly fluctuating, full conductance state.

DISCUSSION

This chapter has shown that photooxidation of rose bengal results in the activation of the Ca^{2+} release channel from SR. In the presence of light, nanomolar concentrations of rose bengal were shown to activate the gating of a rapidly fluctuating, large conductance channel in the SR membrane (Figure 13). The measured conductance (1000 pS) of K^+ through this channel is similar to the K^+ conductance through the Ca^{2+} release channel as reported by Smith et al. (1988). The rose bengal activated channel was completely blocked by micromolar concentrations of the Ca^{2+} channel blocker, ruthenium red (Figure 13). Additionally, analysis of single channel kinetics reveals that while rose bengal stimulated the gating activity of a single Ca^{2+} channel, the ionic selectivity and conductance of this channel remained unchanged (Figure 14). These results indicate that rose bengal acts to activate the Ca^{2+} release channel.

Rose bengal was shown to not activate either the Cl^- or K^+ channels present in the SR. It was observed in Figure 14 that rose bengal does not modify the cation selectivity of the activated channel, nor does it modify the selectivity of the background current. The transport system being activated by rose bengal maintains the cation vs. anion selectivity of the Ca^{2+} release channel. This further indicates that

neither K^+ or Cl^- channels are affected by photooxidation of rose bengal. This conclusion was confirmed by a direct measurement in which the K^+ channels were shown to be unaffected by rose bengal and light (Figure 15).

While SR Ca^{2+} channels are known to be highly cation selective (Smith et al., 1985), they only slightly distinguish between monovalent and divalent cations (Smith et al., 1988). High concentrations of Cs^+ have been shown to inhibit the SR K^+ channel (Coronado et al., 1979). Thus, the use of a high concentration $CsCl$ gradient simplified our analysis in two ways. First, under these ionic conditions the SR K^+ channels are strongly inhibited. Second, the high selectivity of the Ca^{2+} release channel for Cs^+ causes the reversal potential for Cs^+ to be far removed from the reversal potential for Cl^- . Thus, we were able to measure large Cs^+ currents at positive membrane potentials near the reversal potential for Cl^- , where the nonregulatable Cl^- currents were relatively insignificant. These results provide further evidence that photooxidation of rose bengal activates only the Ca^{2+} release channel of the SR.

Stimulation of the Ca^{2+} release channel has been shown to be Ca^{2+} concentration dependent with maximal activation occurring between 1 and 10 μM Ca^{2+} . At Ca^{2+} concentrations as low as 10 nM the channel has been shown to be inhibited (Smith et al., 1988). As shown in Stuart et al. (1992), rose bengal-induced Ca^{2+} release from SR vesicles is insensitive

to both the Ca^{2+} and Mg^{2+} concentrations. This chapter shows that rose bengal activation of the Ca^{2+} release channel is also insensitive to the free Ca^{2+} concentration (Figures 15 and 16). It is likely that the molecular mechanism underlying rose bengal-induced Ca^{2+} release is different from that observed with other activating reagents.

Stuart et al. (1992) has suggested that rose bengal-stimulated Ca^{2+} release from SR vesicles is mediated by singlet oxygen ($^1\text{O}_2$) formed during the photooxidation of the dye. If activation of the Ca^{2+} release channel is via a similar mechanism, it should not matter which side of the BLM the rose bengal is added. The lifetime of singlet oxygen ($^1\text{O}_2$) in H_2O has been measured to be between 2 and 5 us (Cadenas, 1985). Given the high diffusion coefficient of O_2 in water ($D=10^{-9} \text{ m}^2\text{s}^{-1}$), it is likely that $^1\text{O}_2$ can diffuse at least 10 times the thickness of the bilayer before decaying. Thus, $^1\text{O}_2$ formed by photooxidation of rose bengal on one side of the bilayer membrane would still be able to activate Ca^{2+} release on the other side of the bilayer. Therefore, it is not surprising that photoactivation of the release channel is independent of the side to which the rose bengal is added.

In spite of the somewhat unusual mechanism by which of rose bengal stimulates Ca^{2+} release, it is clear that photooxidation of rose bengal induces a direct interaction with the Ca^{2+} release protein from skeletal muscle SR.

PORPHYRIN-INDUCED CALCIUM RELEASE FROM SKELETAL MUSCLE SARCOPLASMIC RETICULUM

SUMMARY

This chapter shows that micromolar concentrations of the porphyrin meso-tetra(4-N-methylpyridyl)porphine tetraiodide (TMP_yP) induces the rapid release of Ca²⁺ from skeletal muscle sarcoplasmic reticulum (SR) vesicles. In particular, TMP_yP-induced Ca²⁺ release is shown to be stimulated by millimolar ATP and micromolar Ca²⁺, and inhibited by millimolar Mg²⁺ and micromolar ruthenium red. TMP_yP is also shown to stimulate high-affinity [³H]ryanodine binding to its receptor. The effect of TMP_yP is to sensitize the receptor to activation by Ca²⁺. Finally, TMP_yP is shown to activate a single Ca²⁺ release channel which has been fused with a bilayer lipid membrane (BLM). The TMP_yP activated channel is shown to be blocked by micromolar ruthenium red and to have a biphasic dependence on the Ca²⁺ concentration in a manner similar to that seen with SR vesicles. These results indicate that porphyrin-induced Ca²⁺ release is caused by a direct interaction of the porphyrin with the Ca²⁺ release protein from sarcoplasmic reticulum.

INTRODUCTION

Porphyrins are prosthetic groups for a large number of biological molecules which carry out diverse roles in nature. The basic structure of a porphyrin consists of a cyclic tetrapyrrole coordinated to a central metal ion. The central ion is usually the primary reactive site of the porphyrin and can determine the porphyrin's biological role. For example, oxygen transport and storage, associated with myoglobin and hemoglobin, are comprised of porphyrin molecules complexed with Fe^{2+} . The cytochromes and chlorophylls, which are associated with electron and energy transfer processes, contain porphyrins complexed with Mg^{2+} , while the coenzymes and cytochromes, which are porphyrins complexed with Co^{2+} , are involved with biocatalysis.

Our interest in the interaction of porphyrins and the Ca^{2+} release mechanism from sarcoplasmic reticulum was motivated by earlier work carried out in this laboratory which demonstrated that the structurally similar phthalocyanine dyes were potent stimulators of Ca^{2+} release from SR vesicles (Abramson et al., 1988).

In this chapter all bilayer work was performed by E. Buck. All other figures were generated by Abramson et al. at Portland State University with the exception of Figures 25, 26, and 27 which were generated by Pessah et al at the University of California, Davis. Abramson and Pessah were

collaborators on the associated publication and the figures were included here for completeness. This work was published in the Archives of Biochemistry and Biophysics (Abramson et al., 1993).

METHODS AND MATERIALS

Preparation of SR Vesicles

For all Ca^{2+} flux studies, and for single channel measurements, rabbit skeletal muscle sarcoplasmic reticulum vesicles were prepared according to the method of MacLennan et al., as described in detail under "Preparation of SR Vesicles" in Chapter II.

Protein concentrations were determined as described in Chapter II.

Measurement of Ca^{2+} Efflux

Ca^{2+} fluxes across SR vesicles were monitored using a calcium selective electrode (WPI, Cal-1), as described in detail under "Active Ca^{2+} Efflux" in Chapter II, with the following modifications: In all experiments not designed to measure the effects of varying ATP concentrations, the uptake of Ca^{2+} was initiated by the addition of 0.5 mM Mg^{2+} -ATP to the solution. Upon completion of Ca^{2+} uptake by the SR, as indicated by the leveling off of the signal, an appropriate concentration of porphyrin (1-60 μM) was added to induce release.

In experiments where the ATP concentration was varied, an ATP regenerative system was used. To maintain the ATP concentration at a fixed level during the experiment, creatine phosphate (5 mM) and creatine phosphokinase (5 U/ml) was added to the SR prior to the addition of the ATP. Since the ATP concentration can affect the free Mg^{2+} concentration, an appropriate amount of Mg^{2+} was added prior to Ca^{2+} uptake to maintain a free Mg^{2+} concentration of 170 μM . Ca^{2+} release was initiated by the addition of 10 μM TMP_{yP} .

In experiments where the Mg^{2+} concentration was varied, the quantity of additional Mg^{2+} necessary to achieve a desired free Mg^{2+} concentration (170-400 μM) was calculated using Mg^{2+} -ATP stability constants described by Fabiato and Fabiato (1979). The Mg^{2+} was added prior to the initiation of Ca^{2+} uptake by the SR. Ca^{2+} release was initiated by the addition of 10 μM TMP_{yP} . In all other respects the experiments were as described in Chapter II.

[3H]Ryanodine Binding Assays

For all [3H]ryanodine binding studies rabbit skeletal muscle sarcoplasmic reticulum vesicles were prepared according to the method of Inui et al., as described in detail under "Preparation of SR for [3H]ryanodine Binding Studies" in Chapter II.

[3H]Ryanodine binding to SR vesicles was determined as described in detail under "[3H]Ryanodine Binding Assay" in

Chapter II, with the following modifications: Junctional SR membranes (30 $\mu\text{g/ml}$) were incubated at 37°C for 2 h in a medium consisting of 250 mM KCl, 15 mM NaCl, 0.8 nM [^3H]ryanodine, 20 mM Hepes-Tris, pH 7.1. Depending on the conditions of the assay, Mg^{2+} (1 mM), caffeine (10 mM), Mg^{2+} -AMP-PCP (0.5 mM), or Ca^{2+} (140 μM + various concentrations of EGTA) were present with and without TMPyP (30 μM) during the incubation procedure.

Equilibrium binding curves were performed in the presence of 1 nM [^3H]ryanodine and varying concentration (0.5-64 nM) of unlabeled ryanodine in an assay medium consisting of 250 mM KCl, 15 mM NaCl, 50 μM CaCl_2 , 20 mM Hepes-Tris, pH 7.1. Samples were incubated for 3 h to assure near steady state conditions and then processed as described in Chapter II. The resulting data were fit to a one-site model using the nonlinear regression program ENZFITTER (Elsevier Biosoft).

In all other respects the experiments were performed as described in Chapter II.

Bilayer Lipid Membrane Studies

Reconstitution experiments were carried out by fusion of SR vesicles to a planar bilayer lipid membrane (BLM). Bilayer formation and vesicle fusion were performed in 500 mM CsCl, as described in detail under "Bilayer Lipid Membrane Studies" in Chapter II, with the exception that 1 mM MgCl_2 was present in the *cis* chamber at all times.

In experiments designed to measure the channel open probability (P_o) as a function of the Ca^{2+} concentration, Ca^{2+} was added to the *cis* chamber in 200-300 μM aliquots to a final concentration of greater than 1.4 mM. After each Ca^{2+} addition, the channel was allowed to stabilize for at least 30 seconds and channel activity was then recorded for at least 1 minute. Following the Ca^{2+} titration, the *cis* chamber was re-perfused with the starting buffer and the experiment repeated with the additional presence of 10 μM TMPyP . The data collected was analyzed with the pCLAMP program (Axon Instruments, Burlingame, CA), as described in Chapter II.

Materials

All reagents were analytical grade. TMPyP and TSPP were purchased from Strem Chemicals Inc. (Newburyport, MA). Dithiothreitol and Hepes were obtained from Research Organics (Cincinnati, OH). [^3H]Ryanodine was purchased from New England Nuclear (Wilmington, DE). Ryanodine-dehydroryanodine was purchased from Agrisystems Int. (Wind Gap, PA). All other chemicals were obtained from Sigma Chemical Co (St. Louis, MO).

RESULTS

Porphyrins Stimulate Ca^{2+} Release from SR Vesicles

Figure 20 shows the rate of Ca^{2+} release as a function of concentration for the porphyrin, TMPyP . Over the

concentration range tested (1-60 μM), TMP_yP induced a concentration dependent increase in the rate of Ca^{2+} release. The data presented in Figure 20 was analyzed according to the method of Hill. The maximal Ca^{2+} release rate (V_{max}), the Hill coefficient (h), and the porphyrin concentration at which the rate of Ca^{2+} release is half-

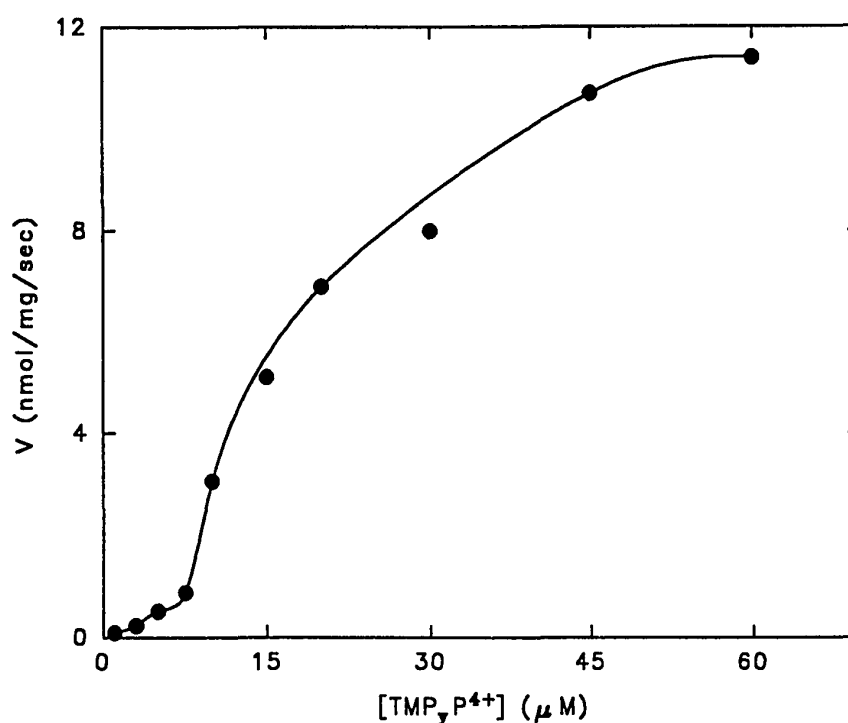


Figure 20. Rate of Ca^{2+} release as a function of TMP_yP concentration. SR vesicles at 0.2 mg/ml were actively loaded in a buffer containing 100 mM KCl, 20 mM Hepes-Tris, 20 μM CaCl_2 , pH 7.0, by addition of 0.5 mM Mg^{2+} -ATP. Prior to addition of porphyrin, the Ca^{2+} concentration was adjusted to 1.5 μM . Ca^{2+} release was initiated by the addition of the indicated amount of TMP_yP . Ca^{2+} release rates were determined from the initial slope of free Ca^{2+} concentration vs. time following addition of the porphyrin.

maximal, $(K_d)^{1/h}$, was determined to be 12.0 ± 0.74 (nmol/mg)/s, 2.10 ± 0.26 , and $18.3 \mu\text{M}$, respectively.

The stimulation of Ca^{2+} release from SR vesicles by many compounds is known to depend on the free Ca^{2+}

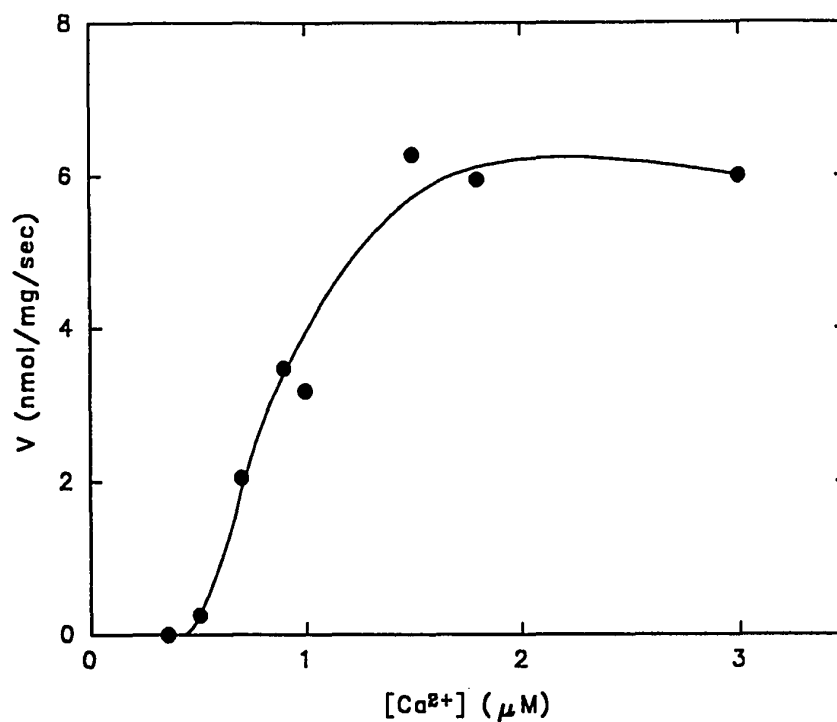


Figure 21. Rate of TMPyP -induced Ca^{2+} release as a function of free Ca^{2+} concentration. SR vesicles were actively loaded as described in Figure 20. Prior to Ca^{2+} release the free Ca^{2+} concentration was adjusted to the value shown on the abscissa. Ca^{2+} release was initiated by the addition of $10 \mu\text{M}$ TMPyP .

concentration. Figure 21 shows that TMPyP -induced Ca^{2+} release is also sharply dependent on the free Ca^{2+} concentration. In these experiments, the Ca^{2+} concentration was adjusted to the desired level (0.4 to $3.0 \mu\text{M}$) by the

addition of Ca^{2+} from a 100x stock, after active loading of the SR. Ca^{2+} release was initiated by the addition of 10 μM TMPyP . Kinetic analysis of Figure 21 revealed that Ca^{2+} activation of TMPyP -induced Ca^{2+} release showed a great deal of cooperativity with a Hill coefficient (h) of 7.6 ± 2.8 . The Ca^{2+} concentration at which the rate of Ca^{2+} release is half-maximal, $(K_d)^{1/n}$, was determined to be 0.93 μM .

Since adenine nucleotides are known to enhance Ca^{2+} release, TMPyP -induced Ca^{2+} release was measured in the presence of a range of ATP concentrations. To preclude any effects which might result from a change in the Mg^{2+} concentration during the ATP titration, the free Mg^{2+} concentration was held constant at 170 μM . The ATP concentration was also maintained constant at all times by the use of a creatine phosphate/creatine phosphokinase regenerative system. The presence of adenine nucleotides stimulated TMPyP -induced Ca^{2+} release (Figure 22).

The stimulatory effects of adenine nucleotides were further examined by comparing the rates of release induced by TMPyP in the presence and absence of ATP. The Ca^{2+} release rate triggered by 10 μM TMPyP was three times faster in the presence of adenine nucleotides than in the presence of the non-adenine nucleotide containing substrate, AcPO_4 (data not shown). In spite of the same amount of Ca^{2+} loading and the same free Mg^{2+} concentration, release was enhanced by ATP.

Two well recognized inhibitors of Ca^{2+} release from SR vesicles are Mg^{2+} and ruthenium red. The sensitivity of TMPyP -induced Ca^{2+} release to inhibition by Mg^{2+} is

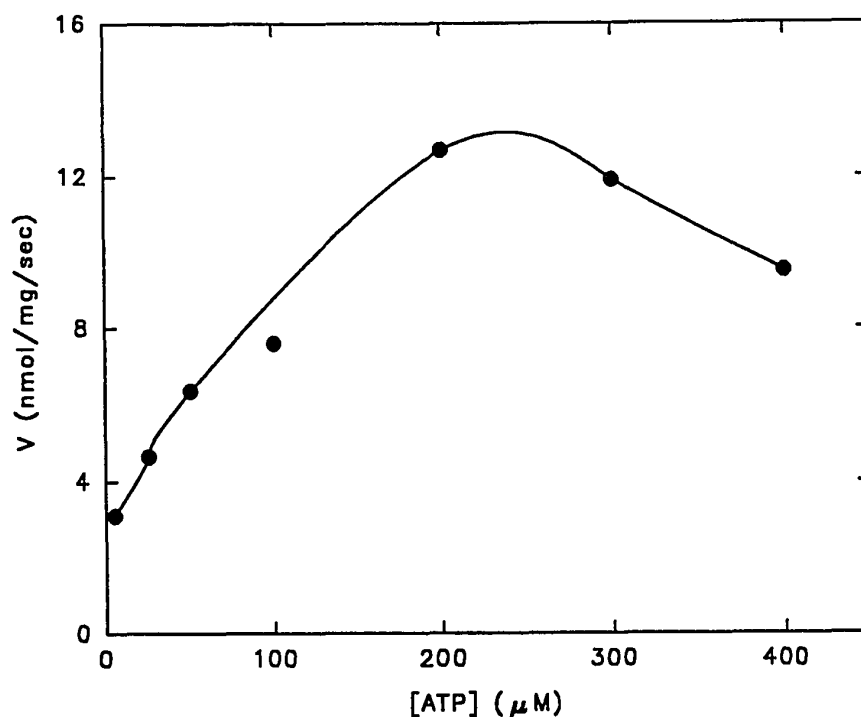


Figure 22. Rate of TMPyP -induced Ca^{2+} release as a function of ATP concentration. SR vesicles actively loaded in as described in Figure 20. The ATP concentration was maintained by an ATP regenerative system consisting of 5 mM creatine phosphate plus 5 U/ml creatine phosphokinase. Mg^{2+} was added at each ATP concentration to maintain a free Mg^{2+} concentration of 170 μM . Ca^{2+} release was initiated by the addition of 10 μM TMPyP .

shown in Figure 23. The concentration at which inhibition was half-maximal (K_i) is approximately 220 μM . Ruthenium red is also a potent inhibitor of Ca^{2+} release induced by TMPyP .

As is shown in Figure 24, the concentration of ruthenium red at which inhibition is half-maximal (K_i) is approximately 7.0 nM.

The anionic porphyrin, tetrasodium-meso-tetra(4-

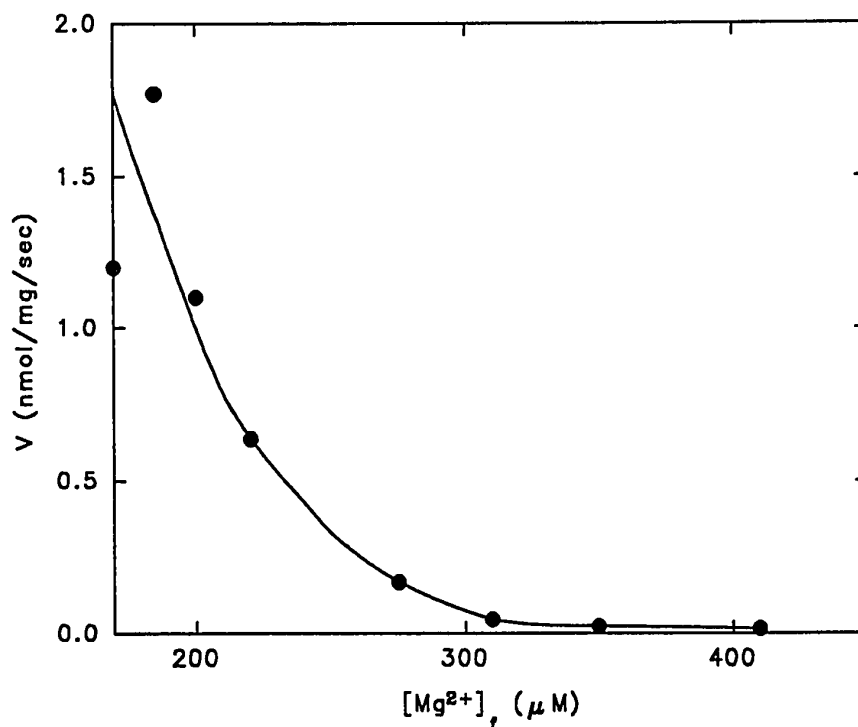


Figure 23. Rate of TMPyP-induced Ca^{2+} release as a function of free Mg^{2+} concentration. SR vesicles were actively loaded with 0.5 mM Mg^{2+} -ATP plus added Mg^{2+} to yield the free Mg^{2+} concentration shown on the abscissa. Ca^{2+} release was initiated by the addition of 10 μM TMPyP.

sulfonatophenyl)porphine dodecahydrate (TSPP) was also assayed for its ability to release Ca^{2+} . TSPP was a considerably less potent stimulator of Ca^{2+} release from SR

vesicles than was the cationic porphyrin TMP_yP. The rate of Ca²⁺ release stimulated by 100 μM TSPP is 0.8 (nmol/mg)/sec, as compared to a release rate of 3.0 (nmol/mg)/sec observed with 10 μM TMP_yP. In spite of this reduced potency, TSPP-induced Ca²⁺ release is also inhibited by submicromolar concentrations of ruthenium red and submillimolar concentrations of Mg²⁺ (not shown).

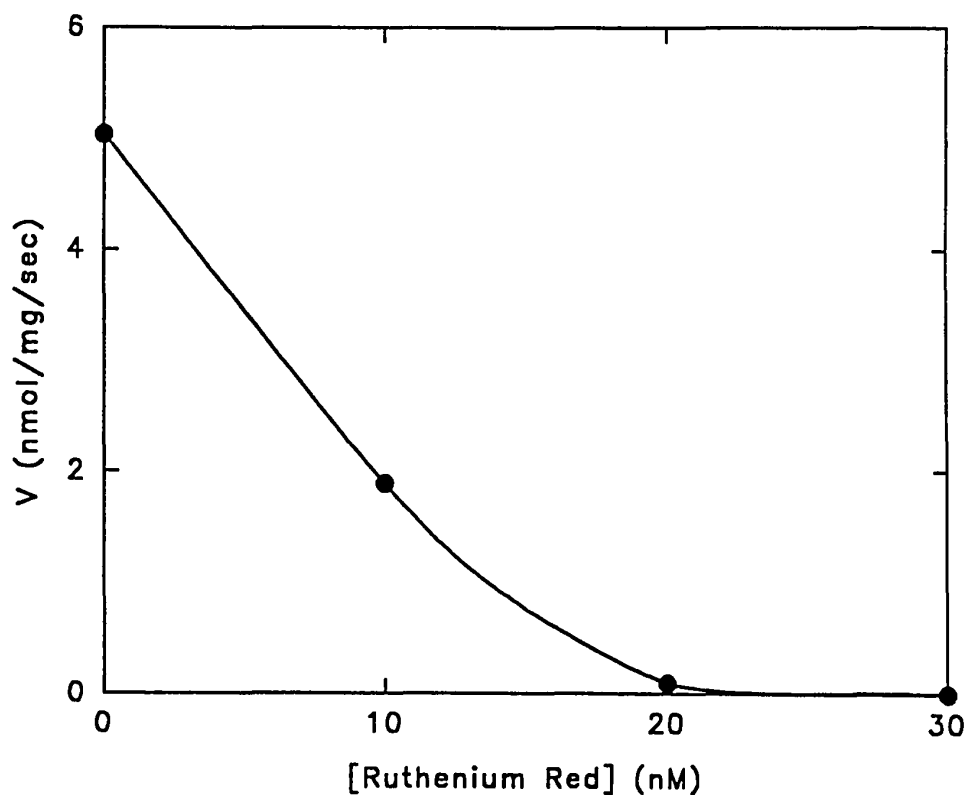


Figure 24. Ca²⁺ release induced by TMP_yP is inhibited by nanomolar concentrations of ruthenium red. SR vesicles were actively loaded as described in Figure 20. Prior to addition of TMP_yP, the indicated amount of ruthenium red was added. Ca²⁺ release was initiated by the addition of 10 μM TMP_yP.

Porphyryns Stimulate [^3H]Ryanodine Binding

To determine the mechanism by which TMPyP influences Ca^{2+} release, we examined the Ca^{2+} dependence of [^3H]ryanodine binding. $30\ \mu\text{M}$ TMPyP , in the absence of Mg^{2+} , was seen to enhance [^3H]ryanodine binding more than two fold (Figure 25A). However, in the presence of $1\ \text{mM}$ Mg^{2+} , $30\ \mu\text{M}$ TMPyP not only increased [^3H]ryanodine binding (as before), but also sensitized the receptor to activation by Ca^{2+} (Figure 25B).

In Chapter III, both caffeine and doxorubicin were shown to decrease the threshold for Ca^{2+} activation (K_d/Ca^{2+}) of [^3H]ryanodine binding without increasing the maximal number of binding sites (B_{max}). In contrast, adenine nucleotides have been observed to increase B_{max} without influencing K_d/Ca^{2+} (Pessah et al., 1987).

In Figure 26A, shows that in the presence of $1\ \text{mM}$ Mg^{2+} and $0.5\ \text{mM}$ AMP-PCP, $30\ \mu\text{M}$ TMPyP enhanced only the Ca^{2+} sensitivity of the ryanodine receptor (K_d/Ca^{2+}) without increasing B_{max} . On the other hand, Figure 26B shows that in the presence of $1\ \text{mM}$ Mg^{2+} and $10\ \text{mM}$ caffeine, $30\ \mu\text{M}$ TMPyP increased only the B_{max} without further effecting K_d/Ca^{2+} . These results indicate that TMPyP influences the ryanodine receptor in a manner similar to doxorubicin (Chapter III), in that both receptor occupancy and Ca^{2+} sensitivity are enhanced.

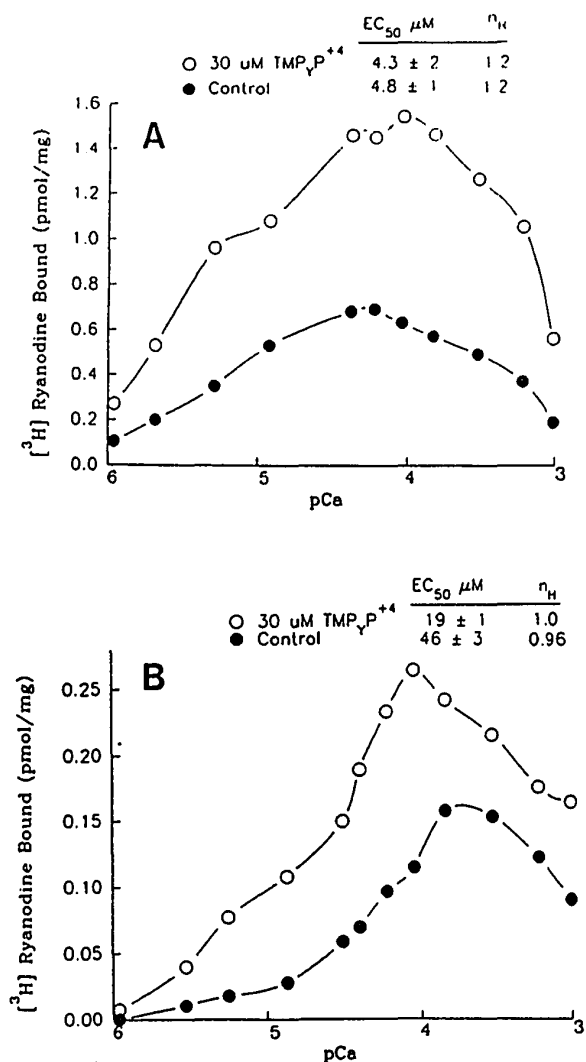


Figure 25. Ca²⁺ dependence of TMP_yP-stimulated high-affinity [³H]ryanodine binding. [³H]Ryanodine binding was carried out as described in Methods. Assay buffer contained either no Mg²⁺ (A) or 1 mM Mg²⁺ (B). Ryanodine binding was measured in the absence (●) or presence (○) of 30 μM TMP_yP. The free Ca²⁺ concentration below 140 μM was obtained by addition of the appropriate amount of EGTA. The half-activation constant (ED₅₀) and Hill coefficient (n_H) are mean ± SD (n=3).

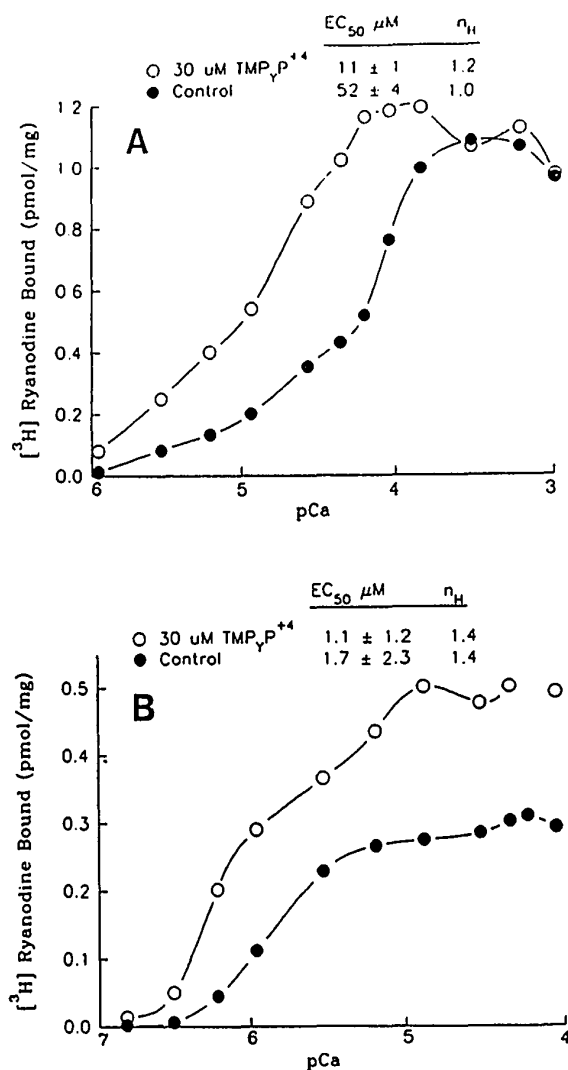


Figure 26. The effect of AMP-PCP and caffeine on $TMPyP$ -stimulated ryanodine binding. $[^3H]$ Ryanodine binding was measured as described in Figure 25. Assay buffer contained either 0.5 mM Mg^{2+} -AMP-PCP (A) or 10 mM caffeine (B). All assay buffers contained 1 mM Mg^{2+} and Ca^{2+} -EGTA buffered as described. Ryanodine binding was measured in the absence (●) or presence (○) of 30 μM $TMPyP$. The free Ca^{2+} concentration below 140 μM was obtained by addition of the appropriate amount of EGTA. The half-activation constant (ED_{50}) and Hill coefficient (n_H) are mean \pm SD ($n=3$).

[³H]Ryanodine equilibrium binding experiments, performed in the absence and presence of 30 μ M TMPyP demonstrate that receptor activation by TMPyP stems from a 30% increase in both the binding affinity and maximal capacity of the SR membranes to bind [³H]ryanodine (Figure 27).

Single Channel Measurements

Figure 28 shows the effect of TMPyP on a single Ca^{2+} release channel fused to the BLM in the presence of 1 mM Mg^{2+} . At this high Mg^{2+} concentration, 600 μ M Ca^{2+} was necessary to activate the channel (trace A). The addition of 10 μ M TMPyP greatly stimulated the channel activity (trace B). Verification that TMPyP had activated the Ca^{2+} release channel is seen in trace C; the TMPyP activated Ca^{2+} channel was completely inhibited by the addition of 10 μ M ruthenium red.

In a separate experiment, the open probability (P_o) of the channel was measured as a function of free Ca^{2+} in the absence and presence of 1 mM Mg^{2+} . In a manner analogous to the ryanodine binding experiment described in Figure 25B, it is seen that the presence of Mg^{2+} sensitizes the reconstituted Ca^{2+} release channel to activation by Ca^{2+} (Figure 29). Despite the fact that the physiological Mg^{2+} concentration is approximately 1 mM, BLM experiments are consistently performed in the absence of Mg^{2+} . As is

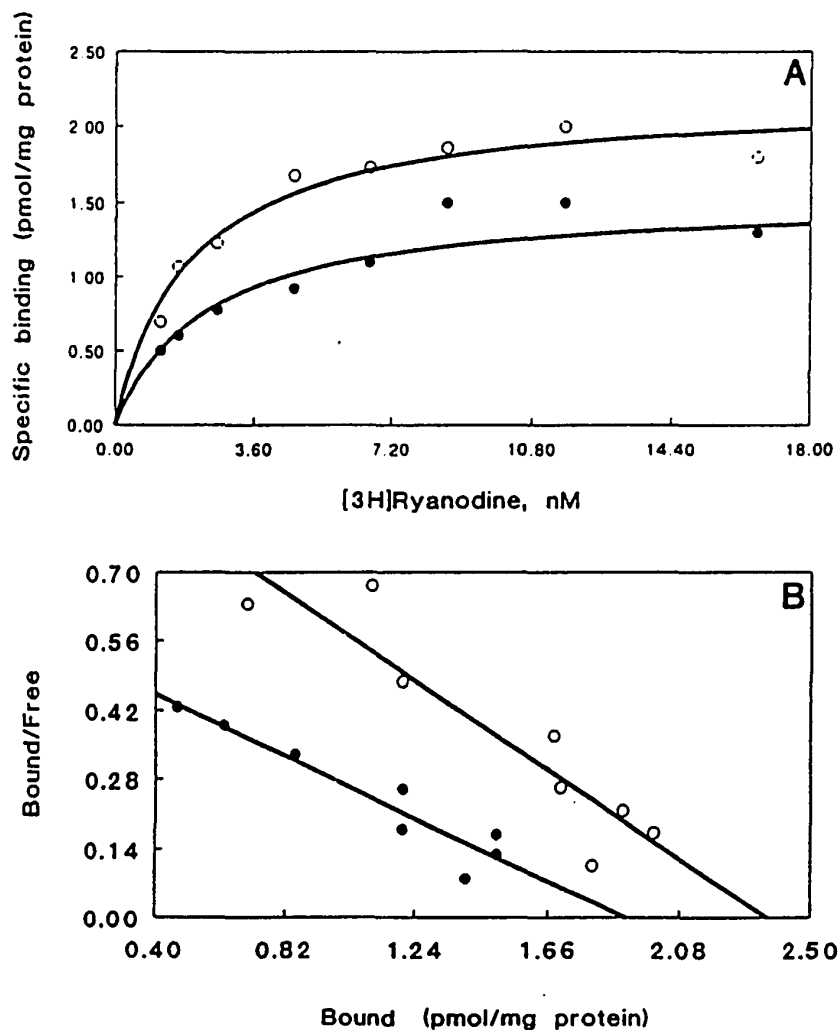


Figure 27. TMPyP stimulates ryanodine binding by altering K_d and B_{max} . Equilibrium binding measurements were generated in the absence (●) or presence (○) of 30 μ M TMPyP. Data shown are representative of three determinations. Scatchard analysis gave K_d and B_{max} values (mean \pm SD) of 2.6 ± 0.2 and 1.7 ± 0.1 for control, and 2.0 ± 0.1 and 2.2 ± 0.1 for TMPyP treated SR.

shown in Figure 29, the Ca^{2+} concentration required to activate the channel in the presence of 1 mM Mg^{2+} is considerably higher than has been observed in the absence of Mg^{2+} .

Figure 30 is a plot of the single channel current as a function of the holding potential in the absence and presence of 1 mM Mg^{2+} . Calculations yielding the conductance of the channel show no change due to the high Mg^{2+} concentration, measuring 451 ± 40 pS in the absence of Mg^{2+} , and 503 ± 72 pS in the presence of Mg^{2+} . In contrast, Mg^{2+} is seen to decrease the voltage intercept at zero current, and hence the cation vs. anion selectivity of the channel. Analysis of this data reveals a change in selectivity ($\text{P}_{\text{Cs}^+}/\text{P}_{\text{Cl}^-}$) from 45.1 in the absence of Mg^{2+} to 3.4 in the presence of 1 mM Mg^{2+} .

Effect of Reducing Agents

To investigate if porphyrins induced Ca^{2+} release via an oxidation reaction, the effects of the reducing agents dithiothreitol (DTT) and dithionite were examined. A concentration of 1.0 mM DTT had no effect on Ca^{2+} release induced by 10 μM TMP_yP . Additionally, the absorption spectrum of TMP_yP was not altered by DTT. Since DTT did not reduce TMP_yP , it was not surprising that DTT had no effect on porphyrin-induced Ca^{2+} release from SR vesicles.

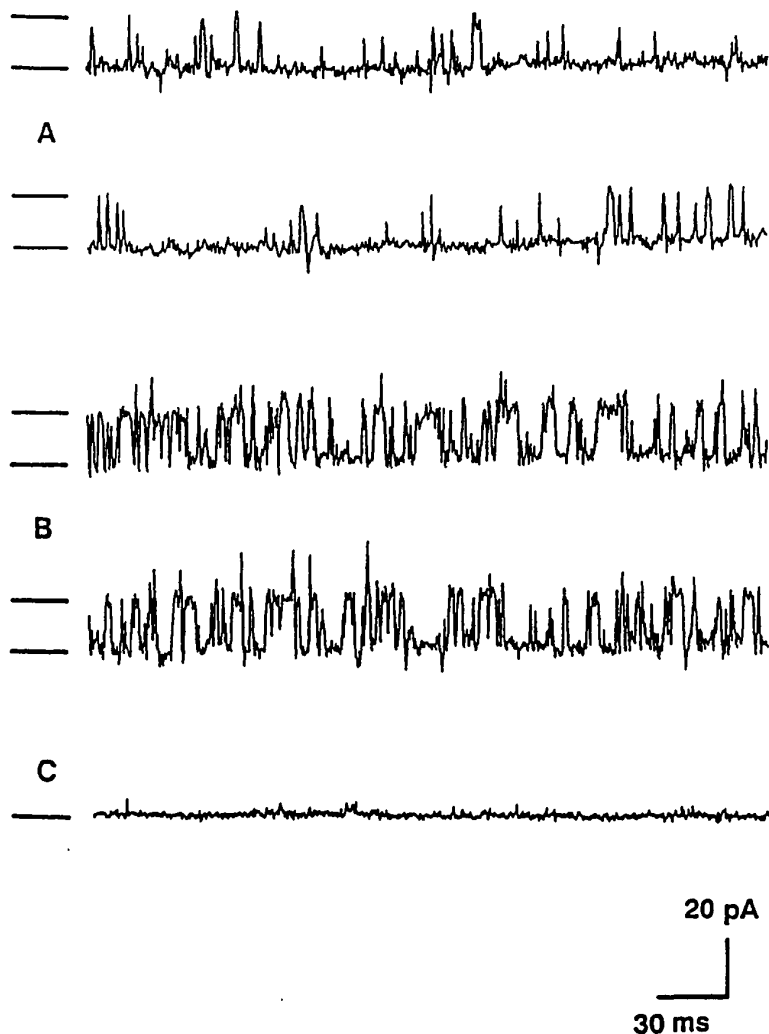


Figure 28. Ca^{2+} release channels of SR are activated in the presence of TMPyP . Following fusion of an SR vesicle to the BLM in the presence of a 5:1 CsCl gradient, single channel fluctuations were examined in the presence of 1 mM Mg^{2+} . (A) Single channel fluctuations in the presence of 600 μM Ca^{2+} . (B) Addition of 10 μM TMPyP . (C) Addition of 10 μM ruthenium red.

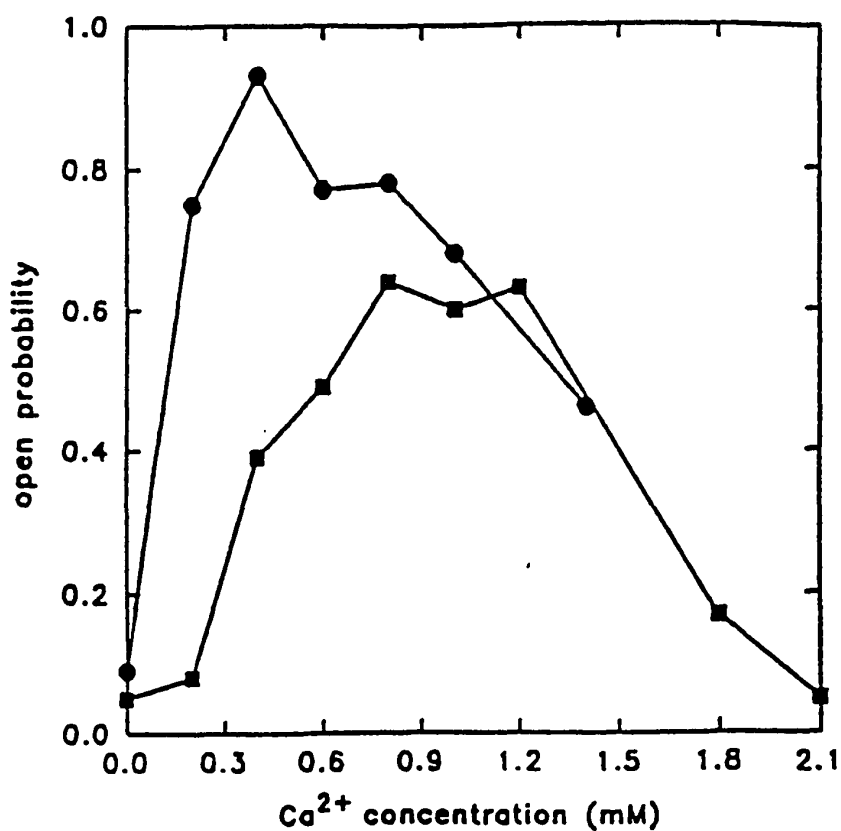


Figure 29. Open probability of a single channel as a function of the Ca^{2+} concentration. Single channel fluctuations were examined as in Figure 28. Open probabilities were determined as described in Methods in the absence (●) and presence (■) of 10 μM TMPyP. P_o values were determined from data sets containing at least 300 transitions (15-30 s).

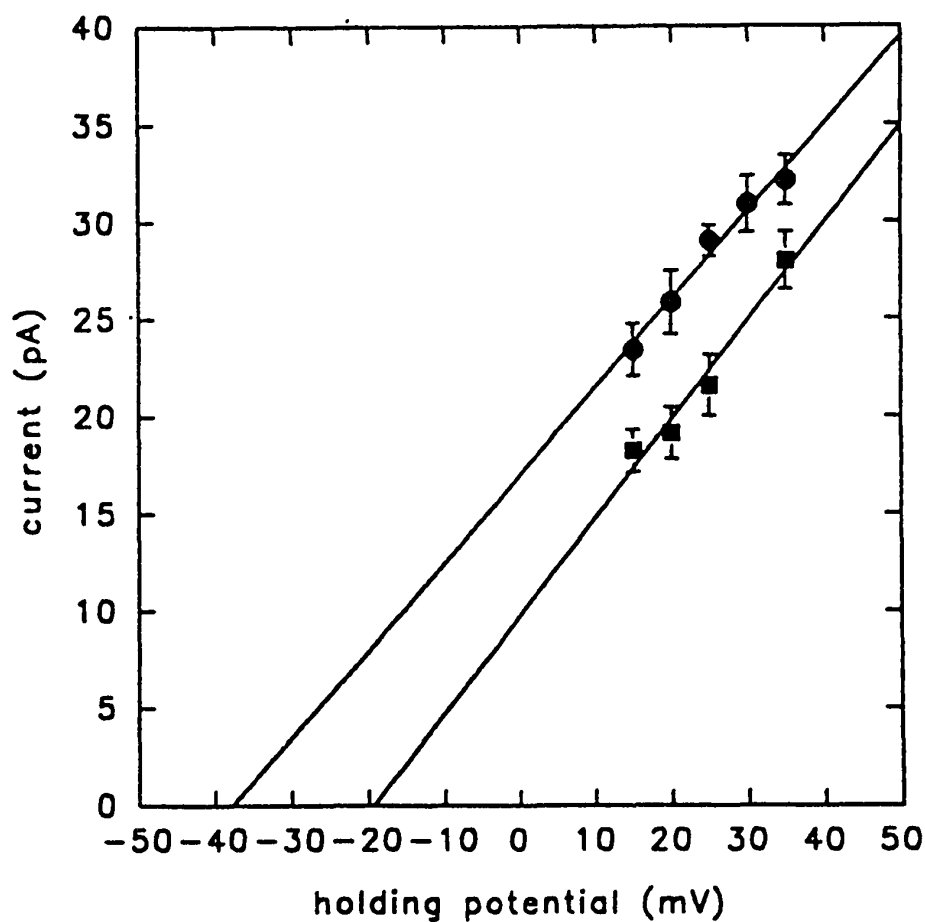


Figure 30. Selectivity of the Ca^{2+} release channel is decreased by 1 mM Mg^{2+} . Under conditions similar to those for Figures 28 and 29, single channel fluctuations were recorded as a function of holding potential in the absence (●) and presence of 1 mM Mg^{2+} (■). Control data was accumulated at 100 μM Ca^{2+} , while 1 mM Mg^{2+} data was generated in the presence of 400 μM Ca^{2+} .

In contrast, dithionite, which is a stronger reducing agent, was able to reduce TMP_YP as indicated by changes in the absorption spectrum. When TMP_YP was incubated with dithionite prior to addition to the SR, Ca²⁺ release was inhibited. The Ca²⁺ release rates as induced by 10 μM TMP_YP, 10 μM TMP_YP treated with dithionite, and 10 μM TMP_YP treated with previously oxidized dithionite were 3.03 ± 0.08 , 0.93 ± 0.31 , and 3.03 ± 0.21 (nmol/mg)/s, respectively. Neither reduced nor oxidized dithionite had any effect on SR Ca²⁺ release. The fact that reduced porphyrin was less effective than oxidized porphyrin in stimulating Ca²⁺ release implies that at least part of the underlying mechanism involved an oxidation reaction.

It has been suggested here that porphyrins interact with the Ca²⁺ release system via an oxidation reaction. Based on this assumption, one would expect that following channel activation, removal of porphyrin would not change the activity of the channel. In a control experiment, the reconstituted Ca²⁺ release channel yielded an P_o of 0.58 in the presence of 200 μM Ca²⁺ and no added Mg²⁺. Addition of 20 μM TMP_YP to this channel increased P_o to 0.83. Exchanging the solution in the *cis* chamber with an identical buffer which contained no porphyrin resulted in a P_o of 0.79. The subsequent addition of 1 mM DTT had only a small effect on the P_o . Thus, TMP_YP appears to increase the open probability

of the reconstituted Ca^{2+} release channel in an irreversible manner. This data is shown in Table VII.

TABLE VII
TMP_YP-INDUCED Ca^{2+} RELEASE IS IRREVERSIBLE

Additions	Open probability (P_o)
200 μM Ca^{2+}	0.58
+ 20 μM TMP _Y P	0.83
+ wash	0.79

Representative sample of data from single channel measurements made with SR vesicles fused with the BLM. Data were collected and analyzed for the open probability (P_o) as described in Methods.

DISCUSSION

In this chapter, we have examined the interaction between porphyrins and the Ca^{2+} release system of SR. These compounds were found to stimulate Ca^{2+} release from SR vesicles in a concentration dependent manner (Figure 20). Of the two porphyrins tested, TMP_YP⁴⁺ (cationic) was a more potent stimulator of Ca^{2+} release than was TSPP⁻ (anionic) (not shown).

Ca^{2+} release induced by TMP_YP was sharply activated by both Ca^{2+} (Figure 21) and adenine nucleotides (Figure 22), and was inhibited by low concentrations of either Mg^{2+} (K_i = 220 μM ; Figure 23) or ruthenium red (K_i = 7 nM; Figure 24). The inhibition of porphyrin-induced Ca^{2+} release by Mg^{2+} was not caused by an interaction between the porphyrin and Mg^{2+} .

Spectrophotometric analysis of TMP_yP showed little change in the absorption spectra following addition of 1 mM Mg²⁺ leading to the conclusion that TMP_yP and Mg²⁺ do not interact. Activation of porphyrin-induced Ca²⁺ release by Ca²⁺ exhibited a large degree of cooperativity ($h = 7.6 \pm 2.8$). This enhancement of cooperativity by TMP_yP was similar to that observed for doxorubicin (Chapter III).

The mechanism by which porphyrins induce Ca²⁺ release involve a direct interaction with the [³H]ryanodine binding site. This chapter has shown that TMP_yP increases both the amount of [³H]ryanodine bound to the receptor and the apparent affinity of the Ca²⁺ binding site responsible for activating [³H]ryanodine binding (Figure 27). The effect of TMP_yP on [³H]ryanodine binding is also similar to that of doxorubicin (Chapter III).

In addition, Ca²⁺ flux measurements support the hypothesis that TMP_yP interacts directly with the Ca²⁺ release protein from SR. This was confirmed by examining the effects of TMP_yP on a single channel fused to a BLM. Bilayer experiments were carried out in the presence of 1 mM Mg²⁺ in order to reproduce conditions similar to the [³H]ryanodine study in Figure 25B. Although considerably higher Ca²⁺ concentrations were required to activate the channel in the presence of this high Mg²⁺ concentration, the channel still exhibited a biphasic response to Ca²⁺ (Figure 29). TMP_yP-stimulated channel activity in the presence of 1 mM Mg²⁺ was

inhibited by 10 μ M ruthenium red (Figure 28C), and the single channel conductance remained unchanged (Figure 30). TMAPyP both increased the open probability of the channel and enhanced its Ca^{2+} sensitivity (Figure 29).

The observation that physiological levels of Mg^{2+} decreased the cation vs. anion selectivity of the channel suggests that the Ca^{2+} release channel may be less Ca^{2+} selective in its native state than has been previously deduced. This is in contrast to a report by Smith et al. (1986) in which the Ba^{2+} vs. Tris permeability ratio was measured over a wide range of Mg^{2+} concentrations (0-11 mM). In that study, the Ba^{2+} selectivity was not seen to change as a function of Mg^{2+} concentration.

Porphyrins play a role in many biological electron transport systems where they participate in reversible oxidation-reduction reactions. Other compounds with similar structure, phthalocyanine dyes (Abramson et al., 1988) and anthraquinones (Chapter III), are known to stimulate Ca^{2+} release and modify [^3H]ryanodine binding to SR vesicles at similar concentrations. The presence of porphyrins in the SR, and their possible involvement in the Ca^{2+} release process remains unknown.

RYANODINE STABILIZES MULTIPLE CONFORMATIONAL STATES OF THE CALCIUM RELEASE CHANNEL FROM SARCOPLASMIC RETICULUM

SUMMARY

This chapter shows that ryanodine stabilizes four distinct and unique gating behaviors of the Ca^{2+} release channel from skeletal muscle sarcoplasmic reticulum. These effects of ryanodine on the Ca^{2+} release channel are shown to depend on the ryanodine concentration. High and low-affinity [^3H]ryanodine binding analyses reveal at least three, and possibly four, discrete binding affinities of [^3H]ryanodine in the presence of high concentrations of CsCl. The concentrations of ryanodine required to induce distinct single channel gating behaviors are correlated with discrete binding affinities determined by equilibrium [^3H]ryanodine binding assays.

INTRODUCTION

Ryanodine is a conformationally sensitive, highly specific probe of the Ca^{2+} release system of skeletal and cardiac muscle SR. The binding of ryanodine reflects the functional state of the Ca^{2+} release channel in that conditions which enhance the open probability (P_o) of the channel also enhance the rate of binding. Ryanodine binding

is stimulated by the presence of Ca^{2+} , adenine nucleotides, caffeine, and other activators of channel activity and is inhibited by Mg^{2+} and ruthenium red, inhibitors of channel activity. In addition, the ryanodine binding site is only available when the channel is in an open configuration.

Ryanodine has been shown to exert a biphasic effect on the function of Ca^{2+} release channels incorporated into a bilayer lipid membrane (BLM). At low μM concentrations, ryanodine is observed to induce a transition from a rapidly fluctuating, full conductance state to a slowly fluctuating, 1/2 conductance state (the apparent consequence of ryanodine binding to a 'high-affinity' site), while mM concentrations of ryanodine are seen to close the channel entirely (the apparent consequence of ryanodine binding to a 'low-affinity' site).

However, analysis of [^3H]ryanodine binding suggests that the interaction between ryanodine and the Ca^{2+} release channel is more complex than has been previously thought. Recent evidence has revealed the existence of up to four ryanodine binding sites on the Ca^{2+} release protein (Lai et al., 1989; Pessah et al., 1991; Carroll et al. 1991).

Therefore, there appears to be a lack of correlation between the reported binding constants of [^3H]ryanodine in SR vesicles when compared to the effect of the alkaloid on the Ca^{2+} release channel in the BLM. The quantitative discrepancy between ryanodine receptor binding and the

ability of the alkaloid to influence the gating of the channel in the BLM has been attributed to its slow association kinetics (Smith et al., 1988).

In this chapter [^3H]ryanodine binding analyses and single channel measurements are made under identical ionic conditions to demonstrate that discriminating concentrations of ryanodine stabilize distinct gating behaviors of a single channel which can be correlated with the observed ryanodine binding affinities.

In this chapter all figures were generated by E. Buck with the exception of Figures 31-33 which were generated by Pessah et al. at the University of California, Davis. Pessah was a collaborator on the associated publication and the figures were included here for completeness. This work was published in the Journal of Biological Chemistry (Buck et al., 1992).

METHODS AND MATERIALS

Preparation of SR Vesicles

For all single channel measurements, rabbit skeletal muscle sarcoplasmic reticulum vesicles were prepared according to the method of MacLennan et al. as described in detail under "Preparation of SR Vesicles" in Chapter II.

Protein concentrations were determined as described in Chapter II.

[³H]Ryanodine Binding Assays

For all [³H]ryanodine binding studies, rabbit skeletal muscle SR vesicles were prepared according to the method of Inui et al., as described in detail under "Preparation of SR for [³H]Ryanodine Binding Studies" in Chapter II.

Equilibrium Binding Assay. Specific equilibrium binding of [³H]ryanodine was performed as described in detail under "[³H]Ryanodine Binding Assay" in Chapter II, with the following exceptions: [³H]Ryanodine binding was measured under the same ionic conditions as the BLM studies (500 mM CsCl, 100 μ M CaCl₂, 5 mM Hepes-Tris, pH 7.2, at 25°C). To determine the binding constants (K_d and B_{max}) of the high and low affinity binding sites, SR vesicles were incubated for 4.5 h in the presence of either 0.5-500 or 50-5050 nM [³H]ryanodine, respectively. The assay was terminated as described in Chapter II and in all other respects the experiment was as described.

Association Binding Assay. Experiments designed to measure the association kinetics of [³H]ryanodine binding were performed in the following manner: SR vesicles (30 μ g) were incubated in the presence of [³H]ryanodine in a solution consisting of 500 mM CsCl, 100 μ M CaCl₂, 5 mM Hepes-Tris, pH 7.2, at 25 or 37°C, for various times up to 420 minutes. For high affinity binding a [³H]ryanodine concentration 1 nM was used, while for low affinity [³H]ryanodine binding concentrations of 50, 250, 500, 1000,

and 3000 nM were used. Samples were quenched at appropriate times, as described in Chapter II.

Bilayer Lipid Membrane Studies

SR vesicles were reconstituted into a planar bilayer lipid membrane (BLM), as described in detail under "Bilayer Lipid Membrane Studies" in Chapter II.

Data were acquired as described and were analyzed for the open probability (P_o) and mean open time (τ) in the following manner: Each data point is the average \pm SE of 6-11 data blocks, randomly selected from the raw data. Each data block is at least 5 seconds in length and contains approximately 3200 gating events. Data blocks were acquired 5-10 minutes after the addition of ryanodine to the BLM. The computer program pCLAMP (Axon Instruments) is used to analyze the data blocks and fits the data to a biexponential of the form:

$$p(t) = w_1 e^{-t/(\tau_1)} + w_2 e^{-t/(\tau_2)}$$

where $p(t)$ is the probability of the channel being open or closed after t seconds, τ_1 and τ_2 are time constants, and $w_1 + w_2 = 100\%$

Materials

Unlabeled ryanodine was purified according to the method of Waterhouse et al. (1984). All other reagents were

analytical grade and were purchased as described in Chapters III-V.

RESULTS

[³H]Ryanodine Receptor Binding in the Presence of CsCl.

[³H]Ryanodine binding to skeletal muscle SR membranes was performed in the presence of 500 mM CsCl as described in Methods. Binding was measured within two concentration ranges (0.5-500 nM and 50-5050 nM) to measure both high and low affinity binding, respectively.

In Figure 31, the data from both binding assays (0.5-5050 nM [³H]ryanodine) are plotted together. In general, total ryanodine binding is comprised of both specific and non-specific components. Subtracting non-specific binding from the total binding yields the specific binding, which are represented by filled circles in this figure.

Figure 32A shows the specific [³H]ryanodine binding from 0.5-150 nM ryanodine, while Figure 32B shows similar data from 500-5050 nM ryanodine. The data for these plots are derived from Figure 31 and show that [³H]ryanodine binding within the two concentration ranges are saturable. Analysis of the data in these figures yields the binding constants, K_d and B_{max} .

Figure 32C is a Scatchard plot of the data contained in Figure 32A. Within this concentration range (0.5-150 nM [³H]ryanodine) the data is best fit by a two-site model with

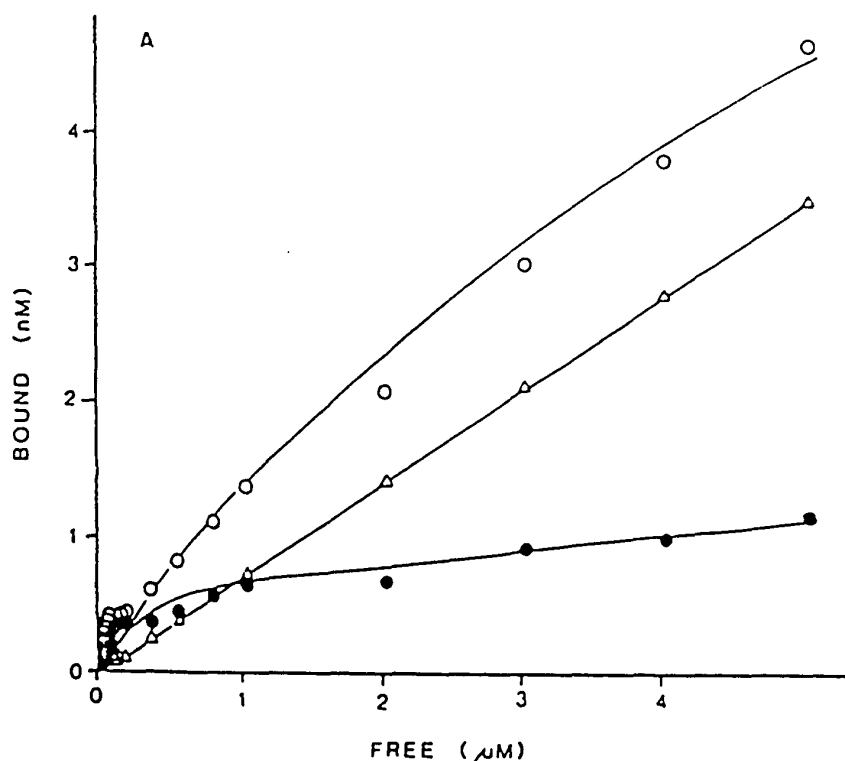


Figure 31. Equilibrium binding of 0.5-5050 nM [^3H]ryanodine in the presence of 500 mM CsCl and 100 μM CaCl_2 . Equilibrium binding was determined as described in Methods. Non-specific binding was determined in the presence of 100 fold excess of unlabeled ryanodine. Specific (●) binding was determined by subtracting non-specific (Δ) binding from total (○) binding.

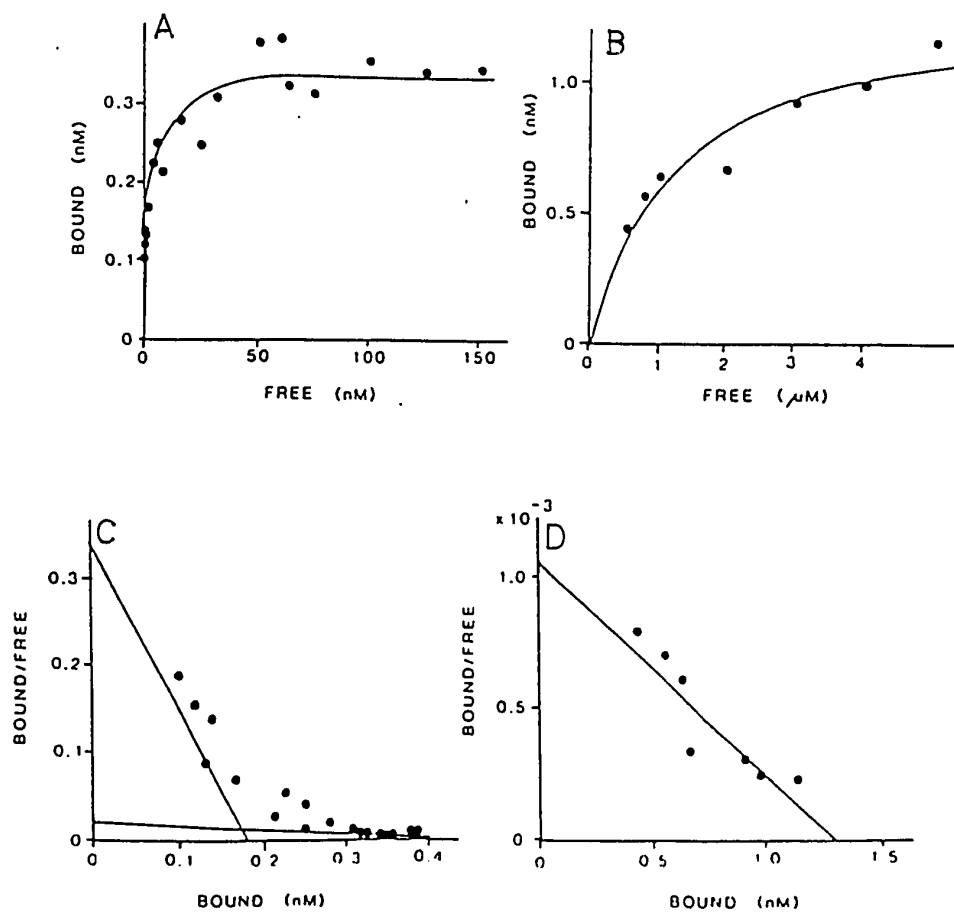


Figure 32. Scatchard analysis of specific binding in the range 0.5-5050 nM ryanodine. The data in Figure 31 was analyzed for the kinetic binding constants. (A) Specific binding in the range of 0.5-150 nM [3 H]ryanodine. (B) Specific binding in the range of 550-5050 nM [3 H]ryanodine. (C) Scatchard analysis of data in (A). (D) Scatchard analysis of data in (B). Results presented in Table VIII.

K_d s of 0.7 and 22.9 nM and B_{max} 's of 3.3 and 12.2 pmol/mg of protein. Figure 32D shows a similar analysis of the data from Figure 32B. Within this concentration range (500-5050 nM [3 H]ryanodine) the data is best fit by a one site model with a K_d of 1.4 μ M and a B_{max} of 18.5 pmol/mg of protein. These result are summarized in Table VIII.

The existence of a fourth binding site is not ruled out. In Figures 32A and 32B, the specific binding has plateaued from 50-150 nM [3 H]ryanodine and then rises again above 500 nM up to and beyond 5050 nM. This suggests the possibility of a fourth site which is not saturated at 5050 nM ryanodine.

Further evidence for a fourth binding site is also presented in Table VIII. This table summarizes the K_d and B_{max} values of up to four different binding sites, as measured in 250 mM KCl buffer and in 500 mM CsCl buffer. The multiple [3 H]ryanodine binding affinities reported here for KCl have been previously measured (Pessah et al., 1991). Clearly, the presence of CsCl markedly increases the affinity of the two highest affinity binding sites without altering B_{max} . In contrast, CsCl decreases the affinity of the third binding site, again without significantly altering B_{max} . If a fourth binding site is available in the presence of CsCl, one would expect its affinity to also decrease in a similar manner to that of the third binding site. The existence of this fourth binding site, which is difficult to

quantify with equilibrium experiments in KCl buffer, is not detectable within the range of [^3H]ryanodine utilized in the present experiments.

TABLE VIII
EFFECT OF 500 mM CsCl AND TEMPERATURE ON
BINDING CONSTANTS OF [^3H]RYANODINE

Affinity site	250 mM KCl at 37°C		500 mM CsCl at 25°C	
	K_d (nM)	B_{\max} (pmol/mg)	K_d (nM)	B_{\max} (pmol/mg)
1	4.6±1.9	5.8±0.2	0.7±0.3	3.3±0.8
2	52.8±17.1	12.9±4.1	22.9±11.9	12.2±2.5
3	554.5±66.5	26.1±1.9	1480±880	18.5±7.7
4	2800±100%	67.2±100%	?	?

Equilibrium binding of 0.5-500 and 50-5050 nM [^3H]ryanodine is measured as described in Methods. All experiments are performed in duplicate and repeated twice. Data are mean \pm SE (n=3).

The observed rate of association (k_{obs}) of [^3H]ryanodine binding was measured from 1-3000 nM ryanodine. As shown in Figure 33, this association rate exhibits biphasic behavior in the presence of 500 mM CsCl. Although k_{obs} is a linear function of the [^3H]ryanodine concentration in the range of 1 to 50 nM (inset, Figure 33), there is a decrease in the rate of association at [^3H]ryanodine concentrations greater than 250 nM. This decrease in association rate is also linearly dependent on the ryanodine concentration (not shown). The half-time to equilibrium under these conditions are 112, 22, and 4.9 minutes at 1, 10, and 50 nM [^3H]ryanodine, and 6, 8, 50, and 41 minutes at

250, 500, 1000, and 5000 nM [^3H]ryanodine, respectively. These results are summarized in Table IX. The decrease in k_{obs} at high ryanodine concentrations is in agreement with the decreased affinities measured in equilibrium binding experiments.

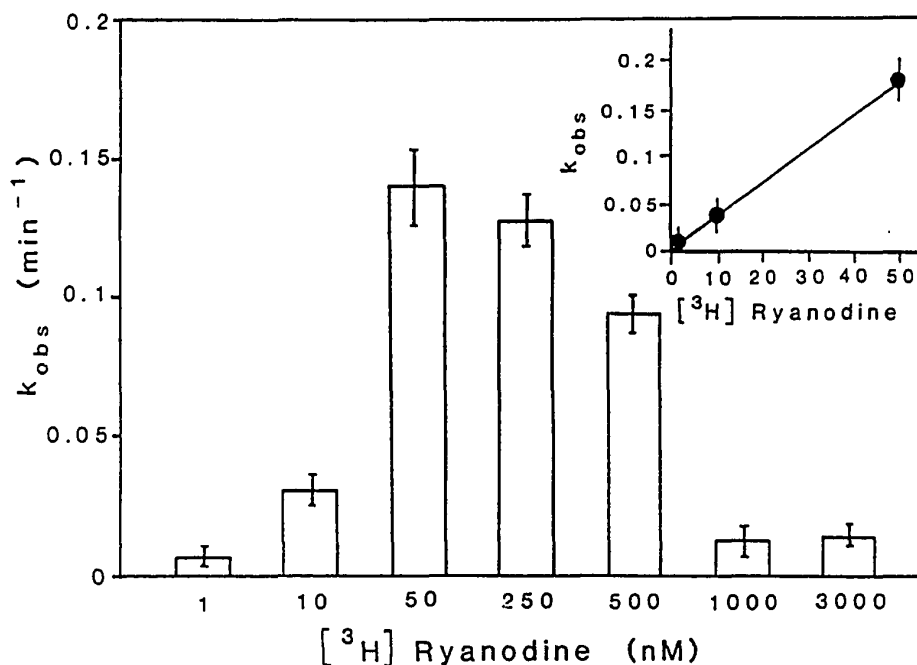


Figure 33. Biphasic association rate for [^3H]ryanodine in the presence of 500 mM CsCl. Experiments were performed in the presence of the indicated [^3H]ryanodine concentration. Inset shows the observed rate (k_{obs}) of association is linearly dependent on the ryanodine concentration in the range 1-50 nM ryanodine. The decline in k_{obs} between 250 and 1000 nM ryanodine is also linear.

Nanomolar Ryanodine and Single Channel Kinetics

As shown in Chapter IV, fusion of SR vesicles to a BLM results in discrete fluctuations which correspond to the gating of the Ca^{2+} release channel.

TABLE IX

ASSOCIATION RATE CONSTANTS (k_{obs}) FOR [^3H]RYANODINE
BINDING IN THE PRESENCE OF CsCl

Ryanodine concentration (nM)	k_{obs} (min^{-1})	$t_{1/2}$ (min)
1	0.006	112
10	0.032	22
50	0.141	4.9
250	0.116	6
500	0.087	8
1000	0.014	50
3000	0.017	41

Analysis of data from Figure 33. Time to half-saturation ($t_{1/2}$) of available binding sites are determined from the exponential equation described in Methods.

The effect of nanomolar concentrations of ryanodine on the Ca^{2+} release channel were examined. In the presence of $100\ \mu\text{M}$ CaCl_2 , the probability of open time (P_o) for a single channel ranged between 0.12 and 0.36, depending on the SR preparation. Nevertheless, addition of 5 to 40 nM ryanodine resulted in a concentration dependent increase in P_o of the channel. Figure 34A summarizes a typical result from one of three SR preparations where ryanodine (5-40 nM) increased the P_o of the full conductance state 2.7 fold.

The mean time (τ) of the open and closed states are best fit by the sum of two exponentials having time

constants τ_{11} and τ_{22} (where $\tau_{11} < \tau_{22}$). As shown in Figure 34B, kinetic analysis reveals that as P_o increases with increasing ryanodine concentration, so does the time constants (τ_{11} , τ_{22}) associated with channel opening. Conversely, as the probability of channel closure decreases with increasing ryanodine concentration, so does the associated time constants (Figure 34C).

In one SR preparation, addition of 10 nM ryanodine dramatically slowed the fluctuation of the channel (Figure 35). This resulted in a large increase in P_o from 0.36 to 0.70 (trace B). To determine if this effect of nanomolar ryanodine was reversible, the *cis* chamber was perfused with an identical medium which did not contain either ryanodine or Ca^{2+} . Subsequent addition of 100 μM Ca^{2+} resulted in the near complete disappearance of the prolonged open states (trace C).

Ryanodine Stabilizes 1/2 Conductance States of the Ca^{2+} Release Channel

Although 5-40 nM ryanodine significantly increased P_o of the full conductance state of the channel, occasionally a subconductance state of approximately 50% of the full conductance value could be seen. As is shown in Figure 36 (trace B), such a transition is seen in the presence of 10 nM ryanodine.

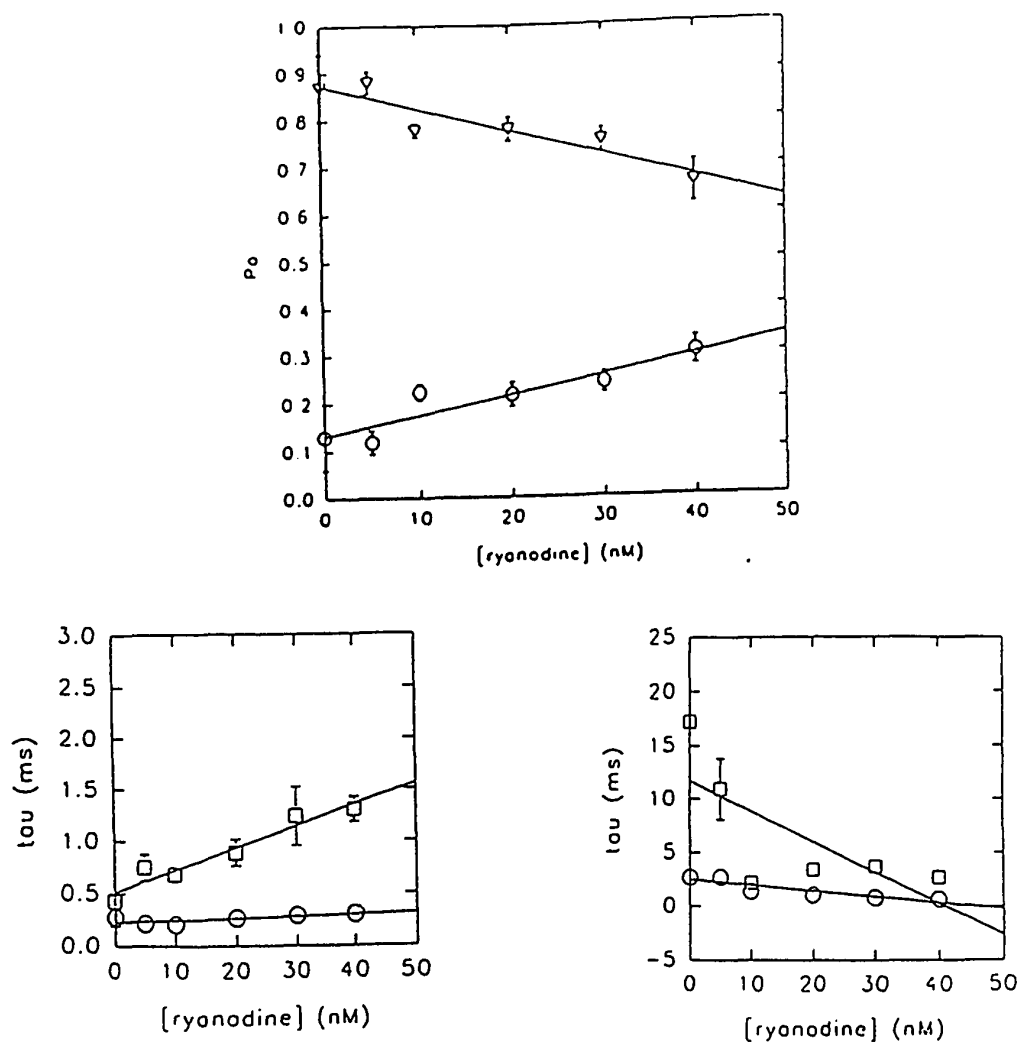


Figure 34. Addition of nanomolar ryanodine increases channel open time. Fusion of SR vesicles to a BLM was performed as described in Methods. (A) Probability of open (○) state or closed (▽) state is modified by nanomolar ryanodine. Each data point is derived from 6-11 randomly selected data blocks (5 sec) which were acquired 5 min after the addition of ryanodine. Dwell times (mean \pm SD) for open state (B) and for closed state (C) are modified by nanomolar ryanodine.

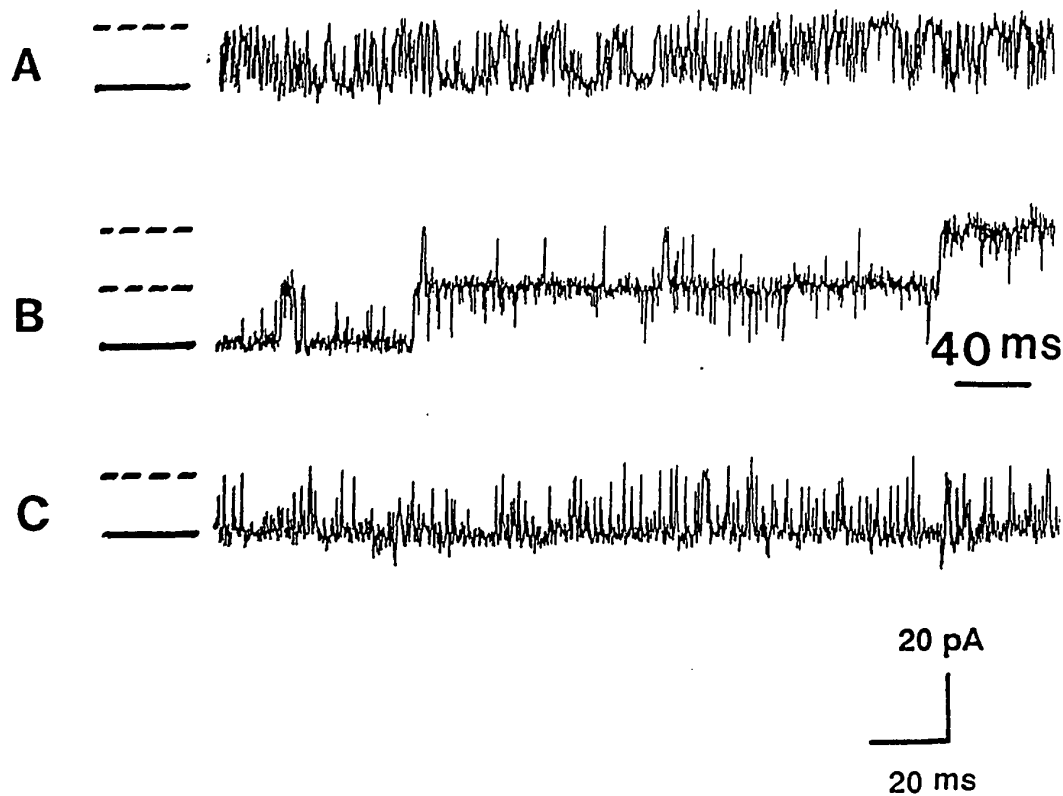


Figure 35. Nanomolar ryanodine increases channel open time in a reversible manner. (A) Single Ca^{2+} channel in the presence of 100 μM Ca^{2+} . (B) Channel modified by 10 nM ryanodine. (C) The solution on the *cis* chamber was perfused with Ca^{2+} free buffer and 100 μM Ca^{2+} subsequently added. The solid bar to the left of each trace represent the closed state of the channel. The time mark in trace 2 is 40 ms, whereas the time mark for all other traces is 20 ms.

Nevertheless, raising the ryanodine concentration to 50 nM consistently resulted in a persistent transition from the rapidly fluctuating full conductance state to a long-lived 1/2 conductance state after a delay of nearly 10 min (trace C). The delay in appearance of the 1/2 conductance state from the full conductance state is found to depend on the ryanodine concentration. For example, in the presence of 10 μ M ryanodine the transition from the full conductance state to the 1/2 conductance state occurs within a few seconds (trace D). Once the channel has made the transition to the more slowly fluctuating state, only discrete 1/2 conductance fluctuations are observed.

Micromolar concentrations of ryanodine permanently altered the Ca^{2+} release channel. Removal of ryanodine by perfusion of the *cis* chamber with a Ca^{2+} free buffer, followed by the addition of 100 μ M Ca^{2+} were ineffective in restoring the rapid full conductance gating behavior of the channel (trace E). A final addition of 20 μ M ruthenium red closed the channel completely (trace F).

Ryanodine Stabilizes 1/4 Conductance States of the Ca^{2+} Release Channel

While micromolar concentrations of ryanodine stabilize 1/2 conductance transitions in the Ca^{2+} release channel, ryanodine at concentration greater than 70 μ M cause the channel to fluctuate in both 1/2 and 1/4 conducting states. As is shown in Figure 37, these effects are most clearly

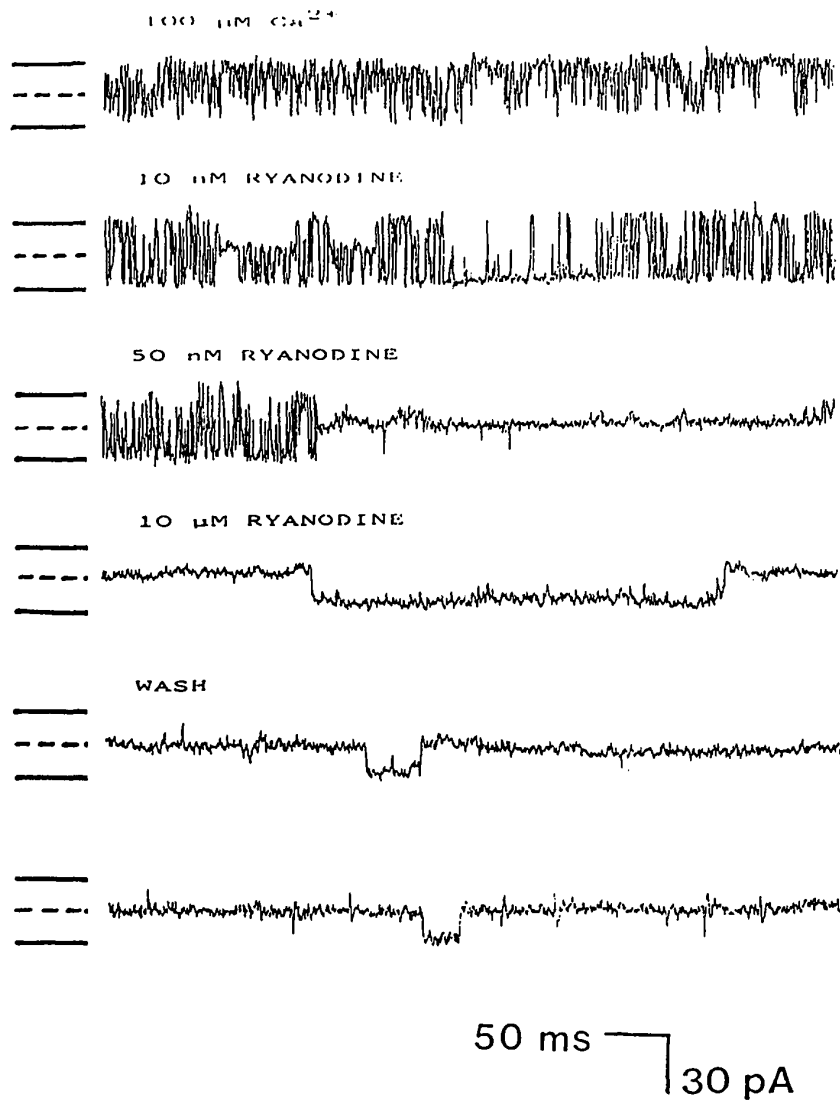


Figure 36. Ryanodine produces both occasional and persistent 1/2 conductance fluctuations with increasing concentration. (A) Control data in the presence of $100\ \mu\text{M}\ \text{Ca}^{2+}$. (B) Addition of $10\ \text{nM}$ ryanodine. (C) Addition of $40\ \text{nM}$ ryanodine (total ryanodine concentration $50\ \text{nM}$). (D) Addition of $10\ \mu\text{M}$ ryanodine. (E and F) The *cis* chamber perfused with Ca^{2+} free buffer, and $100\ \mu\text{M}\ \text{Ca}^{2+}$ subsequently added. The lower solid line represents the closed state of the channel.

demonstrated when several channels are incorporated into the BLM. In trace A several channels are fused with the BLM in the presence of 100 μM ryanodine. Upon addition of ryanodine, the channels rapidly make transitions to the slowly fluctuating 1/2 conductance state. Trace B is an expanded view of a small section of trace A. Notice the occasional 1/4 state transitions. These ryanodine stabilized 1/4 states are highly reproducible and have been observed in each of 11 independent bilayer experiments, on at least 4 different SR preparations. Interestingly, in all observations of the 1/4 state (several hundred), they always appear as closures from the 1/2 conductance state. Openings from the closed state to a 1/4 open state are not observed and transitions from the 1/4 state to the full conductance state are also not observed. The addition of 20 μM ruthenium red completely closed the channel and neither 1/2 nor 1/4 state transitions were subsequently observed (trace C).

In Table X the P_o , mean open time, and conductance for both the 1/2 and 1/4 state transitions are shown, as derived from the data in Figure 37. Comparison of the 1/2 conductance state to the 1/4 conductance state shows that the 1/4 state is relatively short lived, having a mean open time of only 8.5 ms.

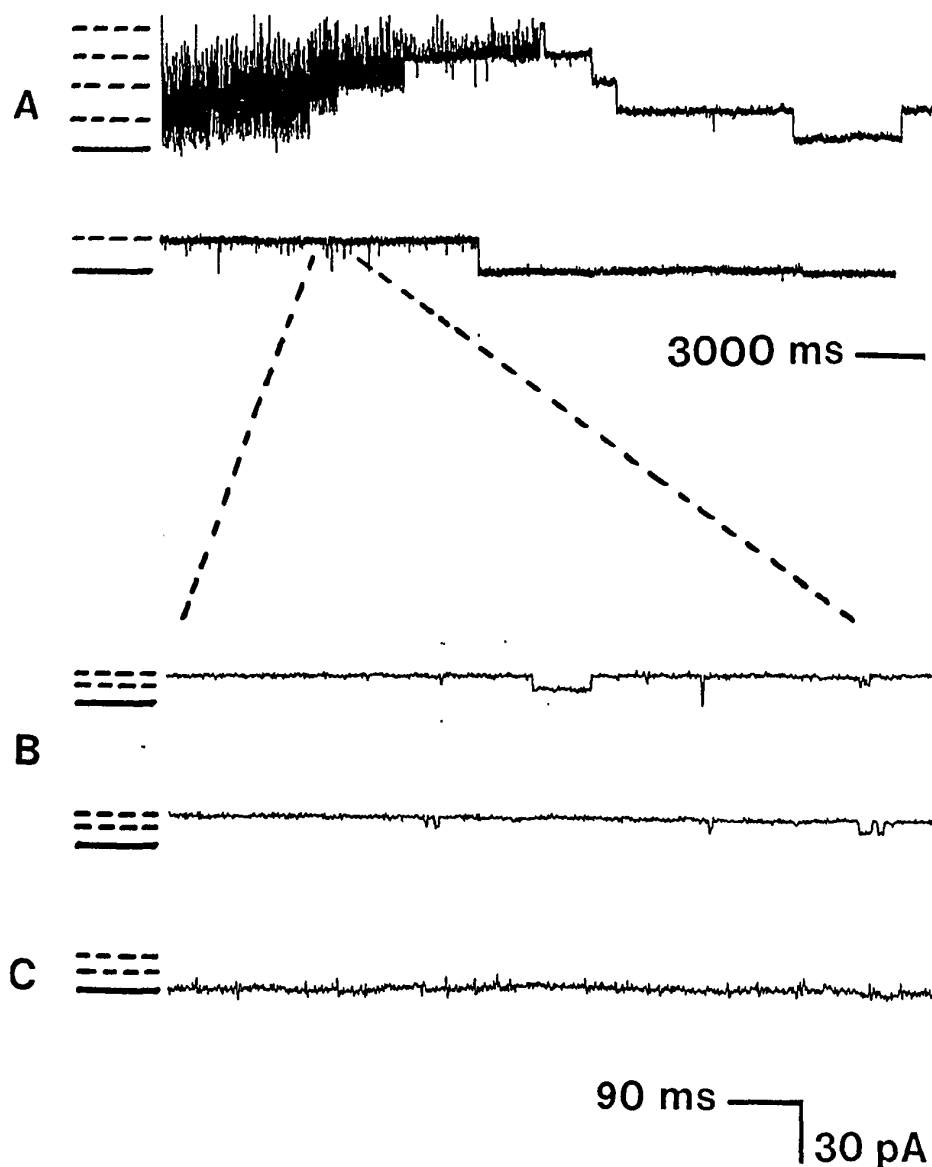


Figure 37. Addition of 100 μM ryanodine causes SR channels to fluctuate in both 1/2 and 1/4 subconducting states. (A) 100 μM ryanodine added to *cis* chamber in the presence of many channels. (B) Expanded view of section of Trace A showing 1/4 state transitions. (C) Inhibition of all transitions by the addition of 20 μM ruthenium red.

Figure 38 shows the current through the open channel as a function of the holding potential for a single channel in the presence of 0, 10, and 100 nM ryanodine. The data which represents the unmodified Ca^{2+} release channel and the channel in the presence of 10 nM ryanodine are fit by the same line. Therefore, nanomolar concentrations of ryanodine

TABLE X

OPEN PROBABILITY, MEAN OPEN TIME, AND CONDUCTANCE OF
THE Ca^{2+} RELEASE CHANNEL IN THE PRESENCE OF
100 μM RYANODINE

Transition	Open probability (P_o)	Mean open time	Conductance (pS)
1/2 state	0.35	12.2 s	225 \pm 68
1/4 state	0.008	8.5 ms	129 \pm 25

The P_o for the 1/2 conductance state transition represents the probability of finding the channel in the 1/2 open state, whereas P_o for the 1/4 conductance state transition is the probability of the channel closing from the 1/2 state to the 1/4 state. Before the addition of ryanodine, the single channel conductance is 468 ± 205 pS. The results are calculated from two of six independent bilayer experiments.

induce slower channel kinetics without altering the voltage-current relationship. With the 5:1 CsCl gradient used in this study, the voltage intercept at zero current (-36 ± 17 mV) and the conductance (468 ± 205 pS) remains unchanged in the presence of 0-40 nM ryanodine.

Both 1/2 state transitions and 1/4 state transitions are derived from the same Ca^{2+} release channel. While both

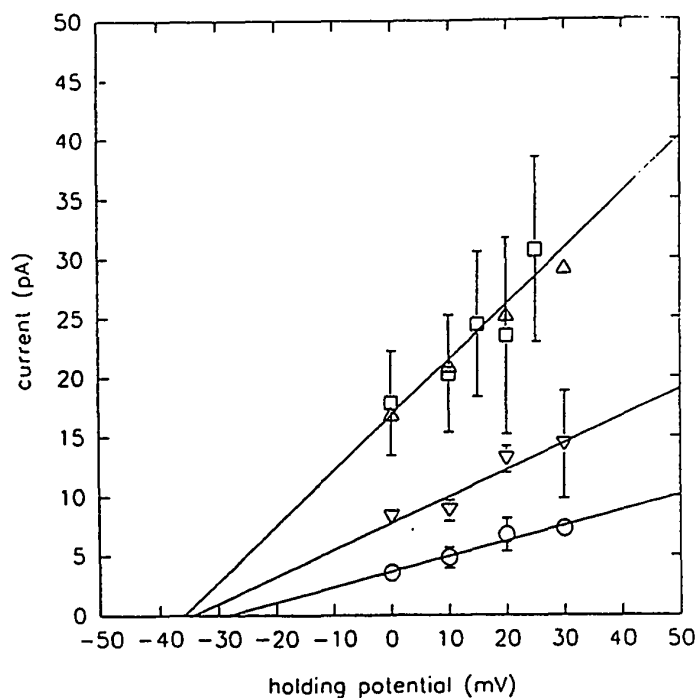


Figure 38. Current-voltage plot of control and ryanodine modified Cs^+ conducting Ca^{2+} channel. Data from the rapidly fluctuating full conductance state in the absence (\square) of ryanodine, the slower full conductance state in the presence of 10 nM ryanodine (\triangle), the 1/2 conductance state (∇) and the 1/4 conductance state (\circ) in the presence of 100 μM ryanodine. Each current-voltage relationship is fit by least squares linear regression analysis. The single channel conductance for the full, 1/2, and 1/4 conductance states are 468 ± 205 , 225 ± 68 , and 129 ± 25 pS, respectively. The voltage intercepts are -36 ± 17 , -34 ± 12 , and -28 ± 7 mV, respectively. Values are mean \pm SD.

show similar, although not identical, voltage intercepts at zero current, the conductance of the 1/4 state (129 ± 25 pS) is half that of the 1/2 state (225 ± 68 pS). In addition, all transitions (full conductance, 1/2 state, and 1/4 state) are inhibited by ruthenium red.

The shift in the reversal potentials of the 1/2 and 1/4 states to slightly more positive values, as seen in Figure 38, suggests a change in the selectivity of the channel. However, variability associated with calculation of the reversal potential precludes definitive conclusions regarding a change in the selectivity.

Ryanodine concentrations greater than 200 μ M induce complete closure of the Ca^{2+} release channel such that no further gating activity is observed.

DISCUSSION

Studies which involve the binding of [^3H]ryanodine to its high-affinity binding site have contributed greatly to understanding the function of the Ca^{2+} release channel. However, there appears to be some discrepancy between the number of reported ryanodine binding sites and the consequences of ryanodine binding on channel function.

This chapter has presented work which directly addresses this issue by examining the coupling between receptor occupancy and the associated single channel behavior. Effects due to temperature or other assay

conditions, were minimized by performing radioligand binding assays and BLM studies under identical ionic conditions and in the presence of 100 μM Ca^{2+} (optimal conditions for both high-affinity ryanodine binding and for single channel activation).

Equilibrium ryanodine binding curves, performed in the presence of KCl, have revealed multiple binding sites with up to four affinities. Similar measurements, performed here in the presence of CsCl, revealed three distinct ryanodine binding sites and suggested the presence of a fourth site (Table VIII). Comparison of ryanodine binding as measured in the two salts showed that CsCl increased the affinity of the two highest affinity sites (K_{d1} and K_{d2}) over that of KCl, while CsCl decreased the affinity of the third binding site (K_{d3}). The possibility of a fourth binding site in CsCl was not ruled out since the ryanodine binding curves did not saturate at high ryanodine and CsCl could have shifted the fourth binding site beyond the range of the assay.

The observed rate of association (k_{obs}) of ryanodine was measured in the presence of CsCl and was found to exhibit biphasic behavior. As the ryanodine concentration was increased, the time required to saturate 1/2 of the available binding sites at first decreased linearly (up to 50 nM), then increased linearly at higher concentrations (Figure 33 and Table IX). The significance of these findings relates to the rapidity with which various concentrations of

ryanodine would be expected to alter the gating behavior of a single channel.

The k_{obs} values reported in Table IX allow quantitative predictions to be made. The data shown in Figure 33 was generated from measurements of ryanodine binding as a function of time. These measurements were fit to an exponential equation of the form:

$$B(t) = B_{\text{max}}(1 - e^{-kt})$$

where k is k_{obs} . Based on this equation, ryanodine at concentrations of 1, 5, 10, 20, and 40 nM would be expected to reach 2.4, 7.5, 12.4, 22.1, and 41.5% of equilibrium occupancy, respectively, 5 min after the addition of ryanodine, which is the time frame of the bilayer experiments.

Exposure of the Ca^{2+} release channel to 5-40 nM ryanodine resulted in a concentration dependent increase in P_0 (Figure 35). It is not surprising that within this concentration range, ryanodine had only a moderate influence on the channel gating behavior. Based on the numerical considerations above, only a small number of productive collisions between ryanodine and its receptor would be predicted during the lifetime of a bilayer experiment. However, increasing the ryanodine concentration would be expected to increase the frequency of successful collisions, assuming that the binding of ryanodine was reversible. In

fact, the binding of nanomolar concentrations of ryanodine has been shown to be reversible (Pessah *et al.*, 1991), as are the transitions induced by low nanomolar ryanodine concentrations reported here (Figure 35). The observation that ryanodine can effect an increase in channel open time without altering the conductance is a new and unique observation. However, a somewhat similar conclusion regarding the open and closed dwell times of the full conductance state has also been reported by Bull *et al.* (1989) working with frog SR in the BLM. This suggests that the findings presented here are not limited to a single species, but reflect a common mechanism of ryanodine action. These results indicate that ryanodine binding to its highest affinity site ($K_{d1}=1$ nM) results in an increase in open time of the full conductance state of the channel.

Micromolar concentrations of ryanodine, known to cause an irreversible transition to a slowly fluctuating, $1/2$ conductance state, has been attributed to high-affinity ryanodine binding. This chapter has shown that the binding of ryanodine to its highest affinity site resulted only in a moderate increase in the channel open time. The irreversible transition to the $1/2$ conductance state is, instead, correlated with ryanodine binding to its second highest affinity site ($K_{d2}=22$ nM). While a ryanodine concentration of 50 nM was sufficient to modify the channel, the rapidity with which this occurred was highly dependent on the

ryanodine concentration (Figure 36). Exposure of the channel to 50 nM ryanodine was found to require almost 10 min to induce the transition to the 1/2 state, while 10 μ M ryanodine is seen to affect a very rapid transition (Figure 36).

The observation that k_{obs} decreased linearly between 200 and 3000 nM [3 H]ryanodine (and possibly beyond) suggests a change in channel conformation coincident with the transition to the long lived, 1/2 conductance state. In support of this hypothesis, a highly persistent action of micromolar ryanodine on channel function was recently reported (Zimanyi et al., 1992).

The observation of 1/4 states seen with ryanodine concentrations between 70-200 μ M (Figure 37) represent the binding of ryanodine to its third highest affinity binding site ($K_{d3}=1.5 \mu$ M). The 1/4 states are a true manifestation of the Ca^{2+} release channel as deduced from the following observations: The conductance of the 1/4 state was measured to be one fourth of the full conductance state (129 pS as opposed to 468 pS), the selectivity of the 1/4 state is the same as the 1/2 state (Figure 38), and the 1/4 state transitions are blocked by μ M concentrations of ruthenium red (Figure 37).

Two points can explain the apparent lack of correlation between the third binding affinity (1.4 μ M) and the ryanodine concentration required to alter channel gating

(70 μM) in BLM studies. First, CsCl is seen to reduce the affinity of the third binding site (increase K_d) compared to 250 mM KCl. Second is the finding that the observed rate of association (k_{obs}) decreases at higher ryanodine concentrations. In the time frame of the bilayer experiments (5-10 min) only 6.7 and 8.1% of receptor occupancy is expected at 1 and 3 μM ryanodine, respectively. Based on these results, a low-affinity binding constant measured under equilibrium conditions (4.5 hr) would be expected to lack quantitative correlation with the concentrations necessary to induce a change in single channel behavior.

Although the presence of a fourth ryanodine binding site was not directly observed in CsCl (K_{d4} not measured), it is proposed that the binding of ryanodine to its fourth binding site is associated with complete channel closure.

In conclusion, the present results suggest that discriminating concentrations of ryanodine can stabilize four discrete gating behaviors of the Ca^{2+} release channel from SR which strongly supports the existence of multiple, ryanodine binding sites.

CONCLUDING REMARKS

The work presented in this thesis has addressed two aspects of the Ca^{2+} release system from skeletal muscle sarcoplasmic reticulum. Chapters III, IV, and V showed that SR Ca^{2+} release can be mediated by an oxidation-reduction reaction. On the other hand, Chapter VI investigated various functional states of the Ca^{2+} release channel.

The mechanism of oxidation-induced Ca^{2+} release has been extensively developed in this laboratory over the last ten years. The initial finding was that the heavy metals Hg^{2+} , Cu^{2+} , Ag^+ , and Cd^{2+} stimulated the rapid release of Ca^{2+} from SR vesicles (Abramson et al., 1983). The Ca^{2+} releasing potency of these metals was found to parallel their binding affinity to SH groups. Heavy metal-induced release was found to be modulated by all the pharmacological modifiers of Ca^{2+} release, with the exception that Ag^+ -induced Ca^{2+} release was seen to occur at physiological Mg^{2+} concentrations. Based on the above evidence, it was deduced that heavy metals were activating the Ca^{2+} release system of SR.

Recognizing that heavy metal-induced Ca^{2+} release probably has no physiological basis, the authors suggested that the oxidation of a critical sulfhydryl was the

mechanism of Ca^{2+} release. While direct evidence for the function of critical sulfhydryls in Ca^{2+} release has not yet been demonstrated, the evidence suggesting the role of an oxidation-reduction reaction is overwhelming. In addition to heavy metals, numerous other compounds known to participate in oxidation-reduction reactions have been found to induce Ca^{2+} release. These include Cu^{2+} /cysteine (Trimm et al., 1986), phalocyanine dyes (Abramson et al., 1988), quinones (Zorzato et al., 1985, Chapter III), and porphyrins (Chapter V). Each of these compounds has been shown to induce Ca^{2+} release by a direct interaction with the Ca^{2+} release protein.

Oxidative stress results when a physiological process which regulates the intracellular level of reactive oxygen species is either inhibited or overwhelmed. The subsequent rise in the concentrations of superoxide (O_2^-), hydroxyl radicals (OH), singlet oxygen ($^1\text{O}_2$), and hydrogen peroxide (H_2O_2) can have deleterious effects on biological systems. These reactive oxygen species are commonly produced either as a side product in oxidation-reduction reactions, or as a direct product in redox cycling. To combat the effects of these species, the body has developed defense systems which regulate the level of oxygen metabolites. These defense mechanisms are either enzymatic or scavenger based and fall under the general heading of antioxidants. Examples of biological antioxidants include superoxide dismutase,

glutathione reductase, and beta-carotene. Compounds such as glutathione, dithiothreitol and dithionite are known as reducing agents. They prevent the formation of reactive oxygen species by maintaining a reduced environment, thus inhibiting oxidation-reduction reactions.

Since both quinones and porphyrins participate in reactions which produce reactive oxygen species, we investigated the ability of side products to induce Ca^{2+} release. The presence of superoxide dismutase in the assay medium had no effect on Ca^{2+} release induced by either quinones or porphyrins. This indicates that neither superoxide dismutase, nor the free radical superoxide, stimulate Ca^{2+} release from the SR. In addition, the presence of oxidized dithionite in the assay medium had no effect on oxidation-induced Ca^{2+} release. This suggests that side or end products of dithionite oxidation are also not involved in Ca^{2+} release. However, the reduction of either the quinone or the porphyrin by dithionite was sufficient to inhibit its ability to induce Ca^{2+} release. These results, coupled with the pharmacology of oxidation-induced Ca^{2+} release, demonstrate that Ca^{2+} release induced by these compounds is via a direct oxidation-reduction reaction with the SR protein.

In a previous report (Stuart et al., 1992) it was observed that the photooxidation of rose bengal induced the rapid release of Ca^{2+} from SR vesicles. Since rose bengal-

induced Ca^{2+} release does not have the same pharmacological characteristics as quinone- or porphyrin-induced Ca^{2+} release, it is probably interacting with the Ca^{2+} release channel in a different manner. As suggested by Stuart, the effect of rose bengal is probably mediated by singlet oxygen ($^1\text{O}_2$) produced during photooxidation of the dye. This suggestion was supported by the observation that histidine, an active scavenger of $^1\text{O}_2$, inhibited Ca^{2+} release induced by photooxidation of rose bengal.

The effects of $^1\text{O}_2$ on biological systems include lipid peroxidation and inactivation of cellular enzymes. Since these effects are non-specific, and since Stuart's study was performed only with SR vesicles, the study presented in Chapter IV was performed with a single channel incorporated into the BLM. It was found that photooxidation of rose bengal directly stimulated the Ca^{2+} release channel of SR. This result was verified by showing that the activated channel was inhibited by ruthenium red, and was not either the K^+ or Cl^- channels present in the SR. The suggestion that $^1\text{O}_2$ was mediating Ca^{2+} release was supported by the observation that rose bengal photooxidation-induced release was independent of the side of the bilayer to which the rose bengal was added. In the time frame of these experiments, $^1\text{O}_2$ produced on one side of the BLM had sufficient mobility and longevity to diffuse across the BLM and induce release.

The plant alkaloid ryanodine is a functional probe of the Ca^{2+} release channel of skeletal muscle sarcoplasmic reticulum. Micromolar concentrations are observed to induce release of Ca^{2+} from SR vesicles and to lock single channels in an open 1/2 conductance state, while millimolar concentrations have been observed to irreversibly close the channel. These two characteristics of ryanodine binding have traditionally been associated with ryanodine binding to either its 'high' affinity or its 'low' affinity binding sites, respectively. However, recent evidence has indicated that the binding of ryanodine is more complicated than has been previously thought. Several investigators have reported multiple ryanodine binding affinities in the presence of various salts with either positive or negative cooperativity (Lai et al., 1989; Pessah et al., 1991; Carroll et al., 1991). Since there appears to be a discrepancy between the action of ryanodine on SR preparations and the reported number of binding sites, the study presented in chapter IV was undertaken.

[^3H]Ryanodine binding to SR membranes measured in the presence of 500 mM CsCl revealed the presence of at least three, and possibly four, ryanodine binding sites. These results were similar to those previously obtained in 250 mM KCl (Pessah et al., 1991). The major difference between the CsCl and KCl data was that the presence of CsCl increased the affinity of ryanodine to its two highest affinity sites,

while reducing the affinity of the third (and possibly fourth) binding site. The presence of a fourth binding site in CsCl was suggested by the data, but was beyond the range of the assay. The reduction in apparent affinity to the lower affinity sites was explained by considering the observed association rate kinetics. It was observed that higher concentrations of ryanodine significantly increased the time to equilibrium in a ryanodine concentration dependant manner.

The focus of this study was to determine if distinct channel gating behaviors, correlated to each binding affinity, could be observed in the BLM. It was observed that ryanodine stabilized four unique and distinct single channel gating behaviors in the presence of various concentrations of ryanodine. These separate behaviors are (1) a concentration dependent increase in the mean open time of a fully conductive channel, seen at ryanodine concentrations below 40 nM, (2) a transition of the channel from a rapidly fluctuating full conductance state to a slowly fluctuating 1/2 conductance state, seen at low micromolar concentrations of ryanodine, (3) the appearance of 1/4 state transitions superimposed on the 1/2 state transitions, seen at ryanodine concentrations greater than 70 μ M, and (4) complete closure of the channel, observed at ryanodine concentrations greater than 200 μ M. Considering the kinetics of ryanodine binding, these effects of ryanodine on the single channel correlate

well with the measured binding affinities measured with SR vesicles.

The data presented in this thesis lends strong support to the mechanism of oxidation-induced Ca^{2+} release and further characterizes the function of the Ca^{2+} release channel.

REFERENCES

- Abramson, J.J., Trimm, J.L., Weden, L., Salama, G. (1983) Heavy metals induce rapid calcium release from sarcoplasmic reticulum vesicles isolated from skeletal muscle. *Proc. Natl. Acad. Sci. U. S. A.* 80:1526-1530.
- Abramson, J.J., Buck, E., Salama, G., Casida, J.E., Pessah, I.N. (1988a) Mechanism of anthraquinone-induced calcium release from skeletal muscle sarcoplasmic reticulum. *J. Biol. Chem.* 263:18750-18758.
- Abramson, J.J., Cronin, J.R., Salama, G. (1988b) Oxidation induced by phthalocyanine dyes causes rapid calcium release from sarcoplasmic reticulum vesicles. *Arch. Biochem. Biophys.* 263:245-255.
- Abramson, J.J., Milne, S., Buck, E., Pessah, I.N. (1993) Porphyrin induced calcium release from skeletal muscle sarcoplasmic reticulum. *Arch. Biochem. Biophys.* 301:396-403.
- Aidley, D.J. (ed): *The Physiology of Excitable Cells*, 3rd ed. Cambridge, Cambridge University Press, 1989.
- Ashley, C.C., Ridgeway, E.B. (1970) On the relationships between membrane potential, calcium transient and tension in single barnacle muscle fibres. *J. Physiol. (Lond)*. 209:105-130.
- Bean, B.P. (1989) Classes of calcium channels in vertebrate cells. *Annu. Rev. Physiol.* 51:367.
- Bennett, H.S., Porter, K.R. (1953) An electron microscope study of sectioned breast muscle of the domestic fowl. *Am. J. Anat.* 93:61.
- Berridge, M.J., Irvine, R.F. (1984) Inositol triphosphate, a novel second messenger in cellular signal transduction. *Nature*. 312:315-321.

- Boucek, R.J., Jr., Olson, R.D., Brenner, D.E., Ogunbunmi, E.M., Inui, M., Fleischer, S. (1987) The major metabolite of doxorubicin is a potent inhibitor of membrane-associated ion pumps. A correlative study of cardiac muscle with isolated membrane fractions. *J. Biol. Chem.* 262:15851-15856.
- Buck, E., Zimanyi, I., Abramson, J.J., Pessah, I.N. (1992) Ryanodine stabilizes multiple conformational states of the skeletal muscle calcium release channel. *J. Biol. Chem.* 267:23560-23567.
- Bull, R., Marengo, J.J., Suarez-Isla, B.A., Donoso, P., Sutko, J.L., Hidalgo, C. (1989) Activation of calcium channels in sarcoplasmic reticulum from frog muscle by nanomolar concentrations of ryanodine. *Biophys. J.* 56:749-756.
- Cadenas, E.: Oxidative stress and formation of excited species, in Sies, H. (ed): *Oxidative stress*. London, Academic Press, 1985, pp. 311-330.
- Caldwell, P.C., Walster, G.E. (1963) Studies on the micro-injection of various substances into crab muscle fibres. *J. Physiol. (Lond)*. 169:353-372.
- Campbell, K.P., Knudson, C.M., Imagawa, T., Leung, A.T., Sutko, J.L., Kahl, S.D., Raab, C.R., Madson, L. (1987) Identification and characterization of the high affinity [^3H]ryanodine receptor of the junctional sarcoplasmic reticulum Ca^{2+} release channel. *J. Biol. Chem.* 262:6460-6463.
- Carroll, S., Skarmeta, J.G., Yu, X., Collins, K.D., Inisi, G. (1991) . *Arch. Biochem. Biophys.* 290:239-247.
- Caswell, A.H., Brandt, N.R., Brunschwig, J.P., Purkerson, S. (1991) Localization and partial characterization of the oligomeric disulfide-linked molecular weight 95,000 protein (triadin) which binds the ryanodine and dihydropyridine receptors in skeletal muscle triadic vesicles. *Biochem.* 30:7507-7513.
- Chu, A., Stefani, E. (1991) Phosphatidylinositol 4,5-bisphosphate-induced Ca^{2+} release from skeletal muscle sarcoplasmic reticulum terminal cisternal membranes. Ca^{2+} flux and single channel studies. *J. Biol. Chem.* 266:7699-7705.
- Coronado, R., Miller, C. (1979) . *Nature*. 280:807-810.
- Costantin, L.L. (1975) Contractile activation in skeletal muscle. *Prog. Biophys. Mol. Biol.* 29:197-224.

- Doroshov, J.H. (1983) Effect of anthracycline antibiotics on oxygen radical formation in rat heart. *Cancer. Res.* 43:460-472.
- Doroshov, J.H., Davies, K.J. (1983) Comparative cardiac oxygen radical metabolism by anthracycline antibiotics, mitoxantrone, bisantrene, 4'-(9-acridinylamino)-methanesulfon-m-anisidide, and neocarzinostatin. *Biochem. Pharmacol.* 32:2935-2939.
- Doroshov, J.H., Tallent, C., Schechter, J.E. (1985) Ultrastructural features of Adriamycin-induced skeletal and cardiac muscle toxicity. *Am. J. Pathol.* 118:288-297.
- Endo, M. (1975) Mechanism of action of caffeine on the sarcoplasmic reticulum of skeletal muscle. *Proc. Jpn. Acad.* 51:479-484.
- Endo, M., Tanaka, M., Ogawa, Y. (1970) Calcium-induced release of calcium from the sarcoplasmic reticulum of skinned skeletal muscle fibers. *Nature London* 228:34-36.
- Fabiato, A. (1983) Calcium-induced release of calcium from the cardiac sarcoplasmic reticulum. *Am. J. Physiol.* 245:C1-C14.
- Fabiato, A. (1985a) Use of aequorin for the appraisal of the hypothesis of the release of calcium from the sarcoplasmic reticulum induced by a change of pH in skinned cardiac cells. *Cell. Calcium.* 6:95-108.
- Fabiato, A. (1985b) Simulated calcium current can both cause calcium loading in and trigger calcium release from the sarcoplasmic reticulum of a skinned canine cardiac Purkinje cell. *J. Gen. Physiol.* 85:291-320.
- Fabiato, A., Fabiato, F. (1979) . *J. Physiol. (Paris)*. 75:463-505.
- Fairhurst, A.S., Jenden, D.J. (1962) Effect of ryanodine on the calcium uptake system of skeletal muscle. *Proc. Natl. Acad. Sci. U. S. A.* 48:807-813.
- Fairhurst, A.S., Hasselbach, W. (1970) Calcium efflux from a heavy sarcotubular fraction. Effects of ryanodine, caffeine, and magnesium. *Eur. J. Biochem.* 13:504-509.
- Ford, L.E., Spotnitz, A.J., Sonnenblick, E.H. (1970) oupling between ionic stimulation and contraction of skeletal muscle cells. *J. Gen. Physiol.* 55:138.

- Ford, L.E., Podolski, R.J. (1972) Intracellular calcium movements in skinned muscle fibers. *J. Physiol. (Lond)*. 223:21-33.
- Fox, M.A., Olive, S. (1979) . *Sci.* 205:582-583.
- Franzini-Armstrong, C. (1970) Studies of the triad. I. Structure of the junction in frog twitch fibres. *J. Cell. Biol.* 47:488-499.
- Franzini-Armstrong, C. (1971) Studies of the triad. II. Penetration of tracers into the junctional gap. *J. Cell. Biol.* 49:196-203.
- Franzini-Armstrong, C., Porter, K.R. (1964) Sarcolemmal invaginations constituting the T system in fish muscle fibers. *J. Cell. Biol.* 22:675-696.
- Franzini-Armstrong, C., Kenney, L.J., Varriano-Marston, E. (1987) The structure of calsequestrin in triads of vertebrate skeletal muscle: a deep-etch study. *J. Cell. Biol.* 105:49-56.
- Garcia, J., Fill, M., Toro, L., Stefani, E. (1990) Functional studies of Ca^{2+} channels from plasmalemma and sarcoplasmic reticulum membranes in muscle cells. *Semin. Cell. Biol.* 1:255-264.
- Gomolla, M., Gottschalk, G., Lüttgau, H.C. (1983) Perchlorate-induced alterations in electrical and mechanical parameters of frog skeletal muscle fibres. *J. Physiol. (Lond)*. 343:197-214.
- Hals, G.D., Stein, P.G., Palade, P.T. (1989) Single channel characteristics of a high conductance anion channel in "sarcoballs". *J. Gen. Physiol.* 93:385-410.
- Harris, R.N., Doroshov, J.H. (1985) Effect of doxorubicin-enhanced hydrogen peroxide and hydroxyl radical formation on calcium sequestration by cardiac sarcoplasmic reticulum. *Biochem. Biophys. Res. Commun.* 130:739-745.
- Hasegawa, T., Kumagai, S. (1989) A G-protein of sarcoplasmic reticulum of skeletal muscle is activated by caffeine or inositol trisphosphate. *FEBS. Lett.* 244:283-286.
- Hess, M.L., Manson, N.H. (1984) Molecular oxygen: friend and foe. The role of the oxygen free radical system in the calcium paradox, the oxygen paradox and ischemia/reperfusion injury. *J. Mol. Cell. Cardiol.* 16:969-985.

- Hirata, M., Suematsu, E., Hashimoto, T., Hamachi, T., Koga, T. (1984) Release of Ca^{2+} from a non-mitochondrial store site in peritoneal macrophages treated with saponin by inositol 1,4,5-trisphosphate. *Biochem. J.* 223:229-236.
- Howell, J.N. (1969) A lesion of the transverse tubules of skeletal muscle. *J. Physiol. (Lond)*. 210:515-533.
- Huxley, A.F., Niedergerke, R. (1954) Structural changes in muscle during contraction. Interference microscopy of living muscle fibers. *Nature*. 173:971-973.
- Huxley, A.F., Taylor, R.E. (1955) Function of Krause's membrane. *Nature*. 176:1068.
- Huxley, H.E., Hanson, J. (1954) Changes in the cross-striations of muscle during contraction and stretch and their structural interpretation. *Nature*. 173:973-976.
- Ikemoto, N., Antoniu, B., Kim, D.H. (1984) Rapid calcium release from the isolated sarcoplasmic reticulum is triggered via the attached transverse tubular system. *J. Biol. Chem.* 259:13151-13158.
- Imagawa, T., Smith, J.S., Coronado, R., Campbell, K.P. (1987) Purified ryanodine receptor from skeletal muscle sarcoplasmic reticulum is the Ca^{2+} -permeable pore of the calcium release channel. *J. Biol. Chem.* 262:16636-16643.
- Inui, M., Saito, A., Fleischer, S. (1987a) Isolation of the ryanodine receptor from cardiac sarcoplasmic reticulum and identity with the feet structures. *J. Biol. Chem.* 262:15637-15642.
- Inui, M., Saito, A., Fleischer, S. (1987b) Purification of the ryanodine receptor and identity with feet structures of junctional terminal cisternae of sarcoplasmic reticulum from fast skeletal muscle. *J. Biol. Chem.* 262:1740-1747.
- Kalckar, H.M. (1947) *J. Biol. Chem.* 196:461-475
- Keynes, R.D., Aidley, D.J. (eds): *Nerve & Muscle*, 2nd ed. Cambridge, Cambridge University Press, 1991.
- Kim, M.S., Akera, T. (1987) . *Am. J. Physiol.* 252:H252-H257.
- Kim, R.S., LaBella, F.S. (1988) The effect of linoleic and arachidonic acid derivatives on calcium transport in vesicles from cardiac sarcoplasmic reticulum. *J. Mol. Cell. Cardiol.* 20:119-130.

- Kukreja, R.C., Okabe, E., Schrier, G.M., Hess, M.L. (1988) Oxygen radical-mediated lipid peroxidation and inhibition of Ca^{2+} -ATPase activity of cardiac sarcoplasmic reticulum. *Arch. Biochem. Biophys.* 261:447-457.
- Lai, F.A., Erickson, H., Block, B.A., Meissner, G. (1987) Evidence for a junctional feet-ryanodine receptor complex from sarcoplasmic reticulum. *Biochem. Biophys. Res. Commun.* 143:704-709.
- Lai, F.A., Anderson, K., Rousseau, E., Liu, Q.Y., Meissner, G. (1988a) Evidence for a Ca^{2+} channel within the ryanodine receptor complex from cardiac sarcoplasmic reticulum. *Biochem. Biophys. Res. Commun.* 151:441-449.
- Lai, F.A., Erickson, H.P., Rousseau, E., Liu, Q.Y., Meissner, G. (1988b) Purification and reconstitution of the calcium release channel from skeletal muscle. *Nature.* 331:315-319.
- Lai, F.A., Misra, M., Yu, X., Smith, H.A., Meissner, G. (1989) . *J. Biol. Chem.* 39:16776-16785.
- MacLennan, D.H. (1970) Purification and properties of an adenosine triphosphatase from sarcoplasmic reticulum. *J. Biol. Chem.* 245:4508-4518.
- MacLennan, D.H., Wong, P.T.S. (1971) Isolation of a calcium-sequestering protein from sarcoplasmic reticulum. *Proc. Natl. Acad. Sci. U. S. A.* 68:1231-1235.
- MacLennan, D.H., Zubrzycka-Gaarn, E., Jorgensen, A.O.: Biogenesis of the sarcoplasmic reticulum, in Entman, M.L., Van Winkle, W.B. (eds): *Sarcoplasmic reticulum in muscle physiology*. Boca Raton, CRC Press, 1986, vol 1, pp. 47-64.
- Manning, A.S., Hearse, D.J. (1984) . *J. Mol. Cell. Cardiol.* 16:497-518.
- Martonosi, A.N. (1984) Mechanisms of Ca^{2+} release from sarcoplasmic reticulum of skeletal muscle. *Physiol. Rev.* 64:1240-1320.
- Meissner, G. (1975) Isolation and characterization of two types of sarcoplasmic reticulum vesicles. *Biochem. Biophys. Acta.* 389:51-68.
- Meissner, G. (1984) Adenine nucleotide stimulation of Ca^{2+} -induced Ca^{2+} release in sarcoplasmic reticulum. *J. Biol. Chem.* 259:2365-2374.
-

- Meissner, G., Darling, E., Eveleth, J. (1986) Kinetics of rapid Ca^{2+} release by sarcoplasmic reticulum. Effects of Ca^{2+} , Mg^{2+} , and adenine nucleotides. *Biochem.* 25:236-244.
- Mikos, G.J., Snow, T.R. (1987) Failure of inositol 1,4,5-trisphosphate to elicit or potentiate Ca^{2+} release from isolated skeletal muscle sarcoplasmic reticulum. *Biochem. Biophys. Acta.* 927:256-260.
- Moore, C.L. (1971) . *Biochem. Biophys. Res. Commun.* 42:298-305.
- Niedergerke, R. (1956) The potassium chloride contracture of the heart and its modification by calcium. *J. Physiol. (Lond).* 134:584-599.
- Numa, S., Tanabe, T., Takeshima, H., Mikami, A., Niidome, T., Nishimura, S., Adams, B.A., Beam, K.G. (1990) Molecular insights into excitation-contraction coupling. *Cold. Spring. Harb. Symp. Quant. Biol.* 55:1-7.
- Oba, T., Takagi, Y., Hotta, K. (1984) Effect of temperature and Zn^{2+} on isometric contractile properties and electrical phenomena of frog (*Rana*) and *Xenopus* skeletal muscle fibers. *Can. J. Physiol. Pharmacol.* 62:1511-1517.
- Ohnishi, S.T. (1979) Calcium-induced calcium release from fragmented sarcoplasmic reticulum. *J. Biochem. (Tokyo).* 86:1147-1150.
- Peachey, L.D. (1965) The sarcoplasmic reticulum and transverse tubules of the frog's sartorius. *J. Gen. Physiol.* 81:337-354.
- Penner, R., Neher, E., Takeshima, H., Nishimura, S., Numa, S. (1989) Functional expression of the calcium release channel from skeletal muscle ryanodine receptor cDNA. *FEBS. Lett.* 259:217-221.
- Pessah, I.N., Waterhouse, A.L., Casida, J.E. (1985) The calcium-ryanodine receptor complex of skeletal and cardiac muscle. *Biochem. Biophys. Res. Commun.* 128:449-456.
- Pessah, I.N., Francini, A.O., Scales, D.J., Waterhouse, A.L., Casida, J.E. (1986) Calcium-ryanodine receptor complex. Solubilization and partial characterization from skeletal muscle junctional sarcoplasmic reticulum vesicles. *J. Biol. Chem.* 261:8643-8648.

- Pessah, I.N., Stambuk, R.A., Casida, J.E. (1987) Ca^{2+} -activated ryanodine binding: mechanisms of sensitivity and intensity modulation by Mg^{2+} , caffeine, and adenine nucleotides. *Mol. Pharmacol.* 31:232-238.
- Pessah, I.N., Durie, E.L., Schiedt, M.J., Zimanyi, I. (1990) Anthraquinone-sensitized Ca^{2+} release channel from rat cardiac sarcoplasmic reticulum: possible receptor-mediated mechanism of doxorubicin cardiomyopathy. *Mol. Pharmacol.* 37:503-514.
- Pessah, I.N., Zimanyi, I. (1991) Characterization of multiple [^3H]ryanodine binding sites on the Ca^{2+} release channel of sarcoplasmic reticulum from skeletal and cardiac muscle: evidence for a sequential mechanism in ryanodine action. *Mol. Pharmacol.* 39:679-689.
- Porter, K.R. (1961) The sarcoplasmic reticulum: Its recent history and present status. *Journal of Biophysical and Biochemical Cytology* 10:219-226.
- Porter, K.R., Palade, G.E. (1957) Studies on the endoplasmic reticulum. III. Its form and distribution in striated muscle cells. *Journal of Biophysical and Biochemical Cytology* 26:269-300.
- Portzehl, H., Caldwell, P.C., Rüegg, J.C. (1964) The dependence of contraction and relaxation of muscle fibres from the crab *Maia squinado* on the internal concentration of free calcium ions. *Biochim. Biophys. Acta.* 79:581-599.
- Pryor, W.A., Hales, B.J., Premovic, P.I., Church, D.F. (1982) . *Sci.* 220:425-427.
- Rardon, D.P., Cefali, D.C., Mitchell, R.D., Seiler, S.M., Jones, L.R. (1989) High molecular weight proteins purified from cardiac junctional sarcoplasmic reticulum vesicles are ryanodine-sensitive calcium channels. *Circ. Res.* 64:779-789.
- Revel, J.P. (1962) The sarcoplasmic reticulum of the bat cricothyroid muscle. *J. Cell. Biol.* 12:571-588.
- Salama, G., Abramson, J. (1984) Silver ions trigger Ca^{2+} release by acting at the apparent physiological release site in sarcoplasmic reticulum. *J. Biol. Chem.* 259:13363-13369.
- Scherer, N.M., Ferguson, J.E. (1985) Inositol 1,4,5-trisphosphate is not effective in releasing calcium from skeletal sarcoplasmic reticulum microsomes. *Biochem. Biophys. Res. Commun.* 128:1064-1070.

- Scheutze, D. (1983) . *Environ. Health Perspect.* 47:65-80.
- Schneider, M.F., Chandler, W.K. (1973) Voltage dependent charge movement in skeletal muscle: a possible step in excitation-contraction coupling. *Nature.* 242:244-246.
- Schultz: *Farbstofftabellen.* Leipzig, Akademisch Verlagsgesellschaft m.b.H., 1885.
- Sies, H.: *Oxidative Stress.* London, Academic Press, 1985.
- Smith, J.S., Coronado, R., Meissner, G. (1985) Sarcoplasmic reticulum contains adenine nucleotide-activated calcium channels. *Nature.* 316:446-449.
- Smith, J.S., Coronado, R., Meissner, G. (1986a) Single-channel calcium and barium currents of large and small conductance from sarcoplasmic reticulum. *Biophys. J.* 50:921-928.
- Smith, J.S., Coronado, R., Meissner, G. (1986b) Single channel measurements of the calcium release channel from skeletal muscle sarcoplasmic reticulum. Activation by Ca^{2+} and ATP and modulation by Mg^{2+} . *J. Gen. Physiol.* 88:573-588.
- Smith, J.S., Imagawa, T., Ma, J., Fill, M., Campbell, K.P., Coronado, R. (1988) Purified ryanodine receptor from rabbit skeletal muscle is the calcium-release channel of sarcoplasmic reticulum. *J. Gen. Physiol.* 92:1-26.
- Stuart, J., Pessah, I.N., Favero, T.G., Abramson, J.J. (1992) Photooxidation of skeletal muscle sarcoplasmic reticulum induces rapid calcium release. *Arch. Biochem. Biophys.* 292:512-521.
- Suarez-Isla, B.A., Alcayaga, C., Marengo, J.J., Bull, R. (1991) Activation of inositol trisphosphate-sensitive Ca^{2+} channels of sarcoplasmic reticulum from frog skeletal muscle. *J. Physiol. (Lond).* 441:575-591.
- Suematsu, E., Hirata, M., Sasaguri, T., Hashimoto, T., Kuriyama, H. (1985) Roles of Ca^{2+} on the inositol 1,4,5-trisphosphate-induced release of Ca^{2+} from saponin-permeabilized single cells of the porcine coronary artery. *Comp. Biochem. Physiol. [A].* 82:645-649.
- Suematsu-E. Hirata-M. Sasaguri-T. Hashimoto-T. Kuriyama-H. (1985) Roles of Ca^{2+} on the inositol 1,4,5-trisphosphate- induced release of Ca^{2+} from saponin-permeabilized single cells of the porcine coronary artery. *Comp. Biochem. Physiol. [A].* 82:645-649.

- Sutko, J.L., Ito, K., Kenyon, J.L. (1985) Ryanodine: a modifier of sarcoplasmic reticulum calcium release in striated muscle. *Fed. Proc.* 44:2984-2988.
- Thorley-Lawson, D.A., Green, N.M. (1977) The reactivity of the thiol groups of the adenosine triphosphate of sarcoplasmic reticulum and their location on tryptic fragments of the molecule. *Biochem. J.* 167:739-748
- Trimm, J.L., Salama, G., Abramson, J.J. (1986) Sulfhydryl oxidation induces rapid calcium release from sarcoplasmic reticulum vesicles. *J. Biol. Chem.* 261:16092-16098.
- Vergara, J., Tsien, R.Y., Delay, M. (1985) Inositol 1,4,5-trisphosphate: a possible chemical link in excitation-contraction coupling in muscle. *Proc. Natl. Acad. Sci. U. S. A.* 82:6352-6356.
- Volpe, P., Salviati, G., Di-Virgilio, F., Pozzan, T. (1985) Inositol 1,4,5-trisphosphate induces calcium release from sarcoplasmic reticulum of skeletal muscle. *Nature.* 316:347-349.
- Waterhouse, A.L., Holden, I., Casida, J.E. (1984) . *J. Chem. Soc. Chem. Commun.*:1256-1266.
- Waterhouse, A.L., Pessah, I.N., Francini, A.O., Casida, J.E. (1987) Structural aspects of ryanodine action and selectivity. *J. Med. Chem.* 30:710-716.
- Watras, J., Benevolensky, D. (1987) Inositol 1,4,5-trisphosphate-induced calcium release from canine aortic sarcoplasmic reticulum vesicles. *Biochem. Biophys. Acta.* 931:354-363.
- Watras, J., Benevolensky, D., Childs, C. (1989) Calcium release from aortic sarcoplasmic reticulum. *J. Mol. Cell. Cardiol.* 21 Suppl 1:125-130.
- Weiss, R.B., Sarosy, G., Clagett-Carr, K., Russo, M., Leyland-Jones, B. (1986) Anthracycline analogs: The past, present, and future. *Cancer. Chemother. Pharmacol.* 18:185-197.
- Wood, D.S., Zollman, J.R., Reuben, J.P., Brandt, P.W. (1975) . *Sci.* 187:1075-1076.
- Xiong, H.: *Modification of the Ca^{2+} release channel from sarcoplasmic reticulum of skeletal muscle* [Dissertation]. Portland State University, 1990. 128 p.

- Xiong, H., Buck, E., Stuart, J., Pessah, I.N., Salama, G., Abramson, J.J. (1992) Rose bengal activates the Ca^{2+} release channel from skeletal muscle sarcoplasmic reticulum. *Arch. Biochem. Biophys.* 292:522-528.
- Zaidi, N.F., Lagenaur, C.F., Hilkert, R.J., Xiong, H., Abramson, J.J., Salama, G. (1989) Disulfide linkage of biotin identifies a 106-kDa Ca^{2+} release channel in sarcoplasmic reticulum. *J. Biol. Chem.* 264:21737-21747.
- Zimanyi, I., Buck, E., Abramson, J.J., Mack, M.M., Pessah, I.N. (1992) Ryanodine induces persistent inactivation of the Ca^{2+} release channel from skeletal muscle sarcoplasmic reticulum. *Mol. Pharmacol.* 42:1049-1057.
- Zorzato, F., Salviati, G., Facchinetti, T., Volpe, P. (1985) Doxorubicin induces calcium release from terminal cisternae of skeletal muscle. A study on isolated sarcoplasmic reticulum and chemically skinned fibers. *J. Biol. Chem.* 260:7349-7355.